HELSINKI UNIVERSITY OF TECHNOLOGY
DEPARTMENT OF AUTOMATION AND SYSTEMS ENGINEERING
CONTROL ENGINEERING LABORATORY

Power Control and Transmission Rate Management in Cellular Radio Systems

Riku Jäntti

Licentiate Thesis

Supervisor: Prof. Heikki Koivo

HELSINKI UNIVERSITY TECHNOLOGY

ABSTRACT OF THE LICENTIATE THESIS

Author: Riku Jäntti

Name of the thesis: Power Control and Transmission Rate Management in Cellular Radio Systems

Language: English

Date: December 10, 1999 Number of pages: 104

Department: Department of Automation and Systems Engineering

Professorship: AS-74

Field of study: Control Engineering

Supervisor: Professor Heikki Koivo

Abstract:

The scarce radio spectrum imposes hard limitations on design of cellular radio systems. To provide communication services with high capacity and good quality of service requires powerful methods for sharing the radio spectrum in most efficient way. In practice, all sharing methods introduce interference, which is proportional to the transmitter powers. The transmitter power control is a key technique to balance the received signal strength and the interference power, which in turn enables more efficient sharing.

Emerging multimedia service can be characterized by different quality of service requirements such as minimum transmission rates. For a real-time service, users must be guaranteed a tolerable minimum rate. However, non-real time applications, i.e. delay insensitive applications, may temporarily lower their transmission rates even to zero, utilizing any excess capacity that the system is able to provide.

For the fixed-rate systems, we study the effect of additional information on the convergence speed of CIR based power control algorithms. For that purpose we suggest two new algorithms and compare them with the distributed constrained power control algorithm (DCPC) [31]. The first algorithm is called second-order power control algorithm (SOPC) and the other is called block power control algorithm (BPC). SOPC utilizes power levels at current as well as previous iterations to compute power update in a distributed fashion. Gain for such a second-order algorithm is in faster convergence. In bunched systems, it is assumed that some of the link gains are available for radio resource management functions. BPC utilizes this partial knowledge of the link gain matrix to increase the convergence speed. In addition, the energy efficiency of power control algorithms is considered. We generalize DCPC not to necessarily utilize maximum power in the case when interference power is high. The generalized algorithm achieves better performance than DCPC in terms of power consumption and outage.

For the multi-rate (multimedia) system, we examine the combined power control and transmission rate selection problem. We improve the selective power control algorithm by adding the active link protection property to it. The new algorithm is shown to achieve the same or slightly higher capacity with less power and smoother outage. In addition, a centralized packet scheduling algorithm based on knapsack packing method is considered.

The emphasis is on spread spectrum systems, although many of the results are applicable to narrow band systems as well.

Keywords: Wireless, multimedia, rate control, power control, transmitter removals, admission control, scheduling algorithms

Preface

This thesis aims at presenting the work that I have done in the field of power control and combined power control and transmission rate management during a time period from November 13, 1997 till December 10, 1999, in a monograph form.

Most of the work presented in this thesis have been made in collaboration together with others. Chapters 4, 5, and 8 are based on the work done in collaboration with assistant professor Seong-Lyun Kim. Material presented in 6 was done in collaboration with Fredrik Berggren and Seong-Lyun Kim. This part of the thesis was initiated during authors research visit at the Radio Communication Systems Group at Royal Institute of Technology in Sweden (24th of August 1998 - 30th of August 1999). Chapter 7 is based on the material done in co-operation with Janne Laakso, Mika Rinne, and Oscar Salonaho from the Nokia Research Center.

I am grateful to everyone that I have been working with. Especially, I would like to thank assistant professor Seong-Lyun Kim for his encouragement and guidance. In addition, I would like to thank my supervisor professor Heikki Koivo for his support.

This work was funded by the Academy of Finland (by granting the author a researcher position in the Graduate School in Electronics, Telecommunication and Automation), Technology Development Center of Finland, Nokia Corporation, and Sonera Corporation. In addition, the author has received grants, that are gratefully acknowledged, from the Nordic Academy of Advanced Study (NORFA), Emil Aaltonen's foundation, and Jenny and Antti Wihuri's foundation.

Espoo, Finland
December 10, 1999 Riku Jäntti

Notation & Abbreviations

Most important symbols

$\mathbf{A}, \mathbf{A}_a$	power control problem matrix
$c_{ij,p}$	tap weight of p^{th} path from transmitter j to receiver i
c_{ij}	fast fading factor in radio channel between receiver i and transmitter j
$\hat{c}_{ij}$	estimate of the fast fading factor
$\mathbf{e}$	eigenvector
$\mathbf{F} = [f_{ij}], \mathbf{H} = [h_{ij}], \mathbf{H}_a$	normalized link gain matrix
g_{ij}	link gain between transmitter j and receiver i
$\mathbf{G}$	link gain matrix
I_i	interference power at receiver i
$\mathbf{I}$	identity matrix
l_{ij}	large scale propagation factor
K	number of possible rates
$\mathbf{L}$	lower triangular matrix
M	number of users
N	number of blocks
$\mathbf{M}, \mathbf{N}$	splitting of $\mathbf{A}$
p_i	transmission power of user i
$\mathbf{p}, \mathbf{p}_i, \mathbf{p}_a, \mathbf{p}_{ai}$	power vector
$\mathbf{p}^*, \mathbf{p}_a^*, \mathbf{p}_{ai}^*$	fixed point solution
$\bar{p}_i$	maximum transmission power allowed for user i
$\bar{\mathbf{p}}$	maximum power vector
$\tilde{p}_i$	transmission power of user i used instead of $\bar{p}_i$
r_{ik}	k^{th} possible transmission rate of user i
$r_i(n)$	transmission rate of user i at iteration n
$R(\mathbf{Z}^n)$	average rate of convergence of $\mathbf{Z}$ at iteration n
$R_\infty(\mathbf{Z})$	asymptotic average rate of convergence of $\mathbf{Z}$
s_{ij}	shadow fading factor in cell i
T_{I_i}	integration time used by user i
u_i, η_i	normalized noise power at receiver i
$\mathbf{u}, \boldsymbol{\eta}, \boldsymbol{\eta}_a$	normalized noise vector
$\mathbf{U}$	upper triangular matrix

w_{ik}	reward rate associated with r_{ik}
$\mathbf{W}$	weight matrix
$\mathbf{Y} = [y_{ij}]$	rate selection matrix
$\mathcal{A}(n)$	set of users in standard mode at iteration n
$\mathcal{B}(n)$	set of users in transition mode at iteration n
$\mathcal{B}_i$	set of users belonging to block i
$\mathcal{C}(n)$	set of users in passive mode at iteration n
$\mathcal{D}(n)$	set of supported users at iteration n
$\mathcal{E}(n)$	set of non-supported at iteration n
$\boldsymbol{\mathcal{G}}(\mathbf{p}) = (\mathcal{G}_i(\mathbf{p}))$, $\boldsymbol{\mathcal{I}}(\mathbf{p}) = (\mathcal{I}_i(\mathbf{p}))$, $\boldsymbol{\mathcal{T}}(\mathbf{p}) = (\mathcal{T}_i(\mathbf{p}))$	power control mapping
$\mathbb{R}$	set of real numbers
$\mathcal{U}_i$	set of iteration indexes at which user i updates its power
Δ	step size
λ_i	i^{th} eigenvalue
$\boldsymbol{\zeta}$	iteration vector ($\mathbf{M}^{-1}\boldsymbol{\eta}$)
$\mathbf{Z}$	iteration matrix ($\mathbf{M}^{-1}\mathbf{N}$)
θ_{ij}	normalized cross-correlation between signals i from transmitter and j at receiver i
γ^t	CIR-target
$\gamma_i, \gamma_i(n)$	receiver CIR of user i at iteration n
$\gamma_i^t, \gamma_i^t(n)$	CIR-target of user i at iteration n
γ_{ij}^t	CIR-target of user i transmitting at rate r_{ij}
$\boldsymbol{\Gamma}$	CIR-target matrix
ν_i	noise power at cell i
$\rho(\mathbf{H})$	spectral radius of matrix $\mathbf{H}$
$\tau_{ij}(n)$	the most recent iteration for which p_j is known to user i
$\boldsymbol{\tau}_i$	time index vector for user i
$\chi(E)$	indicator function of event E
$\mathbf{X}$	a matrix containing CIR-targets divided by measured CIR values on its diagonal
$\boldsymbol{\Psi} = [\psi_{ij}]$	link gain reliability matrix
$\omega, \bar{\omega}, \hat{\omega}, \omega^*$	overrelaxation parameter
$\boldsymbol{\Omega}$	damping factor matrix
$\mathbf{0}$	a vector or a matrix whose all element are zeros
$\mathbf{1}$	a matrix whose all elements are ones

Abbreviations

ALP	Active Link Protection scheme
ARQ	Automatic Repeat reQuest
B-BPC	Bang-Bang Power Control algorithm
BER	Bit Error Rate
BPC	Block Power Control algorithm
CBPC	Constrained BPC
CIR	Carrier-to-Interference+noise Ratio
CDMA	Code Division Multiple Access
CSOPC	Constrained SOPC
D-AMPS	Digital Advanced Mobile Phone Service
DBA	Distributed Balancing Algorithm
DCPC	Distributed Constrained Power Control algorithm
DPC	Distributed Power Control algorithm
DPC-ALP	Distributed power control with active link protection
DS-CDMA	Direct Sequence CDMA
EDGE	Enhanced Data rates for GSM Evolution
FDMA	Frequency Division Multiple Access
FER	Frame Error Rate
FMA	Foschini and Miljanic Algorithm
GDCPC	Generalized DCPC
GRR	Gradual Removal Algorithm
GSM	Global System for Mobile communications
IMT-2000	International Mobile Telecommunications in the year 2000
IS-95	Interim Standard-95
JOR	Jacobi Overrelaxation method
KS	Knapsack packing scheduling algorithm
M-CSOPC	Modified CSOPC
OL	Over Load method
QoS	Quality of Service
SAS	Soft and Safe admission control algorithm
SIR	Signal-to-Interference+noise Ratio
SMIRA	Stepwise Maximum Interference Removal algorithm
SOPC	Second-Order Power Control algorithm
SOR	Successive Overrelaxation method
SPC	Selective Power Control algorithm
SPC-ALP	Extended SPC
SRA	Stepwise Removal Algorithm
TDMA	Time Division Multiple Acess
UMTS	Universal Mobile Telecommunications Systems
USOPC	Unconstrained SOPC
WCDMA	Wideband CDMA

Table of contents

Chapter 1

Introduction

The scarce radio spectrum imposes hard limitations on design of cellular radio systems. To provide communication services with high capacity and good quality of service requires powerful methods for *sharing* the radio spectrum in most efficient way. In practice, all sharing methods introduce *interference* which is proportional to the transmitter powers. The *transmitter power control* is a key technique to balance the received signal strength and the interference power, which in turn enables more efficient sharing.

Emerging multimedia service can be characterized by different quality of service requirements such as minimum transmission rates. For a real-time service, users must be guaranteed a tolerable minimum rate. However, non-real time applications, i.e. delay insensitive applications, may temporarily lower their transmission rates even to zero, utilizing any excess capacity that the system has.

In this thesis, the transmitter power control and the transmission rate management problems are examined. For the fixed-rate systems, we show that considerable improvements in the convergence speed and energy efficiency can be achieved. For the multi-rate (multimedia) system, we examine certain class of combined transmitter power control and transmission rate management algorithms. In addition, implementations of these algorithms are briefly discussed.

In the next two sections, a concise description of the cellular radio system and radio resource management functions are given, focusing on concepts that are important for the understanding of the material that follows.

1.1 Cellular radio systems

A cellular radio system consists of an infrastructure of *base stations* distributed over a *service area*. The service area is a geographical region where the *cellular operator* (*service provider*), provides cellular services. The service area of one base station is called *cell*. The service provided is that *mobile users* are allowed to access a backbone wired network, traditionally *wire-line telephone network*, and communicate with some other user that also has access to the same network. The user is assumed to have a

portable device (e.g. cellular phone) that can both transmit and receive information. We will refer to a mobile user and its device as a *mobile* or just a *user*.

A transmitter receiver pair forms a *connection* if the former one is transmitting information via *radio channel* to the latter one. Transmission from the base station to the mobile is called *downlink* (*forward link*) and the transmission from mobile to base station is called *uplink* (*reverse link*).

The *digital modulator* maps the information sequence into signal waveforms. The *radio channel* is the physical medium that is used to send the signal from transmitter to the receiver. The channel corrupts the transmitted signal by a variety of possible mechanisms, such as distance dependent attenuation, thermal noise, and fading.

Link gain denotes the total attenuation of power due distance and fading at certain time instant i.e. the received power is the transmitted power times the link gain. One important property of communication in cellular systems is large differences in received signal strengths. A signal transmitted from a transmitter close to the receiver is received with a power several magnitude stronger than a signal transmitted far away form the receiver. Therefore if the users are utilizing the same channel, as in CDMA systems, and the transmission powers are not controlled, the user close to the receiver can completely dominate the others, and drown out the signals of other users. This phenomena is called the *near-far* effect.

At the receiver end, the *demodulator* processes the channel-corrupted transmitted waveforms and maps them back to an information sequence. As a measure of how well the demodulator performs the *bit error rate* (BER) in the decode information sequence is used. Another common measure related to BER is the *frame error rate* FER (a rate at which data blocks containing several bits are received incorrectly).

To provide communication services with high capacity, the frequency spectrum must be shared with many simultaneous users. Spectrum sharing methods are called *multiple access* schemes, the most common of which are frequency division multiple access FDMA, time division multiple access TDMA, and code division multiple access CDMA.

In FDMA each user is given a certain narrow band of the spectrum in which only it is allowed to transmit. In TDMA all the bandwidth is available to all the users, but only one user is allowed to transmit at certain time. In CDMA all users transmit on the entire bandwith at all the times. The radio spectrum is shared among the users by spreading them across the entire bandwidth with different *spreading codes*. The *spreading factor* denotes the how much the bandwidth of the signal is increased because of the spreading. Commercial cellular systems utilizing CDMA technique are the narrowband IS-95 system and the emerging UMTS/IMT-2000 wideband CDMA (WCDMA).

We define a *channel* to be either a frequency interval, a time slot or a combination of them depending on the used multiple access scheme.

Ideal FDMA and TDMA do not generate any interference. In such a system the channels are said to be *orthogonal*. Unfortunately such systems have very poor capacity and therefore a hybrid F/TDMA is used in practical systems like D-AMPS and GSM. In addition FDMA is usually utilized for separating the up- and downlinks. The frequency separation between these two is called *duplex distance*.

In F/TDMA multiple users are allowed to use the same bandwidth at certain time instant given that they are far enough away from each other so that the interference that they cause to each other is kept small enough. The minimum distance (in cells) between two base stations using the same frequency band is called *reuse distance*. On the other hand, in CDMA the reuse distance is one, meaning that the same frequency bandwidth is utilized in every cell. In such a systems the interference is limited by the crosscorrelation properties of the spreading codes.

The interference produced in these systems is usually classified into to classes: *Cochannel interference* is the interference originated by the users that are utilizing the same channel and the *adjacent channel interference* is interference coming from transmissions in other channels.

Carrier-to-interference+noise power ratio (CIR) is the signal-to-interference+noise power ratio (SIR) before despreading. That is, CIR would be equivalent to SIR if the spreading code would be the information to be transmitted. BER and FER are highly dependent on the received CIR (or SIR) value. A common assumption is that BER is a monotonous function of CIR so that as CIR approaches infinity (no interference, no noise) BER approaches zero. Consequently, CIR is commonly used as a quality measure.

The system tries to guarantee some *quality of service* (QoS) for every active connection. For example a QoS requirement for voice communication could be that BER must be less or equivalent to 10^{-3}. This can then be mapped to CIR requirement e.g. CIR must be greater or equivalent to 10 dB. If a user achieves its QoS requirement, we say that the user is *supported*.

1.2 Radio resource management

The objective of radio resource management is to maximize the overall *system capacity* in the cellular network. A common definition for capacity is the maximum traffic load that the system can accommodate under some pre-defined *service quality* requirements.

In the previous section, the quality of service was measured in terms of bit error rate. Measures concerning the system as a whole are *blocking probability*, *outage probability* and *dropping probability*. The blocking probability is defined as the probability that a newly arrived user is denied access to the network. Outage probability is the probability that the quality of service, usually in terms of CIR, of one randomly chosen user is below its prefixed target. Dropping probability is the probability that a user is disconnected from the network.

Dropping of an already ongoing call is generally considered to be worse than blocking a new call request. Therefore harder requirements are usually imposed on the dropping probability. *Admission control* determines whether the new user should be admitted access to the network or not. Consequently, it is the radio resource management function that is responsible for making the trade-off between blocking and dropping probabilities.

If the new user is admitted access to the network, then the following has to be decided: coding and modulation schemes, transmission (bit) rate, base station, and

channel assignments and transmission power. Traditionally all these subjects have been studied separately, but recently the trend has shifted to the investigation of combined radio resource functions like the work on combined power control and base station assignment [92, 35], combined power control and transmission rate selection [46] etc.

Most of the above mentioned resources have to be dynamically controlled during the transmission. For example the base station assignment has to be changed as the user moves further away from the base station. The *handover* algorithm takes care this re-assignment of base stations. It may happen that a group of users can not be re-assigned to another base stations and at the same time they can not achieve reasonably QoS in their current cell. In that case the system is said to be congested and some *congestion control* is required. One way of dealing with a congestion situation, is to remove some of the active users. The objective of *connection removal algorithms* is to remove as few users as possible so that all the remaining users achieve their QoS requirements.

The function of *power control* is to assign transmission powers to users so that the QoS requirements of them are fulfilled while the generated interference is minimized. Transmission power control as such is unstable due to user movement and therefore admission control, handover, and connection removal algorithms are required to stabilize it.

1.3 Previous work

We divide this section into two parts. First the work related to the fixed-rate power control algorithms is reviewed and then the work related to the combined transmitter power control and transmission rate selection is treated.

Since power control has been extensively researched, we do not even try to cover all the previous research in this field. Instead we review some of the most important research directions and cite some papers characteristic to each direction.

1.3.1 Fixed-rate systems

Early results in the field of transmitter power control date back to 60's and were considered in the context of broadcast networks [18].

In [2], Aein investigated cochannel interference management in satellite systems. He introduced the concept of CIR-balancing in which the transmission powers of all the users are chosen so that all the receivers experience the same CIR-level. The power control problem was identified as an eigenvalue problem for positive matrixes. In [62, 63], Nettleton and Alavi applied and extended Aein's results to a spread spectrum cellular radio systems. They showed that the system capacity of spread spectrum systems can be substantially improved by utilizing CIR-balancing.

The CIR-balancing concept can also be applied to narrow band systems as in [94] in which a CIR-balancing algorithm was suggested. That algorithm is optimal in the sense that it maximizes the minimum CIR in a cellular network. That is, the algorithm

finds the maximum CIR that all the active connections can achieve. This maximum CIR is referred as *maximum achievable CIR*.

The algorithm in [94] has been extended to the case where receiver noise has been taken in to account [95] and to the case where in addition transmitter powers are upper-bounded [31]. By taking the receiver noise into account the transmission powers in the CIR balancing problem can be unambiguously solved from a set of linear equations provided that the solution exits. In [34], this set of equations was identified to determine the capacity region of the system.

Leung [56] showed that reasonably good approximations of the maximum achievable CIR can be achieved based on limited information about the link gains (link gains between a few strongest interferes and the receiver).

Under certain assumptions (reciprocal link gains, non-orthogonal codes in downlink) it was shown in [62] that the maximum achievable CIR in uplink and the corresponding maximum achievable CIR in downlink of a spread spectrum cellular system are equivalent. Similar result in the case of narrow band systems can be found in [98]. This result means that if one can find a channel allocation in one link (up or down) the same set users can can share the channel in the other direction as well given that the transmitter powers are adjusted appropriately. Numerical results in [24] indicate that the above holds if the transmission powers are constrained.

The above mentioned algorithms are centralized and utilize a lot of information and therefore can be difficult to realize in practice. The alternative to centralized algorithms are of course distributed ones that we briefly review in what follows.

Zander [93] suggested the distributed balancing algorithm (DBA) for solving the maximum achievable CIR and transmission powers in a distributed fashion. For the same purpose Grandhi, Vijayan and Goodman [30] suggested the use of distributed power control (DPC) algorithm originally proposed for satellite systems in [60]. By simulation DPC was shown to converge faster than the DBA. In both algorithms, users update their own power values, in an iterative fashion, based on the local measurement of their received CIR-values. However, the exclusion of the noise in the analysis leads to a problem of setting the absolute power level. Both algorithms had a free parameter for this normalization purpose.

Foschini and Miljanic [23] considered the power control problem in the presence of receiver noise. They introduced QoS requirement dependent prefixed CIR-target that the system should try achieve instead of trying to find the maximum achievable CIR. Their algorithm is shown to converge under stationary link gains to a fixed point where all users achieve the prefixed target conditioned on that the target is strictly less than the maximum achievable CIR. In the noisy case, the free parameter in DPC algorithm can be interpreted as a CIR-target and thus the DPC algorithm can be interpreted to be a special case of the Foschini and Miljanic algorithm.

Mitra [61] proved that an asynchronous version of the Foschini and Miljanic algorithm, in which the users are allowed to perform their power updates using outdated information on the interference caused by others, converges under the assumption of stationary link gains.

DPC has been extended to the case where receiver noise, transmitter power constraints, and asynchronous updates have been taken in to account [31]. This algorithm

is called Distributed Constrained Power Control (DCPC) algorithm.

Blom and Gunnarsson [17] have studied the performance of the local power control loops. They identified the DCPC as an antiwindup I-controller in dB-scale with integration time constant set to one. In addition, they also showed that such a controller is sensitive to delays in the system. As a solution they suggested, among other things, the use of smaller integration time. They noted that in the noisy case the power control algorithm suggested by Lee and Lin [52] can in be interpreted as an I-controller with a tunable integration time constant.

Sung and Wong [78] considered a CIR-balancing algorithm in which some limited signaling between the neighboring cells are allowed. In their algorithm a user updates its power by utilizing information about the minimum CIR within its neighborhood. Numerical results indicated that their algorithm converges faster than the DPC. This kind of approach for power control could be useful in the case of bunched systems.

So far in the QoS based power control it has been assumed that the received CIR can be measured perfectly. One of the first attempts to analyze the roubustness of power control algorithms can be found in [57]. In that paper, the effect of bounded errors in CIR estimation on DBA and DPC algorithms is addressed.

In a recent paper by Ulukus and Yates [83], it was assumed that the received CIR is measured by utilizing the actual matched filter output in the receiver. Ulukus and Yates show that if the link gains are constant the expected squared error (distance between current power vector and the fixed point) of an iterative method similar to the non-stationary Foschini and Miljanic algorithm converges under certain values of free parameters.

In [55], the Foschini and Miljanic type of power control is considered for the packet-switched TDMA system in the case where the received interference power is estimated via Kalman filter. The method is based on the estimation of temporal correlation of cochannel interference and utilizing this information to predict the interference in the next power control interval.

Andersin and Rosberg [5] considered DCPC type of power control based on averaged link gains. Since the actual link gains are distributed around their mean values, the probability that a user is experiencing too low CIR could be high. As a solution they suggested a time varying CIR-margin. Recently Rosberg [69] considered adaptive CIR margins using *duration outage* [59] as a performance measure. Sampath, Kumar and Holzman [74] considered the setting of a SIR-target in a context of IS-95 CDMA system. They suggested an algorithm that adapts the CIR-targets of the power control algorithm based on the measured FER. In [17], a CIR-target adaptation mechanism based on measured statistic of the radio channel was considered for GSM system. References [5], [69], [74], and [17] provide means to adapt the deterministic power control methods to the statistics of the random radio channel.

Besides QoS based power control described above also another class of power control algorithms based on constant received power has been suggested. This scheme is efficient in controlling adjacent intra-cell interference, but has been shown to have limited effects on co-channel inter-cell interference [25, 81].

In most proposals for constant received power, the transmitters update their powers inversely proportional to the link gain in their allocated link. This method is called

full compensation. In [88], Witehead shows that better results can be obtained if only partial compensation is done.

Anderlind [4] has suggested a constant received power control algorithm that has a similar I-controller structure as DCPC has.

Note that if we consider only one cell in a spread spectrum system, the quality based power control and constant received power are equivalent. In that particular case the constant received power algorithms are advantageous since they utilize only the received signal power measurements that are simpler to estimate than the received CIRs.

All the above mentioned distributed power control algorithms required either received CIR or received power values to be transmitted from the receiver to the transmitter. Since in the theoretical algorithms these values are real numbers, infinite bandwidth would be required to transmit the information exactly. Therefore some quantization is required. In [8], two discrete algorithms are presented, both being modifications of the DCPC algorithm; one rounds up to the nearest grid point (ceiling algorithm) and the other rounds down (floor algorithm). Both are shown to converge in a weaker sense to an envelope of powers, but of course oscillations are possible.

Earlier works to consider quantization are [87] and [9] in which the use of a bang-bang type controller in a DS-CDMA system is analyzed. These algorithms can be interpreted as relays in dB-scale. In [87], received CIR is used as a decision variable. Whereas the received signal power is used in [9]. Both these algorithms are practical, since they are reasonably simple to implement and require relatively small overhead. The first one has been suggested for the next generation WCDMA system [1, 21] and the latter one is currently used in the IS-95 system [80, 33].

In a recent paper by Sung and Wong [79], the convergence and active link properties of simple relay with dead-zone controller (in dB-scale) is investigated. This kind of controller has many attractive properties, like noise filtering, compared to the bang-bang power control. The only drawback is that at least two information bits are required to transmit the power control command.

Based on these simple bang-bang controllers some adaptive power control methods have been suggested. The main goal of these algorithms is to quickly track the fast (Rician or Rayleigh) fading [50, 44, 76].

Since the users in general are mobile, the power control problem in one cell is unstable, which means that the power of a user moving away from the base station is increasing all the time. Therefore some handover mechanisms are required. In hard handover the user is handed over to the neighboring cell in the cell boundary. In soft handover the user is connected to two or more base stations, and instantaneously on frame-to-frame basis, the better frame received by either base station is accepted by the network. In [86], it was shown that the soft handover is preferable in terms of coverage and capacity. Understandably soft handover is part of the IS-95 standard [33], and will be part of the third generation WCDMA standard as well [21].

Yates and Huang [92, 37] suggested combined power control and base station assignment, which can be seen as a combination of the power control algorithm suggested by Foschini and Miljanic and the soft handover concept. Independently from their work also Hanly have suggested similar algorithm [35]. Kim [45] proposed that

the base station assignment should only be allowed when the CIR of the user is less than the CIR-target plus some margin. This is to reduce the required amount of signaling and computational complexity while guaranteeing convergence to the minimum power solution.

Reference [90] presents a general framework for analyzing the convergence properties of QoS based power control algorithms like the Foschini and Miljanic algorithm, DCPC and the integrated power control and base station assignment suggested by Yates and Huang. This framework has proven to be useful in the design of new algorithms (see e.g [91]).

Admission control is used for allowing new users to enter the network. Admission control algorithms should prevent new users from dropping any already supported users from the network i.e. a new user should choose its transmission power so that the CIR values of all the already supported users stay greater or equivalent to their prefixed targets. In [12], an active link protection scheme was suggested in which new mobiles start with small power and power up slowly using fixed power up step size while the old already supported users use Foschini and Miljanic algorithm with CIR-margin equal to the fixed power up step. This scheme guarantees that the CIR of no active link is dropped below it's prefixed CIR-target. This power control method is called DPC-ALP (distributed power control with active link protection). The system makes decision whatever to admit or reject the user based on the CIR evolution during the power updates of the new link [11]. In [10], power constrains are considered for DPC-ALP. Since new users cause old users to increase their power it may happen that the power of currently active user drifts to the maximum power value and thus CIR of that user drops below the target value. In order to prevent this, distress signaling is suggested in which the active link drifting towards maximum allowed transmission power value sends a distress signal to all the new links that then drop out.

The problem with DPC-ALP is that the use of CIR-margin reduces the capacity. In [7], a soft and safe admission control (SAS) algorithm was suggested. In this algorithm all the power updates are made by using DCPC, but the new user trying to get admitted into the system has to gradually increase the maximum power level while the already admitted users gradually decrease their protection margin. Since no fixed margin is used, no capacity is lost. The biggest drawback of SAS is that it is designed to admit one user at the time.

Some admission control schemes can make erroneous decision allowing too many users to use the same channel at a given time instant or the link gains of the originally successfully admitted users can change so that the system becomes infeasible. In that case some connections must be either handed over to other cell or removed entirely. Unfortunately the removal problem, i.e. what connections to remove if the system becomes congested, can be shown to be NP-complete [6].

In [94], a Stepwise Removal Algorithm (SRA) has been proposed, which removes connections one-by-one. Given a constant transmission power vector, the SRA removes the connection that has the smallest uplink or downlink CIR whichever is smaller. In the Stepwise Maximum Interference Removal Algorithms (SMIRA) [53] the removal decision is made based on the maximum received interference after the centralized CIR balancing power control has been used. According to the results in [53] the SMIRA

outperforms the SRA algorithm.

In [6], a family of removal algorithms are proposed and analyzed. One of the algorithms proposed in that paper is the gradual removal algorithm. The gradual removal algorithm can be combined with DCPC to yield fully distributed removal algorithm GRR-DCPC in which a connection is removed with certain probability if the transmission power of that connection is set to the maximum value at certain iteration. The GRR-DCPC is capable of removing multiple connections in totally distributed way while maintaining close to optimal performance.

Another heuristic approach for connection removal problem is the Lagrangian relaxation based removal algorithm suggested by Kim and Zander in [47]. This algorithm is fully distributed and performs better than the GRR-DCPC in terms of convergence speed.

One concept related to the connection removal is soft dropping. In soft dropping a connection experiencing bad interference situation is forced to accept decreasing quality of service in terms of CIR. Power control algorithms utilizing this idea can be found in [3, 32, 91].

Rulnick and Bambos [72, 71, 73] consider an idea similar to the soft dropping in which the number of correctly received bits are allowed to vary as the interference varies. In their algorithm minimum power that fulfill the expected throughput criterion (number of correctly received bits in the power control interval) is utilized.

Other approaches to the power control problem include game theoretical approach [39] , soft computing approaches [19, 20, 27] and information theoretical approach [28, 82, 36].

1.3.2 Multi-rate systems

Recently power control has been combined with a variety of things like beamforming [68], modulation [66, 67], and transmission rate selection [46]. The two latter combinations are of interest to us in this section.

Zander [97] considered a radio resource management problem in which the objective is to provide at least some minimum data rates to individual users as well as to maximize the total throughput. The idea is that the system should use any excess bandwidth in the best effort fashion.

In [75], maximizing the total system throughput (transmission rate) is considered in the context of a DS-CDMA system, where each user has a minimum rate requirement, and different rates are represented by varying the *processing gain*. A more general formulation is provided in [77], in which a combined base station assignment, rate control and power control of a DS-CDMA system is formulated into a *quadratic programming problem*. In [66, 67], the problem is addressed in terms of joint power control and adaptive modulation, where powers are controlled within lower and upper limits to maximize the log-sum of users' SIR values. The underlying idea is that, by maximizing the SIR values, we also maximize the total transmission rates through adaptive modulation. Maximization is done over a continuous power domain, assuming that the feasible transmission rates are also continuous. A centralized iterative power

control algorithm that converges to the optimal solution is given and is illustrated by several examples.

The studies mentioned above assume that transmission rates may take any continuous value. That is, the throughput of a radio channel is a *continuous* function of the channel's SIR. The continuity assumption in these works greatly simplifies the problem. Their solutions however, do not lend themselves into distributed power control algorithms.

In practice, the feasible transmission modes are limited to a small number of *discrete* values; finite number of values for the number of bits transmitted in each symbol. For example in EDGE (Enhanced Data rates for GSM Evolution), eight modulation and coding sachems (transmission modes) adapt the bit rate to channel conditions, i.e, SIRs [26]. With this in mind, Kim, Rosberg and Zander [46] focused their attention on the rate selection and power control problem when the feasible transmission rates (modes) are discrete. In their paper two algorithms were described. The first one was based on Lagrangian relaxation technique [22] and the second one, called selective power control (SPC), was based on simple heuristics. Very reacently, there was an interesting work [54] dealing with the same problem as Kim *et al.* In that work, a distributed power control algorithm that reduces packet error while sacrificing some amount of throughput was suggested.

Another approach to the multi-rate systems is to model the cellular system as a queuing system and use transmission rate control to handle the backlog and control the expected delay [64]. In [97] and [46], it is implicitly assumed that the radio resource management time constant is much smaller than the service time constant. Therefore it can in principle be assumed that there is always data to be sent and that the resulting packet delay is approximately one per throughput.

1.4 Scope and contributions

This thesis examines the power control and transmission rate selection problems. The emphasis is on the spread spectrum systems, although many of the results apply for narrow band systems as well.

In the case of fixed rate systems, we examine the CIR based power control and its relations to the iterative methods proposed in the field of numerical linear algebra for solving large linear equation systems. We provide a linear algebra framework for the Foschini and Miljanic type of power control algorithms and by utilizing this frame work, we compare the convergence speeds of different power control algorithms in terms of *asymptotic average rate of convergence*.

Since it has been noted that the convergence speed of DCPC becomes slow as the power vector approaches the fixed point, we suggest two new power control algorithms that are shown to converge faster than DCPC.

Fast convergence is especially important when propagation and traffic conditions are changing rapidly. It is expected that future wireless traffic will become much more bursty than today's voice dominated traffic. With bursty traffic, slow algorithms will

perhaps not even be able to converge before the data burst ends. To track these changes, the power control algorithm must converge quickly.

We show that by utilizing the power control history in computing the power update, the convergence speed of the power control algorithm can be increased. We suggest a Second Order Power Control (SOPC) algorithm that is capable of utilizing this additional information. We show that the SOPC converges to the same fixed point as DCPC but asymptotically faster.

The second power control algorithm suggested in this thesis, called Block Power Control (BPC), utilizes partial knowledge about the link gain matrix to increase the convergence speed. This method is especially suited for bunched systems in which it is assumed that some of the link gains within the bunch can be estimated [14].

In addition, we will address the energy efficiency of the power control algorithms. We revisit DCPC and generalize it not to necessarily use the maximum power when the channel quality is poor. We explain how the generalized algorithm can achieve energy efficiency.

In the convergence analysis, we assume that the system in feasible, but how can we ensure that the system is feasible? One solution is to allow arbitrary number of users transmit simultaneously and then based on some criteria start removing them until all the remaining users can be supported. Another method is to decide beforehand which users are allowed to transmit. We use the first method with the generalized DCPC by combining it with the gradual removal algorithm [6]. The other approach is taken as we suggest a heuristic packet scheduling method based on the knapsack packing optimization method. The performance of which, we evaluate in a highway cellular system in the presence of frequency selective fast fading.

Furthermore we consider the combined power control and transmission rate selection problem and by following in the footsteps of Kim, Rosberg and Zander suggest a new algorithm based on the DPC-ALP and SPC algorithms. In addition, we show that the active link protection property can be achieved by utilizing bang-bang controller and choosing a proper CIR-margin.

Most of the material presented in this thesis are based on the following publications that the author has made in collaboration with other researchers: [41, 40, 15, 42, 48].

1.5 Thesis outline

In chapter 2, the system model and the performance evaluation methods are described. Chapter 3 describes power control and rate selection problems in detail. A new power control method utilizing information about current and previous power values as well as received CIR is described and analyzed in chapter 4. The block power control method utilizing partial knowledge about the link gain matrix is proposed and analyzed in chapter 5. In chapter 6, the energy efficiency of DCPC is considered and new generalized DCPC is suggested. Chapter 7 suggest a centralized (bunched) method for making the system feasible. The suggested method can also be interpreted as a transmission rate selection algorithm if the set of possible rates is limited to zero and some fixed rate. In chapter 8, the combined power control and rate selection problem

is addressed in the case where the set of possible rates is allowed to contain more than two, but finite amount of rates. Finally chapter 9 concludes this thesis.

Chapter 2

Models and methodology

The cellular radio systems are extremely complex and the system design incorporates many details. To be able to focus on parts of it, like the power control problem, simplified models are required. In this chapter, we describe the models, assumptions, and performance evaluation methods used in the text.

2.1 Environment and infrastructure

In this work, we simulate a macro cellular system, typically used in rural environments, to numerically evaluate our algorithms. It should be noted, however, that the proposed algorithms could be directly applied to microcellular systems, used in urban areas, as well.

For the numerical evaluations, two different network configurations are considered. The first one consists of 19 base stations, located in the middle of hexagonal cells as shown in figure 2.1. For simplicity, the system is assumed to be two dimensional, meaning that the base station antenna is on the same level as the mobile antenna. The second configuration is one dimensional. It consists of only five base stations that are equally spaced from each other. A wrap around technique is used to remove possible edge effect. Therefore the latter system can be interpreted as being infinitely long road.

As a multiple access scheme we consider a direct sequence CDMA in which pseudorandom codes are used in the uplink and orthogonal codes in the downlink. It is assumed that the set of orthogonal codes used in one cell is not orthogonal with the set of codes used in another cells; consequently, the capacity of the up- and downlinks are no longer equivalent as assumed in [62, 98, 24].

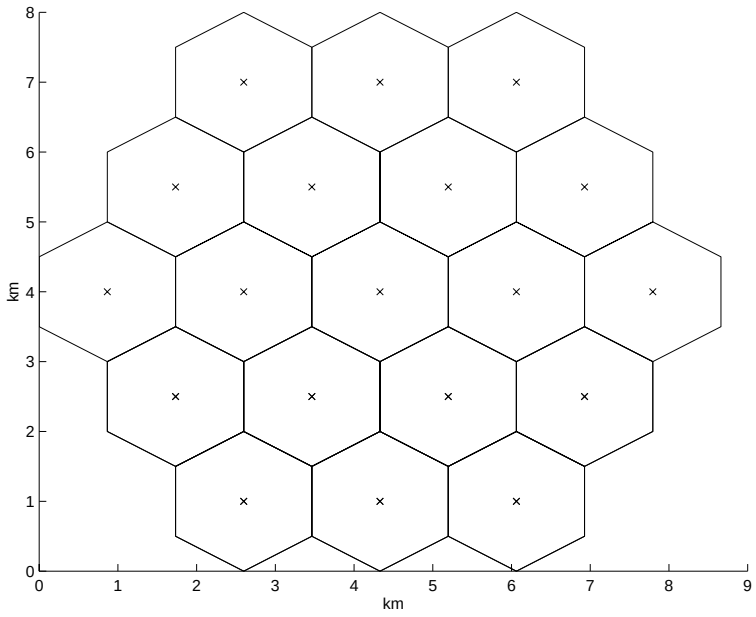

Figure 2.1: Cellular system consisting 19 cells in a hexagonal grid. Location of base stations are marked with 'x'.

2.2 Command control structure

The cellular radio systems are managed and controlled by the base stations, which are interconnected through a high-speed wire-line network. Mobile stations continuously perform measurements in the downlink and report this information back to the base station, while the base station performs the same measurements in the uplink. The wire-line network can be used for exchanging this information between the base stations. We study our algorithm under a variety of assumptions about the available measurements and the distribution of this measurement information in the system.

We consider both *distributed schemes*, in which the radio resource management decisions are made based on local information, and "bunched" schemes, in which it is assumed that certain amount of information can be shared within a set of base stations called a bunch [14]. Furthermore we will slightly generalize the bunch setting by assuming that the information sharing is allowed within an arbitrary set of users called a block.

2.3 Radio wave propagation

In free space, the power density of electromagnetic waves decreases with a factor proportional to the square of the distance between the receiver and the transmitter. In

a typical cellular environment, there are usually many objects upon which the radio waves are *reflected*, *diffracted* or *partially absorbed*. Therefore instead of a single wave-front , an antenna at the receiver encounters several waves of different strength and polarization, coming from different angles and having different phases.

Reflection occurs when propagating radio wave encounters an obstructing object with dimension very large compared to the wavelength of the radio wave. Reflected waves can then interfere either constructively or destructively at the receiver.

The reflection of radio wave in objects with dimensions on the order of wavelength or less, found in the proximity of the receiver causes *scattering*. Which in turn causes rapid variations in received signal strength. This phenomena is called *fast fading*.

Diffraction occurs when the direct path between the transmitter and receiver is obstructed by an impenetrable object. However, the secondary waves may be formed behind the obstructing object. This phenomenon is called *shadowing*.

In addition to the above mechanisms, the received signal is further corrupted by thermal and man-made noise.

Assume that only transmitter j is transmitting at certain time instant. The received power from transmitter j at receiver i, can then be written as $g_{ij}p_i + \nu_i$ in which g_{ij} is the *link gain* between transmitter j and receiver i and ν_i is the noise power at receiver i. Throughout this thesis, we assume that $0 < g_{ij} < \infty$ and $0 < \nu_i < \infty$. In the uplink case, the value p_j means the transmission power of mobile j. However, in the downlink, it denotes the transmission power dedicated to mobile j by the base station to which mobile j belongs.

The link gain is usually partitioned to three parts

$$g_{ij} = \frac{s_{ij}c_{ik}}{l_{ij}} \tag{2.1}$$

The large scale propagation loss l_{ij} is derived from the geometry of the setting and is therefore highly distance dependent. The shadow fading term s_{ij} models the irregularities in the terrain, such as mountains, hills, buildings, etc. The multi-path fading factor c_{ij} models short term variations in the attenuation caused by the mobility of the user and/or the environment.

In macrocellular system, it has been shown empirically [51] that a good model for the large scale propagation is

$$l_{ij} = G_0 L_0 d_{ij}^m \tag{2.2}$$

in which G_0 is a parameter related to antenna heights and gains, L_0 reflects the degree of urbanization, d_{ij} is the distance between transmitter j and receiver i, and m is the propagation constant. In this thesis we scale all the powers so that $G_0 L_0 = 1$. The propagation constant m is in the range $2 \leq m \leq 4.35$ in which $m = 2$ corresponds to free space propagation. In the numerical studies, we use $m = 4$ in the 2-D case and $m = 2$ in the 1-D case.

To model the shadow fading, we use the widely accepted model that the shadow fading has lognormal distribution (see e.g. [38, 51]):

$$s_{ij} = 10^{\frac{\zeta_{ij}}{10}} \tag{2.3}$$

in which the random variable ζ_{ij} has Gaussian distribution with zero mean and σ standard deviation.

In [85], it is assumed that the logarithm of the shadow fading parameters of two or more base stations have jointly Gaussian distribution. That is, ζ_{ij} can be written as a sum of two components:

$$\zeta_{ij} = a\xi + b\xi_i \quad \forall j \tag{2.4}$$

in which $a^2 + b^2 = 1$, $a < 1$. Random variable ξ corresponds to the common near field component and random variable ξ_i is independent from base to base. Since ξ and ξ_i are zero mean Gaussian random variables, it follows that

$$E\{\zeta_{ij}\zeta_{kl}\} = \begin{cases} (a^2+b^2)\sigma^2 & , i = k \\ a^2\sigma^2 & , i \neq k \end{cases} \quad \forall j, l \tag{2.5}$$

In the numerical examples, we use $a = b = \frac{1}{\sqrt{2}}$ and $\sigma = 8$ dB as in [85].

The multi-path fading is due to the summation of radio waves arriving at the receiving antenna with different phases and amplitudes. Depending on the phases and amplitudes of the individual waves the summation may cause a complete or partial signal cancellation, a fade. We assume that the signal bandwidth W_s is much larger than the coherence bandwidth B_m. Thus, the radio channel is frequency-selective and can be modeled as a tapped delay line with statistically independent time-variant tap weights $\{c_{ij,p}\}$ [65].

We assume that a RAKE demodulator with perfect knowledge about all the tap weights is used in the receiver. In the RAKE each of the delayed path (or tap) can be resolved separately. Thus the effect of frequency-selective fading on the received power can be taken into account at certain time instant by using

$$c_{ij} = \sum_{p=1}^{P} c_{ij,p}^* c_{ij,p} \tag{2.6}$$

in which $P = \lfloor W_s T_m \rfloor + 1$ ($\lfloor \cdot \rfloor$ denotes the floor operator) is the number of resolvable paths (or taps) in the receiver and $c_{ij,p}$ is the tap weight of the p^{th} path and $c_{ij,p}^*$ denotes the complex conjugate of $c_{ij,p}$. The signal bandwidth is denoted by W_s and T_m denotes the multipath spread of the channel ($B_m \approx \frac{1}{T_m}$).

A standard assumption in macrocellular environment is that the tap weights $c_{ij,p}$ are Wide-Sense-Stationary and subject to Uncorrelated Scattering (WSSUS). That is,

$$E\left\{c_{ij,p}^* c_{ij,q}\right\} = \begin{cases} \frac{1}{P} & , q = p \\ 0 & , q \neq p \end{cases} \tag{2.7}$$

Furthermore it is assumed that the envelope of the tap weight $|c_{ij,p}|$ is *Rayleigh distributed* [51]. In order to numerically compute these factors we utilize the well-known Jakes model [38].

The fast fading channel has also another negative effect to the received signal. Because of the delayed path, also copies of the previously sent symbols arrive to the receiver at the same instant as the current symbol causing *intersymbol interference*.

Our assumption is that Viterbi decoder (see e.g. [85]) is used so that the effect of *intersymbol interference* can be neglected.

Typically l_{ij} and s_{ij} vary at significantly lower rate than c_{ij}. Therefore, we assume in all the chapters expect chapter 7, that the the multipath fading is resolved by appropriate coding and interleaving techniques i.e. we assume that the effect of fast multi-path fading can be averaged out.

2.4 Communication quality

Suppose a cellular radio system, in which M transmitters are accessing a common frequency channel. Each transmitter communicates with exactly one receiver. For the uplink case, the transmitters are the mobiles and the receivers are their corresponding base stations; and for the downlink case, their roles are reversed. We consider a time instant in which the link gain between every receiver i and every transmitter j is stationary and is given by g_{ij}.

Without loss of generality, we will assume that transmitter i is communicating with receiver i. In a DS-CDMA system, many mobiles will communicate with the same base station through the same channel. Thus, in our notation below, receivers i and j in the uplink may denote the same physical one if the transmitters (mobiles) i and j are assigned to the same base station.

We assume that the signal of transmitter i will be received correctly if the carrier-to-interference-plus-noise ratio (CIR) at the receiver i, γ_i is not less than a given target value γ_i^t. Therefore, we have the following CIR constraint on transmitter i [96]:

$$\gamma_i = \frac{g_{ii}p_i}{\sum_{\substack{j=1 \\ j\neq i}}^{M} g_{ij}\theta_{ij}p_j + \nu_i} \leq \gamma_i^t, \quad i = 1, 2, \ldots, M \tag{2.8}$$

In above the quantity θ_{ij} is the normalized cross-correlation between signals from transmitter i and j at receiver i, i.e. the effective fraction of the received signal power from transmitter j contributes to the interference when receiving the signal from transmitter i. For instance, $\theta_{ij} = 1$ for both up-and downlinks in an F/TDMA system.

In a DS-CDMA system, we assume $\theta_{ij} = 1$ for the uplink case whereas, in the downlink, $\theta_{ij} \in [0, 1]$ if mobiles i and j are assigned to the same base station; otherwise $\theta_{ij} = 1$. This assumption reflects the use pseudorandom spreading code sequences in the uplink and orthogonal spreading code sequences within one cell in the downlink.

A user i is said to be *supported* if inequality (2.8) is fulfilled. Otherwise the user is said to be in *outage*. Unless otherwise noted, we utilize 2 % CIR-tolerance in the outage computations. That is, if $\gamma_i < 0.98\gamma_i^t$ then the user i is assumed to be in outage. We define the *outage probability* as the fraction of users that are in outage at a given time instant.

2.5 Performance evaluation methods

To completely evaluate a radio resource management algorithm, full scale simulation and field trials are required. Instead we choose to utilize two simpler evaluation strategies, the results of which can be interpreted as upper-bounds for the real performance.

The first method is *time independent* analysis in which it is assumed that the power control algorithms converge much faster than it takes for the link gains to change due to mobility. This evaluation approach is called *snapshot analysis* and has been used in most of the power control studies mentioned in section 1.3 with only few exceptions. In a snapshot analysis, the link gains are frozen in time and no measurement and sampling errors occur. This situation could be interpreted as observation of the system at a random instant of time and allowing the radio resource management function, like power controller, perform infinitely fast updates. Clearly the results of this kind of analysis are upper-bounds for the real performance.

However, according to Rosberg and Zander [70], the snapshot analysis could still be useful in the analysis of power control algorithms when some favorite conditions occur. For instance, fast fading is averaged out, mobiles move slowly, and power updates are relatively fast. Under such conditions, the controlled powers are drifted to values which are in the vicinity of a temporary fixed point, in a rate which is much faster than the rate link gains may change. Thus, quasi-convergence and quasi-stability do occur.

As the second evaluation method we still keep the mobile positions fixed, but allow the fast fading factor to vary in time. This kind of model corresponds approximately to a case in which the mobiles are moving slowly at a walking speed.

As a traffic model, we utilize the following simple model that is direct consequence of the snapshot assumption: Fixed number of users uniformly distributed in the service area. We further assume that all the users have infinite amount of data to send i.e. we assume that the time constant of radio resource management is much smaller than the time constant of the the service. This assumption is similar in nature to the snapshot assumption and have been used e.g. in [46].

Chapter 3

Power control

In this chapter we define the problems that we investigate in detail. Firstly, the fixed rate systems are considered and a general framework for analyzing the convergence properties of a certain class of power control algorithms is suggested. Secondly, the problem formulation for the combined rate selection and power control is presented.

3.1 Power control problem

Let us define an $M \times M$ matrix $\mathbf{F} = [f_{ij}]$ such that $f_{ij} = \frac{g_{ij}\theta_{ij}}{g_{ii}}$ for $i \neq j$ and $f_{ij} = 0$ for $i = j$. Furthermore let $\mathbf{\Gamma} = \text{diag}\left\{\gamma_i^t\right\}$ in which γ_i^t is the CIR-target of user i. In addition, let us define a column vector $\mathbf{u} = (u_i)$ such that $u_i = \nu_i / g_{ii}$. Now we can rewrite inequality 2.8 as

$$\mathbf{Ap} \geq \boldsymbol{\eta} \tag{3.1}$$

in which $\mathbf{A} = \mathbf{I} - \mathbf{\Gamma F}$, $\boldsymbol{\eta} = \mathbf{\Gamma u}$ and $\mathbf{p} = (p_i)$ denotes the *power vector*. Since the ideal situation is to make connection with the minimum transmission power, we seek to solve

$$\mathbf{Ap} = \boldsymbol{\eta} \tag{3.2}$$

with respect to $\mathbf{p}$. Since the power of a transmitter is limited, we will consider the following constraint on the power vector:

$$\mathbf{0} \leq \mathbf{p} \leq \bar{\mathbf{p}} \tag{3.3}$$

where $\bar{\mathbf{p}} = (\bar{p}_i)$ denotes the maximum allowed transmission power.

Definition 3.1. If there exists a vector $\mathbf{p}^*$ that solves problem (3.2) within the range of (3.3), we say that the system is *feasible*. Otherwise, we say that the system is *infeasible*.

Let $\mathbf{H} = \mathbf{\Gamma F}$ be a nonnegative matrix and let λ_i denote the i^{th} eigenvalue of it. The constant $\rho(\mathbf{H}) = \max_i |\lambda_i|$ is called *spectral radius* of $\mathbf{H}$. In what follows we state some basic properties of the power control problem using the notation defined here. Note that in our notation $\mathbf{H} \geq \mathbf{0}$ denotes that all the elements of $\mathbf{H}$, h_{ij}, fulfill $h_{ij} \geq 0$ instead of denoting that $\mathbf{H}$ is positive semi-definite as commonly used in linear algebra textbooks. Similarly, in the case of matrixes $\leq$ and $\neq$ denote elementwise relations.

Lemma 3.1 (lemma 2.1 in [29]). $\mathbf{H}$ *is an irreducible nonnegative matrix.*

Proposition 3.1 (Perron-Frobenius Theorem). *Let* $\mathbf{H} \geq \mathbf{0}$ *be an irreducible* $M \times M$ *matrix. Then,*

1. $\mathbf{H}$ *has a positive real eigenvalue equal to its spectral radius.*
2. *To* $\rho(\mathbf{H})$ *there corresponds an eigenvector* $\mathbf{e} > \mathbf{0}$.
3. $\rho(\mathbf{H})$ *increases when any entry of* $\mathbf{H}$ *increases.*
4. $\rho(\mathbf{H})$ *is a simple eigenvalue of* $\mathbf{H}$.

For proof see e.g. Theorem 2.1 in [84].

Proposition 3.2 (Theorem 3.7 in [84]). *If* $\mathbf{H}$ *is an arbitrary complex* $M \times M$ *matrix with* $\rho(\mathbf{H}) < 1$, *then* $\mathbf{I} - \mathbf{H}$ *is nonsingular, and*

$$(\mathbf{I} - \mathbf{H})^{-1} = \sum_{k=0}^{\infty} \mathbf{H}^k$$

the series on the right converging. Conversely, if the series on the right converges, then $\rho(\mathbf{H}) < 1$.

Proposition 3.3 (Theorem 3.9 in [84]). *If* $\mathbf{H} \geq \mathbf{0}$ *is an* $M \times M$ *matrix and* $\alpha > 0$, *then the following are equivalent:*

1. $\alpha > \rho(\mathbf{H})$
2. $\alpha\mathbf{I} - \mathbf{H}$ *is nonsingular, and* $(\alpha\mathbf{I} - \mathbf{H})^{-1} > \mathbf{0}$

The meaning of the above proposition, in terms of power control, is that a necessary (but not sufficient) condition for feasibility is $\rho(\mathbf{H}) < 1$. That is, if the system is feasible then $\mathbf{A}^{-1} > 0$ and thus $\rho(\mathbf{H}) < 1$.

In the next section, we will describe a framework for power control that utilizes the above mentioned properties.

3.2 A framework for power control

3.2.1 Unconstrained power control

Consider first a relaxed problem in which the transmission power constraint is relaxed. Then the power control problem is reduced to solving equation (3.2) with respect to $\mathbf{p}$. Since the number of users in the cellular system M is in general large, inverting $\mathbf{A}$ becomes computationally intensive. Solving of very large linear equation systems like (3.2) is extensively studied in the field of numerical linear algebra [84, 89]. Let us follow the approach taken in [84, 89] and divide $\mathbf{A}$ to two parts such that $\mathbf{A} = \mathbf{M} - \mathbf{N}$, $\mathbf{M} \neq \mathbf{0}$; then a general method for solving (3.2) can be written as

$$\mathbf{p}(n+1) = \mathbf{M}^{-1}\mathbf{N}\mathbf{p}(n) + \mathbf{M}^{-1}\boldsymbol{\eta} \stackrel{\text{def}}{=} \boldsymbol{\mathcal{I}}\left(\mathbf{p}(n)\right) = \left(\mathcal{I}_i\left(\mathbf{p}(n)\right)\right) \tag{3.4}$$

or equivalently as a function of initial value $\mathbf{p}(0)$ as

$$\mathbf{p}(n) = \left(\mathbf{M}^{-1}\mathbf{N}\right)^n \mathbf{p}(0) + \sum_{k=0}^{n-1} \left(\mathbf{M}^{-1}\mathbf{N}\right)^k \mathbf{M}^{-1}\boldsymbol{\eta} \tag{3.5}$$

From proposition 3.2, we can conclude that the above iteration converges if and only if the spectral radius of the iteration matrix $\mathbf{M}^{-1}\mathbf{N}$ fulfills $\rho\left(\mathbf{M}^{-1}\mathbf{N}\right) < 1$. If it converges, then

$$\lim_{n\to\infty} \mathbf{p}(n) = \left(\mathbf{I} - \mathbf{M}^{-1}\mathbf{N}\right)^{-1} \mathbf{M}^{-1}\boldsymbol{\eta} = \mathbf{A}^{-1}\boldsymbol{\eta} = \mathbf{p}^* \tag{3.6}$$

An interesting question is how fast the above iteration converges. We answer it, by following the steps taken in [84]. Consider the distance between the current power vector $\mathbf{p}(n)$ and the fixed point solution $\mathbf{p}^*$ given by $\|\mathbf{p}(n) - \mathbf{p}^*\|_2$ in which $\|\cdot\|_p$ denotes the p-norm (if $p = 2$, it is equivalent to the Euclidean norm). For simplicity let us for now on denote the iteration matrix $\mathbf{M}^{-1}\mathbf{N}$ by $\mathbf{Z}$ and the vector $\mathbf{M}^{-1}\boldsymbol{\eta}$ by $\boldsymbol{\zeta}$. Then,

$$\begin{aligned}
\|\boldsymbol{\mathcal{I}}(\mathbf{p}(n)) - \mathbf{p}^*\|_2 &= \left\| \mathbf{Z}^n\mathbf{p}(0) + \sum_{k=0}^{n-1} \mathbf{Z}^k\boldsymbol{\zeta} - \mathbf{p}^* \right\|_2 && (3.7)\\
&= \left\| \mathbf{Z}^n\mathbf{p}(0) + \sum_{k=0}^{n-1} \mathbf{Z}^k\boldsymbol{\zeta} - \mathbf{Z}^n\mathbf{p}^* - \sum_{k=0}^{n-1} \mathbf{Z}^k\boldsymbol{\zeta} \right\|_2 && (3.8)\\
&= \|\mathbf{Z}^n(\mathbf{p}(0) - \mathbf{p}^*)\|_2 && (3.9)\\
&\leq \|\mathbf{Z}^n\|_2 \, \|\mathbf{p}(0) - \mathbf{p}^*\|_2 && (3.10)
\end{aligned}$$

In (3.10) equality is possible for each n for some $\mathbf{p}(0)$. Thus, if $\mathbf{p}(0) \neq \mathbf{p}^*$, then $\|\mathbf{Z}^n\|_2$ gives us a sharp upper-bound estimate for the ratio $\|\mathbf{p}(n) - \mathbf{p}^*\|_2 \,/\, \|\mathbf{p}(0) - \mathbf{p}^*\|_2$ for n iterations. Since in practice $\|\mathbf{p}(0) - \mathbf{p}^*\|_2$ is unknown, then $\|\mathbf{Z}^n\|_2$ serves as a basis of comparison of different choices of $\mathbf{M}$ and $\mathbf{N}$.

Definition 3.2 (Definition 3.1 in [84]). Let $\mathbf{Z}_1$ and $\mathbf{Z}_2$ be two iteration matrixes. If, for some positive integer n, $\|\mathbf{Z}_1^n\|_2 < 1$, then

$$R(\mathbf{Z}_1^n) \stackrel{\text{def}}{=} -\ln\left\{(\|\mathbf{Z}_1^n\|_2)^{\frac{1}{n}}\right\}$$

is the *average rate of convergence for n iterations* of the matrix $\mathbf{Z}_1$. If $R(\mathbf{Z}_1) < R(\mathbf{Z}_2)$, then $\mathbf{Z}_2$ is *iteratively faster for m iterations* than $\mathbf{Z}_1$.

We remark that because of the norm inequalities, it may happen for a particular vector $\mathbf{p}(0)$ that $\|\mathbf{Z}_2^n(\mathbf{p}(0)-\mathbf{p}^*)\|_2 > \|\mathbf{Z}_1^n(\mathbf{p}(0)-\mathbf{p}^*)\|_2$, while $\|\mathbf{Z}_2^n\|_2 < \|\mathbf{Z}_1^n\|_2$. Nevertheless $\mathbf{Z}_2$ is *iteratively faster for n iterations* than $\mathbf{Z}_1$.

In terms of actual computations, the significance of the average rate of convergence is

$$\left(\frac{\|\mathbf{p}(n)-\mathbf{p}^*\|_2}{\|\mathbf{p}(0)-\mathbf{p}^*\|_2}\right)^{\frac{1}{n}} \leq e^{-R(\mathbf{Z}^n)} \tag{3.11}$$

Unfortunately, the quantity $R(\mathbf{Z}^n)$ is difficult to obtain by analytical means and therefore it is not suitable as a design criterion for power control algorithms. Instead of $R(\mathbf{Z}^n)$, we consider the limit as $n \to \infty$. Then, we have

Proposition 3.4 (Theorem 3.2 in [84]). *Let $\rho(\mathbf{Z}) < 1$, then*

$$\lim_{n\to\infty} R(\mathbf{Z}^n) = -\ln\rho(\mathbf{Z}) \stackrel{\text{def}}{=} R_\infty(\mathbf{Z})$$

The quantity $R_\infty(\mathbf{Z})$ is called *asymptotic average rate of convergence* and it depends only on the spectral radius of the iteration matrix. In consequence, the spectral radius can be used as a tool for choosing $\mathbf{M}$ and $\mathbf{N}$ matrixes. The smaller the spectral radius of the iteration matrix is, the larger is the asymptotic average rate of convergence.

To relate $R_\infty(\mathbf{Z})$ to the norm of the error $\|\mathbf{p}(n)-\mathbf{p}^*\|_2$ consider the following problem: estimate the number of iterations n required for reducing the error reduction factor below some $0 < \delta < 1$. That is, solve

$$\frac{\|\mathbf{p}(n)-\mathbf{p}^*\|_2}{\|\mathbf{p}(0)-\mathbf{p}^*\|_2} \leq \delta \tag{3.12}$$

with respect to n. According to Young [89] a crude estimate for small δ is given by

$$n(\delta) \gtrapprox \frac{-\ln\delta}{R_\infty(\mathbf{Z})} \tag{3.13}$$

which indicates that minimizing spectral radius decreases the number of iterations required to converge close enough to the fixed point solution.

In what follows, we repeat some results that are useful for designing and evaluating power control algorithms.

Definition 3.3 (Definition 3.5 in [84]). For $M \times M$ real matrixes $\mathbf{A}$, $\mathbf{M}$ and $\mathbf{N}$, $\mathbf{A} = \mathbf{M} - \mathbf{N}$ is a *regular splitting of the matrix* $\mathbf{A}$ if $\mathbf{M}$ is nonsingular with $\mathbf{M}^{-1} \geq \mathbf{0}$, and $\mathbf{N} \geq \mathbf{0}$.

Proposition 3.5 (Theorem 3.13 in [84]). *If* $\mathbf{A} = \mathbf{M} - \mathbf{N}$ *is a* regular splitting of the matrix $\mathbf{A}$ *and* $\mathbf{A}^{-1} \geq \mathbf{0}$, *then* $\rho\left(\mathbf{M}^{-1}\mathbf{N}\right) < 1$. *Thus the iteration matrix* $\mathbf{Z} = \mathbf{M}^{-1}\mathbf{N}$ *is convergent and the iteration (3.4) converges to* $\mathbf{p}^*$ *starting from any initial vector* $\mathbf{p}(0)$.

Proposition 3.6 (Theorem 3.15 in [84]). *Let* $\mathbf{A} = \mathbf{M}_1 - \mathbf{N}_1 = \mathbf{M}_2 - \mathbf{N}_2$ *be two regular splittings of* $\mathbf{A}$, *where* $\mathbf{A}^{-1} \geq \mathbf{0}$. *If* $\mathbf{N}_1 \geq \mathbf{N}_2 \geq \mathbf{0}$, *equality excluded, then*

$$1 > \rho\left(\mathbf{M}_1^{-1}\mathbf{N}_1\right) > \rho\left(\mathbf{M}_2^{-1}\mathbf{N}_2\right) > 0$$

So far we have been discussing about general iterative methods. It should be noted that there exists efficient methods for solving (3.2) that can not be written in the form of (3.4). However many of these methods, unlike the general iteration method, do not lend them selves to distributed operation. To motivate our choice of method, we show that the distributed power control algorithms DBA, DPC, and Foschini and Miljanic algorithm are special cases of the general iterative method. Although originally DBA and DPC were suggested for the noiseless case, we analyze these two algorithms in the case where the noise power is not neglected.

The distributed balancing algorithm can be written as

$$p_i(n+1) = \beta p_i(n)\left(1 + \frac{1}{\gamma_i(n)}\right) \tag{3.14}$$

where $\gamma_i(n)$ denotes the received CIR at iteration n defined as

$$\gamma_i(n) = \frac{g_{ii}p_i(n)}{\sum_{\substack{j=1 \\ j\neq i}}^{M} g_{ij}\theta_{ij}p_j(n) + \nu_i} \tag{3.15}$$

By noting that

$$\frac{p_i(n)}{\gamma_i(n)} = \sum_{\substack{j=1 \\ j\neq i}}^{M} f_{ij}p_j(n) + u_i \tag{3.16}$$

we can write (3.14) in the vector form as

$$\mathbf{p}(n+1) = \beta(\mathbf{I} + \mathbf{F})\mathbf{p}(n) + \beta\mathbf{u} \tag{3.17}$$

Proposition 3.7. *If* $\beta < \frac{1}{1+\rho(F)}$, *DBA converges to* $\mathbf{p}^* = \left(\mathbf{I} - \frac{\beta}{1-\beta}\mathbf{F}\right)^{-1}\frac{\beta}{1-\beta}\mathbf{u}$.

Proof. Let $\mathbf{Z}_{DBA} = \beta(\mathbf{I}+\mathbf{F})$ denote the iteration matrix of the distributed balancing algorithm, and let λ_i, $i = 1, \ldots, M$ denote the eigenvalues of $\mathbf{F}$. It follows that $\beta(1+\lambda_i)$ are the eigenvalues of $\mathbf{Z}_{DBA}$; consequently $\rho(\mathbf{Z}_{DBA}) = \beta\,(1+\rho(\mathbf{F}))$. Since the iterative method converges if and only if $\rho(\mathbf{Z}_{DBA}) < 1$ we require that $\beta < \frac{1}{1+\rho(F)}$. If it converges the fixed point fulfills

$$\begin{aligned} \mathbf{p}^* &= \beta\left((\mathbf{I}+\mathbf{F})\mathbf{p}^* + \mathbf{u}\right) && (3.18)\\ &= \frac{\beta}{1-\beta}(\mathbf{F}\mathbf{p}^* + \mathbf{u}) && (3.19)\\ &= \left(\mathbf{I} - \frac{\beta}{1-\beta}\mathbf{F}\right)^{-1}\frac{\beta}{1-\beta}\mathbf{u} && (3.20)\end{aligned}$$

This concludes the proof. □

From the fixed point solution we see that if we choose $\beta = \frac{\gamma^t}{1+\gamma^t}$ then DBA is capable of solving the uncostrained power control problem given that all the user have the same CIR-target and $\gamma^t\rho(\mathbf{F}) = \rho(\mathbf{H}) < 1$ i.e. if the system is feasible.

Foschini and Miljanic have suggested the following algorithm

$$p_i(n+1) = \left(1 - \omega_i + \omega_i\frac{\gamma_i^t}{\gamma_i(n)}\right)p_i(n), \quad 0 < \omega_i \leq 1 \tag{3.21}$$

Actually in the original form $\omega_i = \omega$ and $\gamma_i = \gamma$ for all i, but we shall consider this slightly generalized version and refer to it as the Foschini and Miljanic algorithm (FMA). Note that in the noisy case the DPC becomes equivalent to FMA with the choice $\omega_i = 1$, $\gamma_i^t = \beta$ for all i. For now on, we will refer to the FMA with $\omega_i = 1$ as DPC. The physical meaning of the ω_i-parameter is discussed in chapter 5.

Writing algorithm (3.21) into matrix form yields

$$\mathbf{p}(n+1) = (\mathbf{I}-\mathbf{\Omega})\mathbf{p}(n) + \mathbf{\Omega}(\mathbf{H}\mathbf{p}(n) + \boldsymbol{\eta}) \tag{3.22}$$

where $\mathbf{\Omega} = \operatorname{diag}\{\omega_i\}$. In [23], it was argued that among $\omega \in (0,1]$ the choice $\omega = 1$ is best in terms of convergence speed. However, mathematical proof was omitted. In what follows, we proof that rigorously.

Proposition 3.8. *FMA converges to* $\mathbf{p}^*$ *of a feasible system, starting from any non-negative vector* $\mathbf{p}(0)$. *Furthermore among* $\omega_i \in (0,1]$ *the choice* $\omega_i = 1$ *for all* i *achieves the best asymptotic average rate of convergence.*

Proof. We note that $\mathbf{M} = \mathbf{\Omega}^{-1}$ and $\mathbf{N} = \mathbf{\Omega}^{-1} - \mathbf{I} + \mathbf{H}$. Since $\omega_i \in (0,1]$, it follows that $\mathbf{0} \leq \mathbf{\Omega} \leq \mathbf{I}$, $\det(\mathbf{\Omega}) \neq 0$. Therefore $\mathbf{M}^{-1} = \mathbf{\Omega} \geq \mathbf{0}$, equality excluded, and $\mathbf{\Omega}^{-1} - \mathbf{I} + \mathbf{H} \geq \mathbf{0}$, equality excluded. Thus we can conclude that $\mathbf{M}$ and $\mathbf{N}$ form a regular splitting of $\mathbf{A}$ and by proposition 3.5 the iteration converges. □

Now let $\mathbf{\Omega} \leq \mathbf{I}$, equality excluded, and $\bar{\mathbf{\Omega}} = \mathbf{I}$ and let $\mathbf{Z}_{FMA}(\mathbf{\Omega})$ and $\mathbf{Z}_{FMA}(\bar{\mathbf{\Omega}})$ denote the corresponding iteration matrixes. Clearly, $\mathbf{N}_1 = \mathbf{\Omega}^{-1} - \mathbf{I} + \mathbf{H} \geq \bar{\mathbf{\Omega}} - \mathbf{I} + \mathbf{H} =$

$\mathbf{N}_2$. Therefore by proposition 3.6, $\rho\left(\mathbf{Z}_{FMA}(\mathbf{\Omega})\right) > \rho\left(\mathbf{Z}_{FMA}(\bar{\mathbf{\Omega}})\right) = \rho(\mathbf{H})$ and we can conclude that the choice $\mathbf{\Omega} = \mathbf{I}$ is best in terms of asymptotic average rate of convergence. □

Remark 3.1. The Foschini and Miljanic algorithm (FMA) is equivalent to Jacobi over-relaxation (JOR) iterative method (see e.g. [89]).

The above remark is to show the close resemblance between the power control algorithms and numerical methods of linear algebra.

Let us compare the DBA and FMA in terms of convergence speed. To be able to do so, we choose $\omega_i = \omega$ and $\gamma_i^t = \gamma^t$ for all i and assume that the system is feasible i.e. $\gamma^t\rho(\mathbf{F}) < 1$. If we choose $\omega > \frac{1}{1+\gamma^t}$, then

$$\rho\left(\mathbf{Z}_{DBA}\right) = \frac{\gamma^t}{1+\gamma^t}(1+\rho(\mathbf{F})) > 1 - \omega + \omega\gamma^t\rho(\mathbf{F}) = \rho\left(\mathbf{Z}_{FMA}(\omega\mathbf{I})\right) \tag{3.23}$$

That is, FMA is iteratively faster than the DBA for certain choices of the free parameter ω.

3.2.2 Constrained power control

In this chapter, we consider a general power control algorithm of the following form

$$\mathbf{p}(n+1) = \max\left\{\mathbf{0}, \min\left\{\bar{\mathbf{p}}, \boldsymbol{\mathcal{I}}\left(\mathbf{p}(n)\right)\right\}\right\} \stackrel{\text{def}}{=} \boldsymbol{\mathcal{T}}\left(\mathbf{p}(n)\right) = \left(\mathcal{T}_i\left(\mathbf{p}(n)\right)\right) \tag{3.24}$$

in which the min and max operators work in row by row fashion.

Let us consider the feasible case. Although the fixed point solution $\mathbf{p}^*$ is within the range of (3.3), the general method given by (3.4) could still use power vectors that are outside the range during its convergence. This means that the dynamics of constrained power control algorithms can not in general be replaced by unconstrained dynamics even in the feasible case. Thus we need to investigate the convergence property of (3.24) separately.

Proposition 3.9. *The constrained general power control algorithm given by (3.24) converges to unique* $\mathbf{p}^*$ *of the feasible system starting from any initial power vector* $\mathbf{p}(0)$ *that is in the range of (3.3) if there exists a positive definite diagonal matrix* $\mathbf{W}$ *such that* $\|\mathbf{Z}\|_\infty^{\mathbf{W}} < 1$.

Proof. Consider the weighted maximum norm of the error $\mathbf{p}(n) - \mathbf{p}^*$. Let us choose $\mathbf{W}$ to be positive definite and diagonal matrix such that $\|\mathbf{Z}\|_\infty^{\mathbf{W}} < 1$. Then,

$$\begin{aligned} \|\boldsymbol{\mathcal{T}}\left(\mathbf{p}(n)\right) - \mathbf{p}^*\|_\infty^{\mathbf{W}} &\leq \|\boldsymbol{\mathcal{I}}\left(\mathbf{p}(n)\right) - \mathbf{p}^*\|_\infty^{\mathbf{W}} &(3.25)\\ &\leq \|\mathbf{Z}\|_\infty^{\mathbf{W}}\,\|\mathbf{p}(n) - \mathbf{p}^*\|_\infty^{\mathbf{W}} &(3.26)\end{aligned}$$

The first inequality follows from the fact that if $\mathbf{p}_1 \leq \mathbf{p}_2$, then $\|\mathbf{p}_1\|_\infty^{\mathbf{W}} \leq \|\mathbf{p}_2\|_\infty^{\mathbf{W}}$. Thus, we can conclude that the mapping $\boldsymbol{\mathcal{T}}$ is a pseudo-contraction mapping. Thus it follows, by proposition 1.2 in [16], that it is convergent and its fixed point is unique. □

Remark 3.2. The asymptotic average rate of convergence $R_\infty(\mathbf{Z})$ can be used as convergence speed measure for the general constrained power control.

Since the mapping $\boldsymbol{\mathcal{T}}(\mathbf{p})$ is pseudo-contracting, it follows that there exists $n_0 > 0$ such that $\boldsymbol{\mathcal{T}}(\mathbf{p}(n)) < \bar{\mathbf{p}}$, for all $n > n_0$. Thus for $n > n_0$, the $\boldsymbol{\mathcal{T}}(\mathbf{p}(n)) = \boldsymbol{\mathcal{I}}(\mathbf{p}(n))$ i.e. the power control dynamics can be described by equation (3.4) for which the asymptotic average rate of convergence applies.

As an example, we consider the distributed constrained power control algorithm DCPC in which $\boldsymbol{\mathcal{I}}(\mathbf{p}(n)) = \mathbf{H}\mathbf{p}(n) + \boldsymbol{\eta}$. The mapping $\boldsymbol{\mathcal{I}}$ is equivalent to the mapping used in FMA in the special case in which $\boldsymbol{\Omega} = \mathbf{I}$ i.e the mapping used in DPC. Therefore the DCPC can be interpreted as a constrained version of the Foschini and Miljanic algorithm. Although, the convergence of DCPC has been proven both in synchronous and asynchronous cases in [31], we present here an alternative convergence proof for the synchronous case. This is to illustrate the methodology described above.

Lemma 3.2. *If the system is feasible, there exits a positive definite diagonal weight matrix* $\mathbf{W}$ *such that* $\|\mathbf{H}\|_\infty^{\mathbf{W}} = \rho(\mathbf{H}) < 1$.

Proof. The Perron-Frobenius theorem (proposition 3.1), guarantees that there exits an eigenvector $\mathbf{e} = (e_i)$ corresponding to the largest positive eigenvalue of $\mathbf{H}$ that can be taken to be positive i.e.

$$\mathbf{H}\mathbf{e} = \rho(\mathbf{H})\mathbf{e} > \mathbf{0} \tag{3.27}$$

By choosing $\mathbf{W} = \operatorname{diag}\left\{\frac{1}{e_i}\right\}$ (that clearly is positive definite, since $\mathbf{e}$ is positive), we get

$$\|\mathbf{H}\|_\infty^{\mathbf{W}} = \left\|\mathbf{W}\mathbf{H}\mathbf{W}^{-1}\right\|_\infty = \max_i \left|\frac{1}{e_i}\sum_{j=1}^{M} h_{ij}e_j\right| = \rho(\mathbf{H}) \tag{3.28}$$

Therefore, by constructing such a weight $\mathbf{W}$, we have shown its existence. □

Proposition 3.10. *DCPC converges to* $\mathbf{p}^*$ *of a feasible system starting from any initial power vector* $\mathbf{p}(0)$ *that is in the range of (3.3).*

Proof. By lemma 3.2, we can choose a positive definite diagonal matrix $\mathbf{W}$ such that $\|\mathbf{Z}\|_\infty^{\mathbf{W}} = \|\mathbf{H}\|_\infty^{\mathbf{W}} < 1$. Therefore by proposition 3.9, DCPC converges to $\mathbf{p}^*$. □

Alternative framework has been suggested by Yates [90]:

Definition 3.4. A power control mapping is called *standard interference function* if the following properties are satisfied for all $\mathbf{p} \geq \mathbf{0}$:

1. *Positivity* $\boldsymbol{\mathcal{T}}(\mathbf{p}) \geq \mathbf{0}$
2. *Monotonicity* $\mathbf{p}_1 \leq \mathbf{p}_2$, then $\boldsymbol{\mathcal{T}}(\mathbf{p}_1) \leq \boldsymbol{\mathcal{T}}(\mathbf{p}_2)$
3. *Scalability* $\alpha\boldsymbol{\mathcal{T}}(\mathbf{p}) > \boldsymbol{\mathcal{T}}(\alpha\mathbf{p}) \quad \forall\alpha > 1,\ \alpha \in \mathbb{R}$

A power control algorithm for which $\boldsymbol{\mathcal{T}}(\mathbf{p})$ is standard interference function is called *standard power control algorithm.*

Proposition 3.11 (Theorem 2 in [90]). *If the power control problem is feasible, then for any initial power* $\mathbf{p}(0)$*, the standard power control algorithm converges to a unique fixed point* p^**.*

The framework based on linear algebra and pseudo-contraction mapping is capable of handling algorithms that violate the monotonicity requirement of Yates' framework. On the other hand, Yates' framework is more suitable for some log-linear power control algorithms like the I-controller in dB-scale given by

$$p_i(n+1) = \left(\frac{\gamma_i^t}{\gamma_i(n)}\right)^{\frac{1}{T_{I_i}}} p_i(n), \quad T_i \geq 1 \tag{3.29}$$

where T_{I_i} denotes the integration time. The above algorithm can not be written in the stationary iteration form (3.4), but it can be shown to be standard power control method [17]. To relate these two frameworks described above, we claim that

Proposition 3.12. *A constrained power control algorithm (3.24) is standard if* $\mathbf{M}$ *and* $\mathbf{N}$ *form a regular splitting of* $\mathbf{A}$*.*

Proof. Consider first the unconstrained general iteration given by equation (3.4). By definition of regular splitting (definition 3.3) $\mathbf{Z} = \mathbf{M}^{-1}\mathbf{N} \geq \mathbf{0}$, equality excluded, and $\boldsymbol{\zeta} = \mathbf{M}^{-1}\boldsymbol{\eta} > \mathbf{0}$. Thus it follows that $\boldsymbol{\mathcal{I}}(\mathbf{p}) = \mathbf{Z}\mathbf{p}+\boldsymbol{\zeta}$ fulfills positivity and monotonicity properties. In addition,

$$\begin{aligned} \alpha\boldsymbol{\mathcal{I}}(\mathbf{p}) &= \alpha(\mathbf{Z}\mathbf{p} + \boldsymbol{\zeta}) && (3.30)\\ &= \boldsymbol{\mathcal{I}}(\alpha\mathbf{p}) + (\alpha - 1)\boldsymbol{\zeta} && (3.31)\\ &> \boldsymbol{\mathcal{I}}(\alpha\mathbf{p}) && (3.32) \end{aligned}$$

Thus, $\boldsymbol{\mathcal{I}}(\mathbf{p})$ fulfills scalability condition. Therefore, we can conclude that $\boldsymbol{\mathcal{I}}(\mathbf{p})$ is a standard interference function.

Clearly, the positivity and monotonicity conditions are not violated by adding the maximum power constraint, so we only need to investigate the scalability condition:

$$\begin{aligned} \alpha\boldsymbol{\mathcal{T}}(\mathbf{p}) &= \alpha \min\{\bar{\mathbf{p}}, \boldsymbol{\mathcal{I}}(\mathbf{p})\} && (3.33)\\ &= \min\{\alpha\bar{\mathbf{p}}, \alpha\boldsymbol{\mathcal{I}}(\mathbf{p})\} && (3.34)\\ &> \min\{\bar{\mathbf{p}}, \boldsymbol{\mathcal{I}}(\alpha\mathbf{p})\} = \boldsymbol{\mathcal{T}}(\alpha\mathbf{p}) && (3.35) \end{aligned}$$

The inequality follows from scalability of $\boldsymbol{\mathcal{I}}(\mathbf{p})$. Thus, we can conclude that $\boldsymbol{\mathcal{T}}(\mathbf{p})$ is standard interference function and that the general constrained iteration is standard power control algorithm given that $\mathbf{M}$ and $\mathbf{N}$ form a regular splitting of $\mathbf{A}$. □

3.2.3 Asynchronous algorithms

So far we have been considering synchronous power control methods. The purpose of this section is to expand our framework to the asynchronous cases as well. At iteration n let an integer $\tau_{ij}(n)$ denote the most recent iteration for which p_j is known to user i. Causality requires that $0 \leq \tau_{ij} \leq n$. If user i updates its power at iteration n, the update is based on power vector

$$\mathbf{p}(\boldsymbol{\tau}_i(n)) = (p_j(\tau_{ij}(n))) \tag{3.36}$$

Let $\mathcal{U}_i$ be the set of iteration indexes at which user i updates its power. We assume that the sets $\mathcal{U}_i$ are infinitely long and for any integer n_0 there exits another integer n_1 such that $\tau_{ij}(n) \geq n_0$ for all $n \geq n_1$. Using the notation described here, we can write the asynchronous general power control method as follows:

$$p_i(n+1) = \begin{cases} \mathcal{T}_i(\mathbf{p}(\boldsymbol{\tau}_i(n))) & , n \in \mathcal{U}_i(n) \\ p_i(n) & , n \notin \mathcal{U}_i(n) \end{cases} \tag{3.37}$$

In order to prove the convergence we collect the following result form [16] that hold for arbitrary mapping $\boldsymbol{\mathcal{T}}$.

Proposition 3.13 (Asynchronous convergence theorem). *If there is a sequence of nonempty sets $\{\mathcal{X}(n)\}$ with $\mathcal{X}(n+1) \subset \mathcal{X}(n)$ for all n satisfying the following two conditions:*

1) Synchronous convergence condition: For all n and $\mathbf{p} \in \mathcal{X}(n)$, $\boldsymbol{\mathcal{T}}(\mathbf{p}) \in \mathcal{X}(n+1)$. If $\{\mathbf{y}(n)\}$ is a sequence such that $\mathbf{y}(n) \in \mathcal{X}(n)$ for all n, then every limit point of $\{\mathbf{y}(n)\}$ is a fixed point of $\boldsymbol{\mathcal{T}}$.

2) Box Condition: For every n, there exits sets $\mathcal{X}_i(n) \subset \mathcal{X}_i(0)$ such that $\mathcal{X}(n) = \mathcal{X}_1(n) \times \mathcal{X}_2(n) \times \ldots \times \mathcal{X}_N(n)$.

and $\mathbf{p}(0) \in \mathcal{X}(0)$, then every limit point of $\{\mathbf{p}(n)\}$ is a fixed point of $\boldsymbol{\mathcal{T}}$.

Thus to prove the convergence we need to find the sets $\mathcal{X}(n)$ that fulfill the above proposition.

Proposition 3.14. *The power control method given by (3.37) converges to unique* $\mathbf{p}^*$ *of a feasible system starting from any initial power vector* $\mathbf{p}(0)$ *that is in the range of (3.3) if there exists a positive definite diagonal matrix* $\mathbf{W}$ *such that* $\|\mathbf{Z}\|_\infty^{\mathbf{W}} < 1$.

Proof. By proposition 3.9, $\boldsymbol{\mathcal{T}}$ is a pseudo-contraction mapping having an unique fixed point if $\|\mathbf{Z}\|_\infty^{\mathbf{W}} < 1$. Given an initial power $\mathbf{p}(0)$, we choose

$$\mathcal{X}(n) = \left\{ \mathbf{p} \in \mathbb{R} : \|\mathbf{p} - \mathbf{p}^*\|_\infty^{\mathbf{W}} \leq \left(\|\mathbf{Z}\|_\infty^{\mathbf{W}} \right)^n \|\mathbf{p}(0) - \mathbf{p}^*\|_\infty^{\mathbf{W}} \right\} \tag{3.38}$$

It is straightforward to see that $\boldsymbol{\mathcal{T}}$ and $\mathcal{X}(n)$ fulfill the synchronous convergence condition. Since $\mathcal{X}(n)$ can be interpreted as a sphere in $\mathbb{R}^N$ with respect to the weighted maximum norm, it follows that the box condition holds. That is, if $\mathbf{p}_1 \in \mathcal{X}(n)$ and $\mathbf{p}_2 \in \mathcal{X}(n)$, we can replace any component of $\mathbf{p}_1$ with the corresponding component of $\mathbf{p}_2$ and obtain an element of $\mathcal{X}(n)$. Thus, we conclude that if the mapping $\boldsymbol{\mathcal{T}}$ is pseudo-contracting, i.e. if there exists a positive definite diagonal weight matrix $\mathbf{W}$ such that $\|\mathbf{Z}\|_\infty^{\mathbf{W}} < 1$, then the general asynchronous power control method converges. □

By propositions 3.9 and 3.14, proving the convergence of both synchronous and asynchronous general power control algorithms, given by (3.4) and (3.37) respectively, boils down to finding a diagonal weight matrix $\mathbf{W}$ such that $\|\mathbf{Z}\|_\infty^{\mathbf{W}} < 1$. According to remark 3.2 an increase in the convergence speed of the power control algorithm can be established by minimizing the spectral radius of the iteration matrix $\mathbf{Z}$. This in mind, the next two chapters investigate how the $\mathbf{Z}$ could be chosen to increase the convergence speed while guaranteeing convergence.

3.3 Combined rate selection and power control problem

For combined rate selection and power control problem, we consider the problem formulation suggested by Kim, Rosberg and Zander [46].

For any given physical layer technique, let $r_{i1} < r_{i2} < \ldots < r_{iK}$ be the rates that mobile i can utilize. For the sake of readability, we assume that all mobiles have the same set of feasible data rates. The extension to user-dependent rates is trivial. To properly receive messages transmitted at rate r_{ik}, mobile i is expected to attain an $\gamma_i(n)$ value of at least γ_{ik}^t. Here, the target γ_{ik}^t is a pre-determined CIR value that matches rate r_{ik}.

Let $\mathbf{Y} = [y_{ik}]$ be a 0-1 matrix such that, for every mobile i and rate r_{ik},

$$y_{ik} = \begin{cases} 1, & \text{if mobile } \ i \ \text{ is transmitting with rate } \ r_{ik}, \\ \\ 0, & \text{otherwise.} \end{cases} \tag{3.39}$$

Further, let m_{ik} be an arbitrarily large number satisfying

$$m_{ik} \geq \max_{\mathbf{p}} \ \gamma_{ik}^t \left(\sum_{j=1}^{M} f_{ij} p_j + u_i \right). \tag{3.40}$$

The value m_{ik} can be interpreted as the amount of transmission power that mobile i needs to attain γ_{ik}^t, regardless of the interference power. Then, the combined rate and power control is formulated as the following optimization problem:

$$W \stackrel{\text{def}}{=} \max_{\mathbf{Y},\mathbf{p}} \ \sum_{i=1}^{M} \sum_{k=1}^{K} \ w_{ik} \ y_{ik}, \tag{3.41}$$

subject to the constraints that for every i and k,

$$\begin{gathered} y_{ik} \in \{0, 1\}, \\ \\ \textstyle\sum_{k=1}^{K} \ y_{ik} \leq 1, \end{gathered} \tag{3.42}$$

$$p_i + (1 - y_{ik}) m_{ik} \geq \gamma_{ik} \left(\textstyle\sum_{j=1}^{M} f_{ij} p_j + u_i \right) \tag{3.43}$$

$$0 \leq p_i \leq \overline{p}_i, \tag{3.44}$$

To associate rewards to realized transmission rates, in the objective function (3.41), we assume that so long as mobile i is properly transmitting messages at rate r_{ik}, the system accrues a unit reward with rate w_{ik}. Choosing $w_{ik} = r_{ik}$, aims at the maximization of the instant system throughput, i.e., the sum of effective data rates of all users at the given instant. It may be important to support as many mobiles as possible at least with the minimal rate of r_{i1}. To account for this case, we may set $w_{ik} = R + r_{ik}$, where R is a fixed reward rate for any mobile and is independent of its actual transmission rate, so long as it is positive.

Observe that the controlled powers are not incorporated into the objective function; their sole role is to facilitate proper demodulation under a selected set of rates. This is mathematically expressed in constraint (3.43). For each i and k, if $y_{ik} = 1$, the constraint (3.43) is reduced to the SIR requirement on mobile i for rate r_{ik}. Setting m_{ik} as in (3.40) neutralizes the constraint (3.43) for non-selected rates with $y_{ik} = 0$. Even if we have not considered the powers in the objective function, the amount of data that can be reliably sent using a certain energy allocation may be critical.

The optimization model above has no special structure and belongs to the general *mixed integer linear programming problem* that is known to be *NP-Complete*. Therefore, it calls for heuristic algorithms to get near-optimal values for $\mathbf{Y}$ and $\mathbf{p}$ in *polynomial* time.

We will postpone the description of combined transmission rate selection and power control algorithms to chapter 8.

Chapter 4

Second-order power control

In this chapter, we suggest a new power control algorithm that utilizes the transmitter power levels of both current and previous iterations for power updates. The algorithm is based on the successive overrelaxation (SOR) method for solving large linear equation systems. We start this chapter by describing the unconstrained version of the second-order power control algorithm. Then we expand our analysis to the constrained case. Finally we show numerical results and briefly discuss about implementation aspects. Our analysis assumes that the system is feasible in the sense that we can support every active user by an optimal power control. When the system becomes infeasible because of high traffic load, it calls for other actions such as *transmitter removal*, which is beyond the scope of the present chapter.

4.1 Unconstrained case

Let us consider the general iterative method (3.4) with the matrixes $\mathbf{M}$ and $\mathbf{N}$ defined by

$$\mathbf{M}(\omega) = \frac{1}{\omega}(\mathbf{I} - \omega\mathbf{L}), \quad \mathbf{N}(\omega) = \frac{1}{\omega}((1-\omega)\mathbf{I} + \omega\mathbf{U}), \tag{4.1}$$

where ω is a given number, and $\mathbf{L}$ and $\mathbf{U}$ are strictly lower and upper triangular parts of $\mathbf{H}$ respectively. The iterative method with such matrixes is known as the *successive overrelaxation iterative method* (SOR) and the number ω is called the *relaxation factor* [84, 89].

With SOR, appropriately choosing ω, we can solve the power control problem faster than JOR (Foschini and Miljanic algorithm). However, applying SOR directly to the power control problem (3.2) does not lend itself to a fully distributed power control algorithm. The reason is that it will result in a "*round-robin*" power update, which may require a *center* for scheduling. Furthermore, one iteration of the round-robin update would take as long as it takes for DPC to make M iterations, and thus its performance is expected to be poor. To cope with these drawbacks, we now define the *mirror vectors* $\mathbf{p}_{a1}$ and $\mathbf{p}_{a2}$ of the original power vector $\mathbf{p}$, and consider the following

augmented power control problem:

$$\mathbf{A}_a \mathbf{p}_a = \boldsymbol{\eta}_a \tag{4.2}$$

where

$$\mathbf{A}_a = \begin{bmatrix} \mathbf{I} & -\mathbf{H} \\ -\mathbf{H} & \mathbf{I} \end{bmatrix} \tag{4.3}$$

$$\mathbf{p}_a = \left(\mathbf{p}'_{a1}, \mathbf{p}'_{a2}\right)', \tag{4.4}$$

and

$$\boldsymbol{\eta}_a = \left(\boldsymbol{\eta}', \boldsymbol{\eta}'\right)' \tag{4.5}$$

The unique solution of the augmented problem is $\mathbf{p}_{a1} = \mathbf{p}_{a2} = \mathbf{p}^*$. Let us define $\mathbf{H}_a = \mathbf{I} - \mathbf{A}_a$ and apply SOR to the augmented problem. That is, instead of $\mathbf{H}$, we use $\mathbf{H}_a$ for constructing $\mathbf{L}$ and $\mathbf{U}$. That is, $\mathbf{L} = \begin{bmatrix} \mathbf{0} & \mathbf{0} \\ \mathbf{H} & \mathbf{0} \end{bmatrix}$ and $\mathbf{U} = \begin{bmatrix} \mathbf{0} & \mathbf{H} \\ \mathbf{0} & \mathbf{0} \end{bmatrix}$. From (3.4) and (4.1), we then have the following iterative matrix equation:

$$\begin{bmatrix} \mathbf{p}_{a1}(n+1) \\ \mathbf{p}_{a2}(n+1) \end{bmatrix} = \omega \begin{bmatrix} \mathbf{I} & \mathbf{0} \\ -\omega\mathbf{H} & \mathbf{I} \end{bmatrix}^{-1} \left(\frac{1}{\omega} \begin{bmatrix} (1-\omega)\mathbf{I} & \omega\mathbf{H} \\ \mathbf{0} & (1-\omega)\mathbf{I} \end{bmatrix} \begin{bmatrix} \mathbf{p}_{a1}(n) \\ \mathbf{p}_{a2}(n) \end{bmatrix} + \begin{bmatrix} \boldsymbol{\eta} \\ \boldsymbol{\eta} \end{bmatrix} \right) \tag{4.6}$$

$$= \begin{bmatrix} (1-\omega)\mathbf{I} & \omega\mathbf{H} \\ \omega(1-\omega)\mathbf{H} & \omega^2\mathbf{H}^2 + (1-\omega)\mathbf{I} \end{bmatrix} \begin{bmatrix} \mathbf{p}_{a1}(n) \\ \mathbf{p}_{a2}(n) \end{bmatrix} + \begin{bmatrix} \omega\boldsymbol{\eta} \\ \omega(\omega\mathbf{H} + \mathbf{I})\boldsymbol{\eta} \end{bmatrix} \tag{4.7}$$

$$= \begin{bmatrix} (1-\omega)\mathbf{p}_{a1}(n) + \omega\mathbf{H}\mathbf{p}_{a2}(n) + \omega\boldsymbol{\eta} \\ \omega\mathbf{H}((1-\omega)\mathbf{p}_{a1}(n) + \omega\mathbf{H}\mathbf{p}_{a2}(n) + \omega\boldsymbol{\eta}) + (1-\omega)\mathbf{p}_{a2}(n) + \omega\boldsymbol{\eta} \end{bmatrix} \tag{4.8}$$

$$= \begin{bmatrix} \omega(\mathbf{H}\mathbf{p}_{a2}(n) + \boldsymbol{\eta} - \mathbf{p}_{a1}(n)) + \mathbf{p}_{a1}(n) \\ \omega(\mathbf{H}\mathbf{p}_{a1}(n+1) + \boldsymbol{\eta} - \mathbf{p}_{a2}(n)) + \mathbf{p}_{a2}(n) \end{bmatrix} \tag{4.9}$$

The iterative method (4.9) is interpreted in the following manner. As both sequences of vectors $\{\mathbf{p}_{a1}(n)\}$ and $\{\mathbf{p}_{a2}(n)\}$ converge to $\mathbf{p}^*$ for an appropriately chosen ω, we define a new sequence of vectors $\{\mathbf{p}(n)\}$ by means of

$$\mathbf{p}(2l) = \mathbf{p}_{a1}(l), \quad \mathbf{p}(2l+1) = \mathbf{p}_{a2}(l), \ l = 0, 1, \ldots \tag{4.10}$$

In terms of the vector $\mathbf{p}(n)$, we can rewrite (4.9) in the simpler form

$$\mathbf{p}(n+1) = \omega(\mathbf{H}\mathbf{p}(n) + \boldsymbol{\eta} - \mathbf{p}(n-1)) + \mathbf{p}(n-1), \ n = 1, 2, \ldots \tag{4.11}$$

where $\mathbf{p}(0) = \mathbf{p}_{a1}(0)$ and $\mathbf{p}(1) = \mathbf{p}_{a2}(0)$ (see also figure 4.1). Similar to FMA in (3.21), for each mobile i, the above iterative method can be written as

$$p_i(n+1) = \omega \frac{\gamma_i^t}{\gamma_i^{(n)}} p_i(n) + (1-\omega) p_i(n-1), \ n = 1, 2, \ldots \tag{4.12}$$

where $p_i(0)$ and $p_i(1)$ are arbitrary. Hereafter, we will call the algorithm (4.12) *unconstrained second-order power control* (USOPC). In particular when $\omega = 1$, USOPC is equivalent with the DPC.

l			n
0	$\mathbf{p}_{a1}(0)$	$\rightarrow \mathbf{p}(0)$	0
	$\mathbf{p}_{a2}(0)$	$\rightarrow \mathbf{p}(1)$	1
1	$\mathbf{p}_{a1}(1)$	$\rightarrow \mathbf{p}(2)$	2
	$\mathbf{p}_{a2}(1)$	$\rightarrow \mathbf{p}(3)$	3
$\vdots$	$\vdots$		$\vdots$

Figure 4.1: Representation of $\{\mathbf{p}_{a1}(l)\}$ and $\{\mathbf{p}_{a2}(l)\}$ by $\{\mathbf{p}(n)\}$.

To compare USOPC and DPC consider the following: The power update form (4.12) can be rewritten as $\frac{\gamma_i^t}{\gamma_i^{(n)}}p_i^{(n)} + (\omega^{(n)} - 1)(\frac{\gamma_i^t}{\gamma_i^{(n)}}p_i^{(n)} - p_i^{(n-1)})$. In calculating $p_i^{(n+1)}$, the algorithm first compares the result from DPC, $\frac{\gamma_i^t}{\gamma_i^{(n)}}p_i^{(n)}$ with the previous power value $p_i^{(n-1)}$. If $\frac{\gamma_i^t}{\gamma_i^{(n)}}p_i^{(n)} > p_i^{(n-1)}$, the algorithm tries to choose a power value $p_i^{(n+1)}$ such that $p_i^{(n+1)} > \frac{\gamma_i^t}{\gamma_i^{(n)}}p_i^{(n)}$. The gap between $p_i^{(n+1)}$ and $\frac{\gamma_i^t}{\gamma_i^{(n)}}p_i^{(n)}$ becomes smaller as either $\omega^{(n)} - 1$ or $\frac{\gamma_i^t}{\gamma_i^{(n)}}p_i^{(n)} - p_i^{(n-1)}$ is approaching zero. With the same reasoning, we can see that $p_i^{(n+1)} < \frac{\gamma_i^t}{\gamma_i^{(n)}}p_i^{(n)}$ if $\frac{\gamma_i^t}{\gamma_i^{(n)}}p_i^{(n)} < p_i^{(n-1)}$. When $\frac{\gamma_i^t}{\gamma_i^{(n)}}p_i^{(n)} = p_i^{(n-1)}$, it is easy to see $p_i^{(n+1)} = \frac{\gamma_i^t}{\gamma_i^{(n)}}p_i^{(n)}$ (same as DPC).

Let us denote the iteration matrix

$$\mathbf{M}^{-1}(\omega)\mathbf{N}(\omega) = \begin{bmatrix} \mathbf{I} & \mathbf{0} \\ -\omega\mathbf{H} & \mathbf{I} \end{bmatrix}^{-1} \begin{bmatrix} (1-\omega)\mathbf{I} & \omega\mathbf{H} \\ \mathbf{0} & (1-\omega)\mathbf{I} \end{bmatrix} \tag{4.13}$$

by $\mathbf{Z}_{SOPC}(\omega)$. When $\omega = 1$, we can see from (4.9) that $\mathbf{Z}_{SOPC}(\omega)$ corresponds to the DPC iteration matrix for the case in which two DPC power updates are performed at each iteration. Therefore $\rho(\mathbf{Z}_{SOPC}(1)) = \rho(\mathbf{H})^2$. The question is under what range of ω does USOPC converge to the $\mathbf{p}^*$ of a feasible system faster than DPC in terms of asymptotic average rate of convergence, i.e. $\rho(\mathbf{Z}_{SOPC}(\omega)) < \rho(\mathbf{Z}_{SOPC}(1)) = \rho(\mathbf{H})^2 < 1$. In order to answer, we start investigating the properties of $\rho(\mathbf{Z}_{SOPC}(\omega))$.

Proposition 4.1. *For all real* ω,

$$\rho(\mathbf{Z}_{SOPC}(\omega)) \geq |\omega - 1|$$

Proof. Since $\mathbf{H}_a$ is a square matrix with zero diagonal, the result follows directly from theorem 3.5 in [84]. □

Lemma 4.1. *All eigenvalues of* $\mathbf{H}$ *are also eigenvalues of* $\mathbf{H}_a$ *with multiplicity two.*

Proof. Let λ_i, $i = 1, \ldots, M$ denote the eigenvalues of $\mathbf{H}$. Since

$$\mathbf{H}_a^2 = \begin{bmatrix} \mathbf{H}^2 & \mathbf{0} \\ \mathbf{0} & \mathbf{H}^2 \end{bmatrix} \tag{4.14}$$

it follows that $\det(\lambda_i^2\mathbf{I} - \mathbf{H}_a^2) = \det^2(\lambda_i^2\mathbf{I} - \mathbf{H}^2) = \det^2(\lambda_i\mathbf{I} - \mathbf{H})\det^2(\lambda_i\mathbf{I} + \mathbf{H}) = 0$. Hence, λ_i is an eigenvalue of $\mathbf{H}_a$ with multiplicity two. □

The above lemma implies that if the system is feasible, $\rho(\mathbf{H}_a) < 1$ and it follows that $\mathbf{A}_a^{-1} \geq \mathbf{0}$, equality excluded. Thus we have

Proposition 4.2. *If the system is feasible and* $0 < \omega_1 < \omega_2 \leq 1$ *then* $\rho(\mathbf{Z}_{SOPC}(\omega_2)) < \rho(\mathbf{Z}_{SOPC}(\omega_1)) < 1$

Proof. By definition: $\mathbf{Z}_{SOPC}(\omega) = \mathbf{M}(\omega)^{-1}\mathbf{N}(\omega)$ where

$$\mathbf{M}(\omega) = \frac{1}{\omega}\begin{bmatrix} \mathbf{I} & \mathbf{0} \\ -\omega\mathbf{H} & \mathbf{I} \end{bmatrix} \tag{4.15}$$

and

$$\mathbf{N}(\omega) = \frac{1}{\omega}\begin{bmatrix} (1-\omega)\mathbf{I} & \omega\mathbf{H} \\ \mathbf{0} & (1-\omega)\mathbf{I} \end{bmatrix} \tag{4.16}$$

Clearly, $\mathbf{M}(\omega)^{-1} \geq \mathbf{0}$, equality excluded (see equations (4.6) and (4.1)) and $\mathbf{N}(\omega) \geq \mathbf{0}$, equality excluded, for $0 < \omega \leq 1$. Therefore $\mathbf{M}(\omega)$ and $\mathbf{N}(\omega)$ form a regular splitting of $\mathbf{A}_a$ and therefore by proposition 3.5, we have $\rho(\mathbf{Z}_{SOPC}(\omega)) < 1$ for $0 < \omega \leq 1$.

Now since $\omega_1 < \omega_2 \leq 1$ it follows that $\mathbf{N}(\omega_1) \geq \mathbf{N}(\omega_2)$, equality excluded. Thus by proposition 3.6, we have $\rho(\mathbf{Z}_{SOPC}(\omega_2)) < \rho(\mathbf{Z}_{SOPC}(\omega_1))$. This concludes the proof. □

Since we are interested in the optimum relaxation factor ω^* that minimizes $\rho(\mathbf{Z}_{SOPC}(\omega))$ and satisfies $\rho(\mathbf{Z}_{SOPC}(\omega^*)) < 1$, we have the following optimization problem from propositions 4.1 and 4.2:

$$\min_{\omega} \rho(\mathbf{Z}_{SOPC}(\omega)) = \min_{0<\omega<2} \rho(\mathbf{Z}_{SOPC}(\omega)) = \min_{1\leq\omega<2} \rho(\mathbf{Z}_{SOPC}(\omega)) \tag{4.17}$$

Proposition 4.3. *If the system is feasible, the optimal relaxation factor* ω^* *in USOPC is greater than one, and thus* $\min_\omega \rho(\mathbf{Z}_{SOPC}(\omega)) = \min_{1<\omega<2} \rho(\mathbf{Z}_{SOPC}(\omega))$

Proof. Let us denote the eigenvalue $\lambda = a + b \cdot i$ of $\mathbf{H}_a$ as a point (a, b) in the two dimensional space. Assume $E(x, y)$ denotes the smallest-volume ellipse that contains, in the closed interior, all the pairs (a, b) corresponding to the eigenvalues of $\mathbf{H}_a$. Such an ellipse is given by

$$E(x, y) = (\frac{x}{\bar{a}})^2 + (\frac{y}{\bar{b}})^2 = 1, \tag{4.18}$$

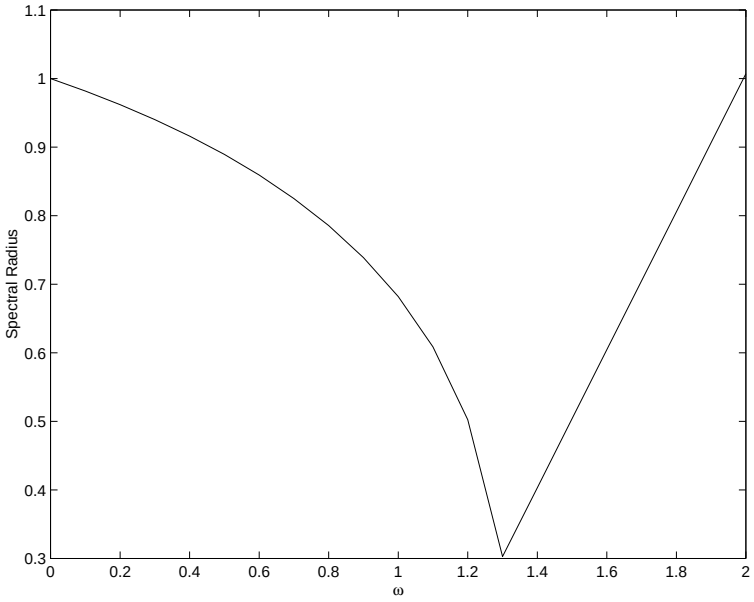

Figure 4.2: $\rho(\mathbf{Z}_{SOPC}(\omega))$ for one typical realization of $\mathbf{H}$.

where $\bar{a}$ and $\bar{b}$ are positive numbers. It is then derived in Chapter 6.4 of [89] for a class of problem matrixes (consistently ordered with nonvanishing diagonal elements and complex eigenvalues), in which our matrix $\mathbf{A}_a$ belongs, that the optimal relaxation factor ω^* is

$$\omega^* = \frac{2}{1 + \sqrt{1 + \bar{b}^2 - \bar{a}^2}} \tag{4.19}$$

Since $\mathbf{H}_a$ is not irreducible, proposition 3.1 does not apply. Fortunately by lemma 4.1, we have that the eigenvalues of $\mathbf{H}$ are also eigenvalues of $\mathbf{H}_a$ with multiplicity two. Thus $\bar{a} = \rho(\mathbf{H}_a) = \rho(\mathbf{H})$ and it follows that $\bar{b} < \bar{a} < \rho(\mathbf{H}_a) = \rho(\mathbf{H}) < 1$. By equation (4.19), $\omega^* > 1$. □

By proposition 3.2 and 4.1, we conclude that USOPC converges to $\mathbf{p}^*$ if ω belongs to the open interval $(0, 1)$. It will be asymptotically faster as ω approaches one, but still slower than DPC ($\rho(\mathbf{Z}_{SOPC}(\omega)) > \rho(\mathbf{Z}_{SOPC}(1))$). However, from proposition 4.3, by selecting optimal ω^* from $(1, 2)$, we can make USOPC asymptotically faster than DPC. We illustrate this property by plotting $\rho(\mathbf{Z}_{SOPC}(\omega))$ for one typical realization of $\mathbf{H}$ in figure 4.2.

Example 4.1. Consider a feasible system, where two mobiles use the same channel at the given instant. The link gain matrix is given by

$$\mathbf{G} = [g_{ij}] = \begin{bmatrix} 0.3288 & 0.0534 \\ 0.0602 & 0.3826 \end{bmatrix} \tag{4.20}$$

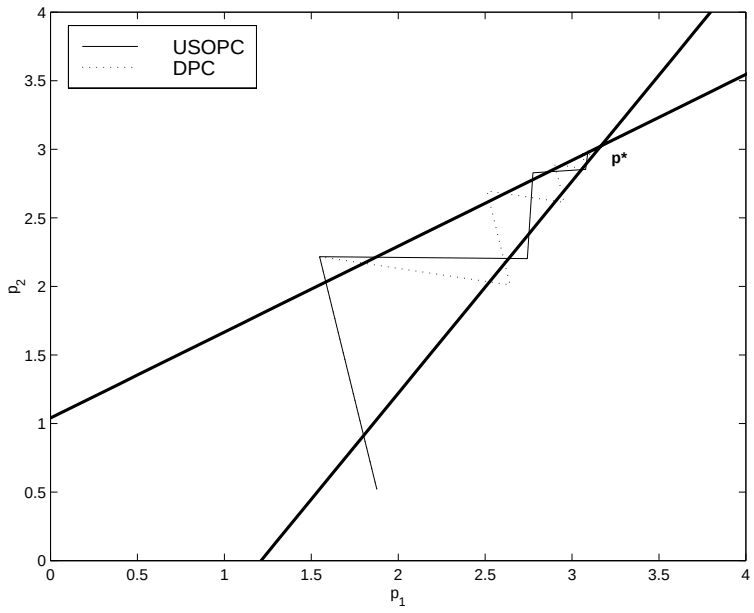

Figure 4.3: Traces of USOPC and DPC. The thick lines denote the CIR constraints.

The receiver noise level is 0.1 and the target CIR is 6 dB. We then have the normalized link gain matrix given by

$$\mathbf{H} = \begin{bmatrix} 0 & 0.6466 \\ 0.6264 & 0 \end{bmatrix} \tag{4.21}$$

The fixed point is known to be $\mathbf{p}^* = (3.1657, 3.0235)$.

We will now apply both USOPC and DPC to the problem to illustrate difference in convergence. It is easy to obtain $\rho(\mathbf{H}) = \rho(\mathbf{H}_a) = 0.6364$, and from (4.19), we have the optimal relaxation factor $\omega^* = 1.1291$ for USOPC ($\bar{a} = 0.6391$ and $\bar{b} = 0$). A randomly chosen initial power vector $\mathbf{p}(0) = (1.8772, 0.5211)'$ is used for both algorithms. In USOPC, the power vector $\mathbf{p}(1)$ is obtained by a one-step iteration of DPC on $\mathbf{p}(0)$. Figure 4.3 shows the traces of the two algorithms, where we can see that both algorithms converge to $\mathbf{p}^*$. Figure 4.4 shows the Euclidean distance between the current power vector and $\mathbf{p}^*$, normalized by $\|\mathbf{p}(0) - \mathbf{p}^*\|_2$. Figures indicate that

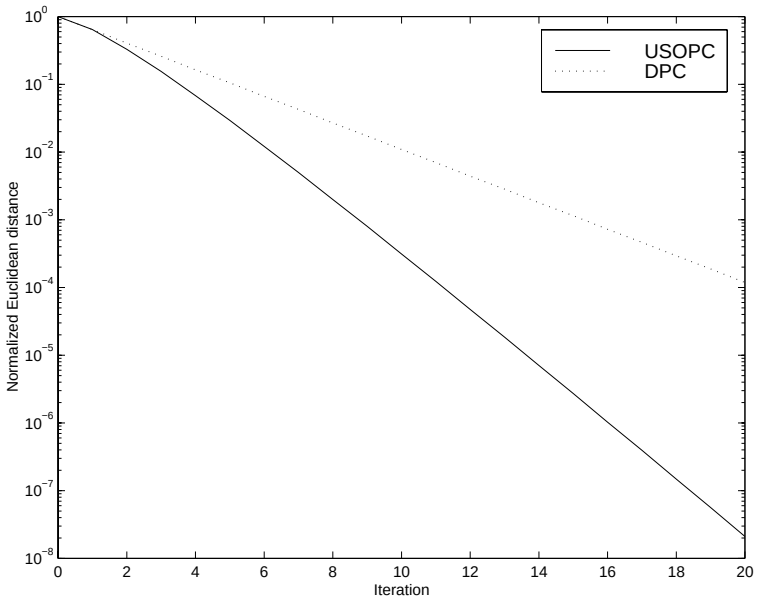

Figure 4.4: Normalized Euclidean distance between the current power vector and $\mathbf{p}^*$ as a function of iteration ($\|\mathbf{p}(n) - \mathbf{p}^*\|_2 \,/\, \|\mathbf{p}(0) - \mathbf{p}^*\|_2$).

USOPC converges faster. The speed difference becomes bigger as USOPC approaches $\mathbf{p}^*$.

Although USOPC is faster than DPC, it seems to be hopeless to apply USOPC to practical problems for two reasons. First, it is difficult to find ω^* since the matrix $\mathbf{H}$ (and thus $\mathbf{H}_a$) is not available in real situations. Second, we have not considered the transmission range described in (3.3). Even if USOPC converges to $\mathbf{p}^*$ of a feasible system, it can generate power vectors that are out of the range of (3.3) during power update. Furthermore, it is even possible that $p_i(n) < 0$ at certain iteration n. In the next section, we show how to cope with such difficulties.

Remark 4.1. We could construct fourth, sixth,... order power control algorithms in the similar manner to the above, but unfortunately they would have the same performance as the second order algorithm. The reason for this is that all even-order iteration matrixes have the same eigenvalues of different multiplicity. The odd-order power controls do not lend themselves into distributed algorithms.

4.2 Constrained case

As the relaxation factor, we now consider a non-stationary number $\omega^{(n)}$ that varies according to the iteration. For this, we suggest the use of a non-increasing sequence $\omega^{(n)}$ that satisfies $\omega^{(1)} > 1$, $\omega^{(1)} = \omega^{(2)} < \omega^{(3)} = \omega^{(4)} < \ldots < \omega^{(2n)} = \omega^{(2n+1)} < \ldots$, and $\lim_{n\to\infty} \omega^{(n)} = 1$. As a result, considering the constraint (3), we confine USOPC to the following version, called CSOPC:

$$p_i(n+1) = \min\left\{\bar{p}_i,\ \max\left\{0,\ \omega(n)\frac{\gamma_i^t}{\gamma_i(n)}p_i(n) + (1-\omega(n))p_i(n-1)\right\}\right\}, \quad n = 1, 2, \ldots \tag{4.22}$$

where the initial values $p_i(0)$ and $p_i(1)$ are arbitrarily chosen from the range of (3.3). In order to prove the convergence of (4.22) we need the following lemma:

Lemma 4.2. *If the system is feasible, there exists a positive definite diagonal matrix* W *and a number* $\hat{\omega} > 1$ *such that* $||\mathbf{Z}_{SOPC}(\omega)||_\infty^{\mathbf{W}} < 1$ *for* $1 < \omega < \hat{\omega}$.

Proof. Let $\mathbf{T}(\omega) = |\mathbf{Z}_{SOPC}(\omega)|$, where $|\cdot|$ is an elementwise absolute value operator. Since $\mathbf{T}(\omega)$ is an irreducible nonnegative matrix, the Perron-Frobenius theorem (proposition 3.1) guarantees that there exists a positive vector $\mathbf{e} = (e_i)$ such that $\mathbf{T}(\omega) = \rho(\mathbf{T}(\omega))\mathbf{e}$. Let us choose a matrix $\mathbf{W} = \mathrm{diag}\{1/e_i\}$. Clearly,

$$\|\mathbf{Z}_{SOPC}(\omega)\|_\infty^{\mathbf{W}} \le \||\mathbf{Z}_{SOPC}(\omega)|\|_\infty^{\mathbf{W}} = \|\mathbf{T}(\omega)\|_\infty^{\mathbf{W}} = \rho(\mathbf{T}(\omega)) \tag{4.23}$$

By Theorem 4-5.9 in [89], $\rho(\mathbf{T}(\omega)) < 1$ if $1 < \omega \le \frac{2}{1+\rho(H)^2}$. From the definition of the weighted matrix norm, it is clear that if we decrease the absolute value of any element in the matrix then the corresponding norm cannot increase and thus $\|\mathbf{T}(\omega)\|_\infty^{\mathbf{W}} < 1$ for $1 < \omega < \hat{\omega}$ must hold for $1 < \hat{\omega} < \frac{2}{1+\rho(H)^2}$. This concludes the proof. □

Proposition 4.4. *CSOPC converges to* $\mathbf{p}^*$ *of a feasible system starting from any initial vector pair* $\{\mathbf{p}(0), \mathbf{p}(1)\}$ *that are in the range of (3.3).*

Proof. Let us *sample* the sequence $\omega^{(n)}$ in (4.22) by taking every second element of it. Then the *sampled sequence* becomes a decreasing one. Now, we redefine $\omega^{(n)}$ to denote the elements of the sampled sequence so that the first element of the sampled sequence has index zero. With help of our sampled sequence, we can rewrite (4.9) as

$$\mathbf{p}_a(n+1) = \mathbf{Z}_{SOPC}(\omega(n))\mathbf{p}_a(n) + \boldsymbol{\zeta}(\omega(n)),\ n = 0, 1, \ldots \tag{4.24}$$

where $\boldsymbol{\zeta}(\omega(n)) = \omega(n)(\mathbf{I} - \omega(n)\mathbf{L})^{-1}\boldsymbol{\eta}_a$. Let us define

$$\boldsymbol{\mathcal{T}}_{SOPC}(\mathbf{p}_a(n), n) \stackrel{\text{def}}{=} \min\{\bar{\mathbf{p}},\ \max\{0, \mathbf{Z}_{SOPC}(\omega(n))\mathbf{p}_a(n) + \boldsymbol{\zeta}(\omega(n))\}\} \tag{4.25}$$

and $\mathbf{p}_a^* = ((\mathbf{p}^*)', (\mathbf{p}^*)')'$ be the solution to the problem (4.2). Then, it is clear that $\boldsymbol{\mathcal{T}}_{SOPC}(\mathbf{p}_a^*, n) = \mathbf{p}_a^*$ for all n. For a given positive definite diagonal matrix $\mathbf{W}$, we have, as in the (3.25),

$$\|\boldsymbol{\mathcal{T}}_{SOPC}(\mathbf{p}_a(n), n) - \mathbf{p}_a^*\|_\infty^{\mathbf{W}} \le \|\mathbf{Z}_{SOPC}(\omega(n))\|_\infty^{\mathbf{W}}\, \|\mathbf{p}(n) - \mathbf{p}^*\|_\infty^{\mathbf{W}} \tag{4.26}$$

Repeating the iteration (4.26), we get

$$\|\boldsymbol{\mathcal{T}}_{SOPC}(\mathbf{p}_a(n), n) - \mathbf{p}_a^*\|_\infty^{\mathbf{W}} \leq \left(\prod_{k=0}^{n} \|\mathbf{Z}_{SOPC}(\omega(k))\|_\infty^{\mathbf{W}} \right) \|\mathbf{p}(0) - \mathbf{p}^*\|_\infty^{\mathbf{W}} \tag{4.27}$$

By lemma 4.2, we can choose a positive definite diagonal matrix $\mathbf{W}$ and a number $\hat{\omega} > 1$ such that $\|\mathbf{Z}_{SOPC}(\omega)\|_\infty^{\mathbf{W}} < 1$ for $1 < \omega < \hat{\omega}$. Since $\omega(n)$ is a decreasing sequence and $\lim_{n\to\infty} \omega(n) = 1$, it is guaranteed that there exists a number n_0 such that $1 < \omega(n) < \hat{\omega}$ for all $n > n_0$. Therefore,

$$\lim_{n\to\infty} \prod_{k=0}^{n} \|\mathbf{Z}_{SOPC}(\omega(k))\|_\infty^{\mathbf{W}} = 0 \tag{4.28}$$

Thus the power vector $\mathbf{p}_a$ converges to $\mathbf{p}_a^*$. □

Remark 4.2. From inequality (4.27), we can see that if the initial value $\omega(0)$ of the sampled sequence is unnecessarily big then the number of iterations needed to decrease $\|\mathbf{Z}_{SOPC}(\omega(n))\|_\infty^{\mathbf{W}}$ below one is going to be large. By $\|\mathbf{Z}_{SOPC}(\omega(n))\|_\infty^{\mathbf{W}} \geq \rho(\mathbf{Z}_{SOPC}(\omega(n)))$ (theorem 2-3.4 in [89]) and $\rho(\mathbf{Z}_{SOPC}(\omega(n))) \geq |\omega(n) - 1|$ (proposition 4.1), it is clear that we do not gain anything by choosing $\omega(0) \geq 2$. Therefore, it is advisable to choose the initial value $\omega(0)$ from the open interval $(1, 2)$.

We would now like to compare CSOPC with DCPC in terms of convergence speed. In order to do so, we need the following lemma:

Lemma 4.3. *If the system is feasible, there exists a nonsingular matrix* $\mathbf{W}$ *and a number* $\hat{\omega} > 1$ *such that* $||\mathbf{Z}_{SOPC}(\omega)||_\infty^{\mathbf{W}} < ||\mathbf{Z}_{SOPC}(1)||_\infty^{\mathbf{W}} < 1$ *for* $1 < \omega < \hat{\omega}$.

Proof. By theorem 2-3.5 in [89], there exits a nonsingular matrix $\mathbf{W}$ and a number $\hat{\omega} > 1$ such that

$$\|\mathbf{Z}_{SOPC}(\hat{\omega})\|_\infty^{\mathbf{W}} \leq \rho(\mathbf{Z}_{SOPC}(\hat{\omega})) + \varepsilon \tag{4.29}$$

where $\varepsilon > 0$ can be made arbitrarily small. Kahan [43] has proved that $\rho(\mathbf{Z}_{SOPC}(\omega))$ is decreasing for $0 < \omega \leq \bar{\omega}$, $\bar{\omega} > 1$. So, if we choose $\hat{\omega} \leq \bar{\omega}$ and a sufficiently small ε, then

$$||\mathbf{Z}_{SOPC}(\hat{\omega})||_\infty^{\mathbf{W}} \leq \rho(\mathbf{Z}_{SOPC}(\hat{\omega})) + \varepsilon < \rho(\mathbf{Z}_{SOPC}(\omega)) \leq ||\mathbf{Z}_{SOPC}(\omega)||_\infty^{\mathbf{W}} \tag{4.30}$$

holds for for $1 \leq \omega < \hat{\omega}$. If we further choose $\hat{\omega}$ arbitrarily close to one, then the norm $\Delta = ||\mathbf{Z}_{SOPC}(1) - \mathbf{Z}_{SOPC}(\hat{\omega})||_\infty^{\mathbf{W}}$ can be made arbitrarily small. Thus for a small enough $\Delta > 0$ and $\varepsilon > 0$

$$||\mathbf{Z}_{SOPC}(1)||_\infty^{\mathbf{W}} \leq ||\mathbf{Z}_{SOPC}(\hat{\omega})||_\infty^{\mathbf{W}} + \Delta < 1 \tag{4.31}$$

holds. This concludes the proof. □

Proposition 4.5. *If the system is feasible, CSOPC is asymptotically faster than DCPC with respect to weighted maximum norm.*

Proof. By proposition 4.4, it is clear that CSOPC converges and thus there exists a number n_0 such that $\mathbf{0} < \boldsymbol{\mathcal{T}}_{SOPC}(\mathbf{p}_a(n), n) < \bar{\mathbf{p}}$ for all $n > n_0$. Therefore, for any nonsingular matrix $\mathbf{W}$, we have

$$||\boldsymbol{\mathcal{T}}_{SOPC}(\mathbf{p}_a(n), n) - \mathbf{p}_a^*||_\infty^{\mathbf{W}} \leq ||\mathbf{Z}_{SOPC}(\omega(n))||_\infty^{\mathbf{W}} ||\mathbf{p}_a(n) - \mathbf{p}_a^*||_\infty^{\mathbf{W}}, \text{ for all } n > n_0 \quad (4.32)$$

Repeating the above, we get

$$\frac{||\boldsymbol{\mathcal{T}}_{SOPC}(\mathbf{p}_a(n), n) - \mathbf{p}_a^*||_\infty^{\mathbf{W}}}{||\mathbf{p}_a(0) - \mathbf{p}_a^*||_\infty^{\mathbf{W}}} \leq C \prod_{k=n_0+1}^{n} ||\mathbf{Z}_{SOPC}(\omega(k))||_\infty^{\mathbf{W}}, \text{ for all } n > n_0 \quad (4.33)$$

where C is a positive constant. We name the right hand side of (4.33) as *error reduction rate*. Consider now the ratio of the error reduction rates of CSOPC and DCPC described by

$$\kappa(n) = C' \frac{\prod_{k=n_0+1}^{n} ||\mathbf{Z}_{SOPC}(\omega(k))||_\infty^{\mathbf{W}}}{(||\mathbf{Z}_{SOPC}(1)||_\infty^{\mathbf{W}})^{n-n_0}}, \text{ for all } n > n_0 \quad (4.34)$$

where C' is a positive constant. By lemma 4.3, we can choose a nonsingular matrix $\mathbf{W}$ and a number $\hat{\omega} > 1$ such that $||\mathbf{Z}_{SOPC}(\omega)||_\infty^{\mathbf{W}} < ||\mathbf{Z}_{SOPC}(1)||_\infty^{\mathbf{W}} < 1$ for $1 < \omega < \hat{\omega}$. Since $\omega(n)$ is a decreasing sequence and $\lim_{n\to\infty} \omega(n) = 1$, it is guaranteed that there exists a number $n_1 > n_0$ such that $1 < \omega(n) < \hat{\omega}$ for all $n > n_1$. Therefore, $\lim_{n\to\infty} \kappa(n) = 0$, and we can conclude that CSOPC converges asymptotically faster than DCPC with respect to weighted maximum norm. □

Remark 4.3. Like the asymptotic average rate of convergence defined in proposition 3.4, the error reduction rate in (4.33) can be used for estimating the minimum number of iterations, $n'(\delta)$ that gives

$$C \prod_{k=n_0+1}^{n'(\delta)} ||\mathbf{Z}_{SOPC}(\omega(k))||_\infty^{\mathbf{W}} = \delta \quad (4.35)$$

In the case of DPC, $n_0 = 0$ and $C = ||\mathbf{Z}_{SOPC}(1)||_\infty^{\mathbf{W}}$. Let us choose a positive definite diagonal matrix $\mathbf{W}$ such that the diagonal entries of $\mathbf{W}^{-1}$ are the components of the eigenvector of $\mathbf{Z}_{SOPC}(1)$ that corresponds to the dominant eigenvalue. Then, $||\mathbf{Z}_{SOPC}(1)||_\infty^{\mathbf{W}} = \rho(\mathbf{Z}_{SOPC}(1))$ and the equation (4.35) can be solved analytically. By noting that $\rho(\mathbf{Z}_{SOPC}(1)) = \rho(\mathbf{H})^2$ and $n'(\delta) = 2n(\delta)$, we get the same result as in (3.13).

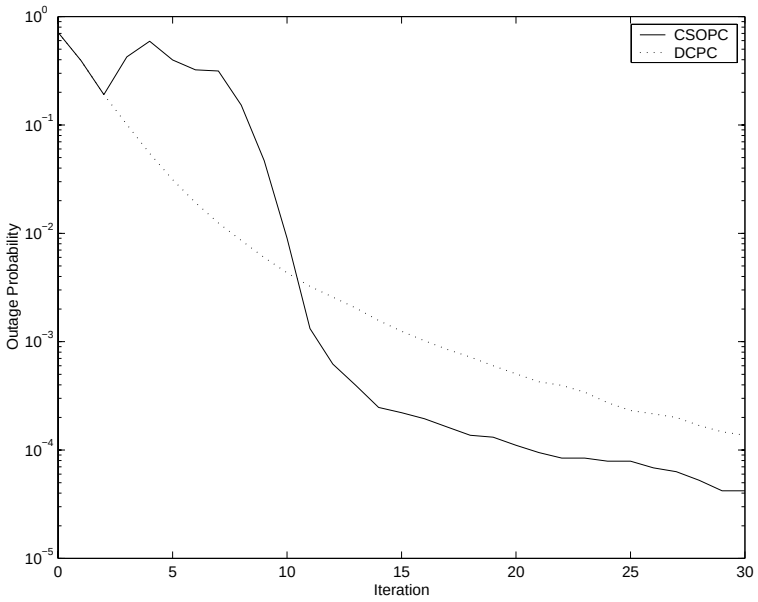

Figure 4.5: Outage probability as a function of iteration

4.3 Computational results

First, we investigate how quickly CSOPC converges to $\mathbf{p}^*$ of a feasible system. DCPC is used as a reference algorithm. An uplink of DS-CDMA system with 19 omni-bases located in the centers of 19 hexagonal cells is used as a test system (figure 2.1). The receiver noise power is taken to be 10^{-12}. The relative maximum mobile power is set to one. The *processing gain* is chosen to be 128 (21 dB) and the SIR-target is set to 8 dB (i.e. CIR target is -13 dB) . For a given instance, a total of 190 mobiles are generated, the locations of which are uniformly distributed over the 19 hexagonal cells.

The *outage probability* is used as a performance measure. To evaluate this, we have taken 1000 independent "feasible" instances of mobile locations and shadow fadings. In each instance, we have performed twenty power control steps. The initial power for each mobile is randomly chosen from the interval [0,1]. Similar to example 4.1 the power vector $\mathbf{p}(1)$ is obtained by a one-step iteration of DCPC on $\mathbf{p}(0)$. CSOPC uses a nonstationary relaxation factor given by

$$\omega(n) = \begin{cases} 1 + \left(\frac{2}{3}\right)^n, & n = 1, 3, \dots \\ 1 + \left(\frac{2}{3}\right)^{n-1} & n = 2, 4, \dots \end{cases} \tag{4.36}$$

The outage probability at each iteration is computed over 1000 instances by counting the portion of the number of non-supported mobiles at the iteration. Figure 4.5 shows the outage probability of each algorithm as a function of iteration. CSOPC takes 22 iterations on average to reach the state with the outage probability of 10^{-4} that we consider as almost the zero-outage. We can see that DCPC requires more than 30

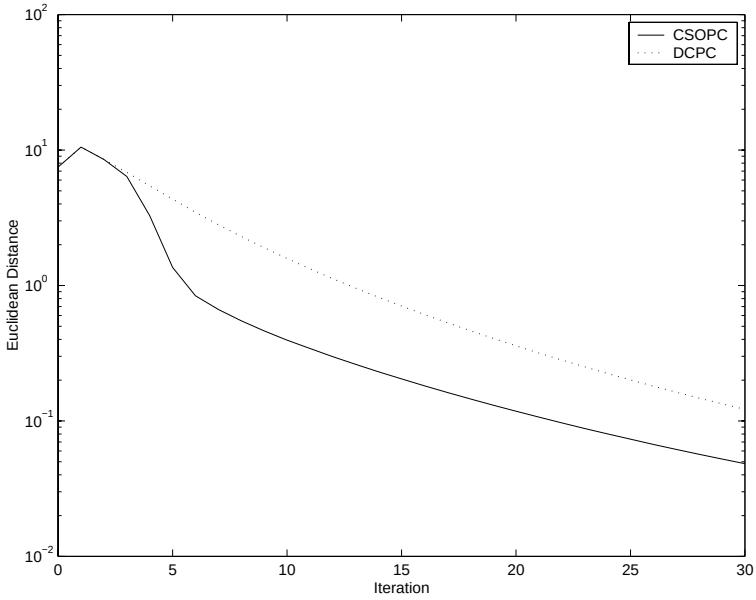

Figure 4.6: Euclidean distance between the current power and $\mathbf{p}^*$ as a function of iteration

iterations on average to reach the point. In the case of CSOPC, the small increase in the outage level in the beginning is caused by the dynamics of the second-order power control. For example, let us assume that there exists a set of users who utilize their maximum power at iteration 1. The existence of such users is very probable because of the random initial power of iteration 0. Then at iteration 2, the powers of the users belonging to that set are decreased because the overall interference level drops. Thus more users are supported and the outage decreases. Now at iteration 3, CSOPC remembers the maximum power values at iteration 1 and utilizes them for reducing the powers of those users further. This may lead to a situation in which the powers of those users become unnecessarily low, many of those users become unsupported, and the outage probability increases. As iterations go on, the power vector rapidly approaches the fixed point solution and thus the power update steps become smaller and the effects of the overshoots to the outage become negligible.

The Euclidean distance between the current power vector and the fixed point is shown in figure 4.6. The result indicates that the CSOPC converges faster than the DCPC which agrees with proposition 4.5; CSOPC is asymptotically faster than DCPC.

There are two major restrictions in implementing power control algorithms in real systems. First, a narrow bandwidth is dedicated to power control commands in general. Second, the dynamic range on power up/down is limited in any implementation of transmitters. Therefore in practical systems, there is only a binary command, power up/down. Transmitters adjust their power levels by increasing/decreasing a fixed (or possibly a variable) amount according the received binary commands. These restric-

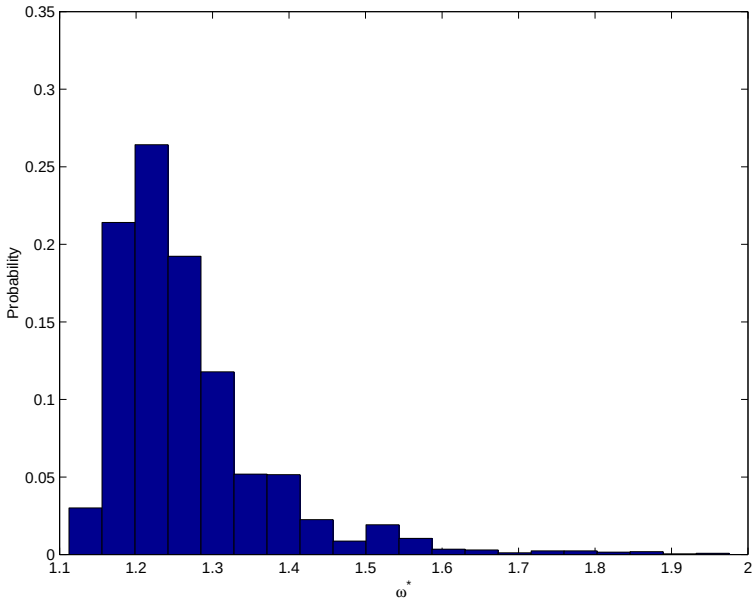

Figure 4.7: Probability density function of ω^*

tions, along with measurement errors and loop delay, contribute to performance gap between the theoretical and the practical algorithms. Furthermore, if we would like to implement CSOPC in a real system, we also have to consider that CSOPC resets the sequence $\omega(n)$ when a change has occurred in $\mathbf{H}$ (thus $\mathbf{H}_a$) due to mobile movement. Detecting such a change in any real environment seems to be hard. With these restrictions in mind, we modify CSOPC to a practical version as follows:

$$p_i(n+1) = \min\{\bar{p}_i, \max\{0, \omega\Delta_i(n)p_i(n) + (1-\omega)p_i(n-1)\}\}, \tag{4.37}$$

where $\Delta_i(n) = \begin{cases} \Delta, & \gamma_i(n) \leq \gamma_i^t \\ \frac{1}{\Delta}, & \gamma_i(n) > \gamma_i^t \end{cases}$. If we choose $\omega = 1$, the above is reduced to the so called "bang-bang" type power control (B-BPC).

We have compared the modified CSOPC (M-CSOPC) with B-BPC, using the same network configuration and assumptions as before. To choose ω in M-CSOPC, we first investigate the probability density function of ω^* of (4.19) through 10000 instances (figure 4.7). The probability that ω^* belongs to the interval $[1.156, 1.286]$ is highest. Accordingly, we set ω to 1.2 in the experiment. The target SIR and the step size Δ are 8 dB and 0.5 dB, respectively. We run M-CSOPC and B-BPC until the iteration number reaches 200. The outage probability at each iteration is computed over 10000 instances by counting the portion of the number of mobiles whose received SIR is less than 7 dB (1 dB margin to the target) at the iteration. Figure 4.8 shows a quite encouraging result. M-CSOPC converges to the stable state (outage probability of $1.9 \cdot 10^{-4}$) after 90 iterations, whereas B-BPC requires approximately 150 iterations. Furthermore, the number of mobiles having SIR below 7 dB (represented by outage in

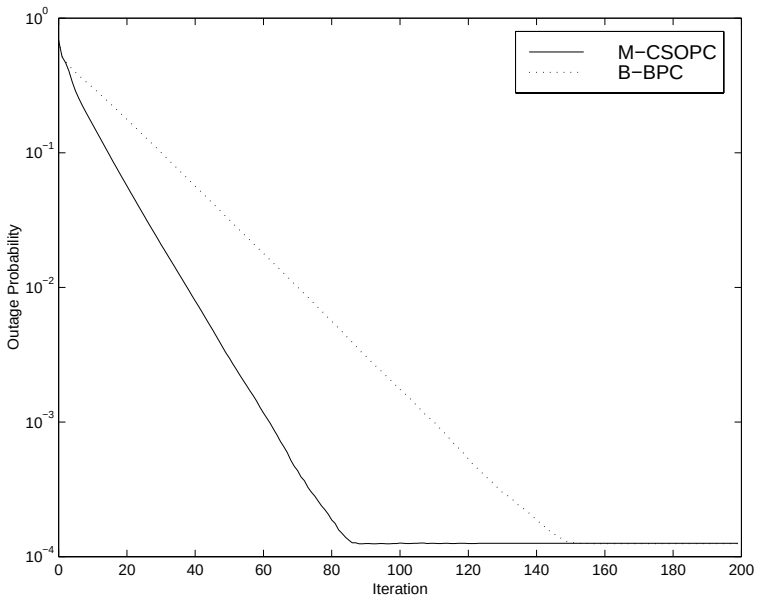

Figure 4.8: Outage probability as a function of iteration

the figure) is less than that of B-BPC over the whole the range of iterations. Thus, it is very likely that M-CSOPC increases the radio network capacity.

4.4 Concluding remarks

A group of the minimal power assignment algorithms including DCPC converge to a fixed point of a feasible system with a geometric rate [37]. In some cases, it takes a long time to reach this fixed point, and this process is especially slow when approaching the fixed point. The second-order power control algorithm will resolve such an undesirable phenomenon due to its asymptotically fast convergence.

From the encouraging computational results, we believe the practical algorithm, M-CSOPC, will significantly improve the network capacity of a real CDMA system, compared with the currently adopted power control scheme. There are, however, some issues requiring further investigation. First, selecting ω for M-CSOPC may need another optimization procedure. Second, M-CSOPC uses one more piece of information $p_i(n-1)$. Because of measurement errors and loop delay, realized power values might differ from the ideal values. Consequently, M-CSOPC uses one more, possibly erroneous value $p_i(n-1)$. This could affect the performance of power control negatively. These problems constitute an interesting future research topic.

Chapter 5

Block Power Control

The purpose of this chapter is to provide a new theoretic framework such that we can utilize partially known link gain information in improving the convergence speed. For the purpose, *block power control* (BPC) is suggested with its convergence properties. BPC is centralized within each *block* in the sense that it exchanges link gain information *within* the same block. However, it is distributed in a block-wise manner and no information is exchanged *between* different blocks. Depending on availability of link gain information, a block can be any set of users, and can even consist of a single user. Computational experiments are carried out on a DS-CDMA system, illustrating how BPC utilizes available link gain information in increasing the convergence speed of the power control.

One possible application of our work is the *bunched* radio resource management scheme [14]. The basic assumption of the scheme is that the link gains within a bunch are, at least partially, known. A bunch is generally equivalent to a block in this text. It may be argued that the bunch concept requires a lot of signaling thus being rather impractical. However, we can imagine an example of "natural" bunches where the signaling can be done locally within one base station controller. In the Wideband CDMA system [21], dedicated pilot bits are associated with each traffic channel in both up- and downlinks, supporting the adaptive antennas. This property may enable the efficient estimation of link gains within one cell which in turn enables the use of bunches having the sizes of one cell.

To present BPC in section 5.1, we start with an algorithm for the relaxed problem that has no constraint on maximum power levels. Next, we develop it to a constrained algorithm. Numerical comparison between BPC and DCPC is contained in section 5.3. Finally, section 5.4 concludes the chapter.

5.1 Unconstrained case

Let us assume that transmitters are grouped into N *blocks*, $\mathcal{B}_1, \mathcal{B}_2, \ldots, \mathcal{B}_N$. A block can be any set of transmitters, and can even consist of a single transmitter. For notational simplicity, we assume that the first $|\mathcal{B}_1|$ transmitters belong to $\mathcal{B}_1$ and the

next $|\mathcal{B}_2|$ transmitters belong to $\mathcal{B}_2$, and so forth ($|\cdot|$ denotes the cardinality of the set). Then, we can represent $\mathbf{H}$ as the following block matrix:

$$\mathbf{H} = \begin{bmatrix} \mathbf{H}_{11} & \mathbf{H}_{12} & \cdots & \mathbf{H}_{1N} \\ \mathbf{H}_{21} & \mathbf{H}_{22} & \cdots & \mathbf{H}_{2N} \\ \vdots & \vdots & \ddots & \vdots \\ \mathbf{H}_{N1} & \mathbf{H}_{N2} & \cdots & \mathbf{H}_{NN} \end{bmatrix} \tag{5.1}$$

The submatrix $\mathbf{H}_{ij}$ has the size of $|\mathcal{B}_i| \times |\mathcal{B}_j|$. In the same manner, we can decompose:

$$\boldsymbol{\eta} = (\boldsymbol{\eta}_1', \boldsymbol{\eta}_2', \cdots, \boldsymbol{\eta}_N')' \tag{5.2}$$

$$\mathbf{p} = (\mathbf{p}_1', \mathbf{p}_2', \cdots, \mathbf{p}_N')' \tag{5.3}$$

To clarify the above mentioned notation, consider the following example:

Example 5.1. Consider a system consisting of three base stations in which each base station is communicating with exactly one mobile station. Let base stations 1 and 2 form a block and let base station 3 form another block (see figure 5.1). Then

$$\mathbf{H} = \left[\begin{array}{cc|c} 0 & \frac{\gamma_1^t g_{12}}{g_{11}} & \frac{\gamma_1^t g_{13}}{g_{11}} \\ \frac{\gamma_2^t g_{21}}{g_{22}} & 0 & \frac{\gamma_2^t g_{23}}{g_{22}} \\ \hline \frac{\gamma_3^t g_{31}}{g_{33}} & \frac{\gamma_3^t g_{32}}{g_{22}} & 0 \end{array}\right] = \left[\begin{array}{c|c} \mathbf{H}_{11} & \mathbf{H}_{12} \\ \hline \mathbf{H}_{12} & \mathbf{H}_{22} \end{array}\right], \tag{5.4}$$

$$\boldsymbol{\eta} = \left[\begin{array}{c} \frac{\gamma_1^t \nu_1}{g_{11}} \\ \frac{\gamma_2^t \nu_1}{g_{22}} \\ \hline \frac{\gamma_3^t \nu_1}{g_{33}} \end{array}\right] = \left[\begin{array}{c} \boldsymbol{\eta}_1 \\ \hline \boldsymbol{\eta}_2 \end{array}\right] \tag{5.5}$$

and

$$\mathbf{p} = \left[\begin{array}{c} p_1 \\ p_2 \\ \hline p_3 \end{array}\right] = \left[\begin{array}{c} \mathbf{p}_1 \\ \hline \mathbf{p}_2 \end{array}\right]. \tag{5.6}$$

Keeping the lesson of proposition 3.6 in mind, we choose $\mathbf{M} = \boldsymbol{\Omega}^{-1}(\mathbf{I} - \boldsymbol{\Psi} \otimes \mathbf{H})$ and $\mathbf{N} = \boldsymbol{\Omega}^{-1} - \mathbf{I} + (\mathbf{1} - \boldsymbol{\Omega}^{-1}\boldsymbol{\Psi}) \otimes \mathbf{H}$, where $\otimes$ denotes element-wise multiplication and $\mathbf{1}$ is a matrix of an appropriate size, consisting of ones. Matrix $\boldsymbol{\Omega}$ has the form

$$\boldsymbol{\Omega} = \begin{bmatrix} \boldsymbol{\Omega}_{11} & \mathbf{0} & \cdots & \mathbf{0} \\ \mathbf{0} & \boldsymbol{\Omega}_{22} & \ddots & \mathbf{0} \\ \vdots & \ddots & \ddots & \vdots \\ \mathbf{0} & \mathbf{0} & \cdots & \boldsymbol{\Omega}_{NN} \end{bmatrix} \tag{5.7}$$

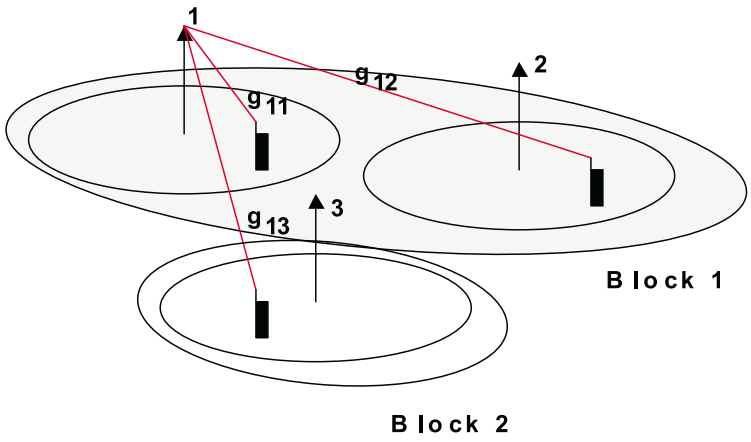

Figure 5.1: Example of a system divided into two blocks

where $\mathbf{\Omega}_{ii}$ is a $|\mathcal{B}_i| \times |\mathcal{B}_i|$ matrix fulfilling

$$\mathbf{0} \leq \mathbf{\Omega}_{ii} \leq \mathbf{I}, \quad \det(\mathbf{\Omega}_{ii}) \neq 0 \tag{5.8}$$

Similarly, $\mathbf{\Psi}$ has the form

$$\mathbf{\Psi} = \begin{bmatrix} \mathbf{\Psi}_{11} & \mathbf{0} & \cdots & \mathbf{0} \\ \mathbf{0} & \mathbf{\Psi}_{22} & \ddots & \mathbf{0} \\ \vdots & \ddots & \ddots & \vdots \\ \mathbf{0} & \mathbf{0} & \cdots & \mathbf{\Psi}_{NN} \end{bmatrix} \tag{5.9}$$

where $\mathbf{\Psi}_{ii}$ is a $|\mathcal{B}_i| \times |\mathcal{B}_i|$ matrix fulfilling

$$\mathbf{0} \leq \mathbf{\Psi}_{ii} \leq \mathbf{\Omega}_{ii}\mathbf{1} \tag{5.10}$$

Then, using these $\mathbf{M}$ and $\mathbf{N}$, we can construct the following iterative power control algorithm, which we will call *unconstrained block power control* (UBPC).

$$\begin{aligned} \mathbf{p}(n+1) &= (\mathbf{I} - \mathbf{\Psi} \otimes \mathbf{H})^{-1}\mathbf{\Omega}\Big((\mathbf{\Omega}^{-1} - \mathbf{I} + (\mathbf{1} - \mathbf{\Omega}^{-1}\mathbf{\Psi}) \otimes \mathbf{H})\mathbf{p}(n) + \boldsymbol{\eta}\Big) \\ &\stackrel{\text{def}}{=} \boldsymbol{\mathcal{I}}_{BPC}(\mathbf{p}(n)) \end{aligned} \tag{5.11}$$

And, by showing that the matrices $\mathbf{M}$ and $\mathbf{N}$ form a regular splitting of $\mathbf{A}$, we have:

Proposition 5.1. *UBPC converges to* $\mathbf{p}^*$ *of a feasible system, starting from an arbitrary initial vector* $\mathbf{p}(0)$.

Proof. The feasibility condition implies that $\rho(\mathbf{H}) < 1$. Since $\mathbf{H}_{ii}$ is a principal submatrix of $\mathbf{H}$, by Lemma 2.4 in [84], we have $\rho(\mathbf{H}_{ii}) < \rho(\mathbf{H}) < 1$. By definition, $\mathbf{\Psi}_{ii} \leq \mathbf{\Omega}_{ii}\mathbf{1} \leq \mathbf{1}$ holds, and Theorem 2.8 in [84] guarantees that $\rho(\mathbf{\Psi}_{ii} \otimes \mathbf{H}_{ii}) \leq \rho(\mathbf{H}_{ii})$. Thus, by proposition 3.3, we have

$$(\mathbf{I} - \mathbf{\Psi} \otimes \mathbf{H})^{-1} = \begin{bmatrix} (\mathbf{I} - \mathbf{\Psi}_{11} \otimes \mathbf{H}_{11})^{-1} & \mathbf{0} & \cdots & \mathbf{0} \\ \mathbf{0} & (\mathbf{I} - \mathbf{\Psi}_{22} \otimes \mathbf{H}_{22})^{-1} & \mathbf{0} & \mathbf{0} \\ \vdots & \ddots & \vdots & \vdots \\ \mathbf{0} & \mathbf{0} & \cdots & (\mathbf{I} - \mathbf{\Psi}_{NN} \otimes \mathbf{H}_{NN})^{-1} \end{bmatrix} \geq \mathbf{0} \tag{5.12}$$

From (5.1), (5.8), (5.10) and (5.12), it is clear that

$$\mathbf{M}^{-1} = (\mathbf{I} - \mathbf{\Psi} \otimes \mathbf{H})^{-1}\mathbf{\Omega} \geq \mathbf{0} \tag{5.13}$$

and

$$\mathbf{N} = \mathbf{\Omega}^{-1} - \mathbf{I} + (\mathbf{1} - \mathbf{\Omega}^{-1}\mathbf{\Psi}) \otimes \mathbf{H} \geq \mathbf{0} \tag{5.14}$$

Thus, by Proposition 3.5, UBPC converges. □

To give the notion of "block-wise" power control, let $\mathbf{X}(n) = \text{diag}\{\frac{\gamma_i^t}{\gamma_i(n)}\}$. This allows us to replace $\mathbf{Hp}(n) + \boldsymbol{\eta}$ in (5.11) by $\mathbf{X}(n)\mathbf{p}(n)$. Since $\mathbf{X}$ is of the same size as $\mathbf{\Omega}$ or $\mathbf{\Psi}$, we can decompose it into blocks in the same manner:

$$\mathbf{X}(n) = \begin{bmatrix} \mathbf{X}_{11}(n) & \mathbf{0} & \cdots & \mathbf{0} \\ \mathbf{0} & \mathbf{X}_{22}(n) & \ddots & \mathbf{0} \\ \vdots & \ddots & \ddots & \vdots \\ \mathbf{0} & \mathbf{0} & \cdots & \mathbf{X}_{NN}(n) \end{bmatrix} \tag{5.15}$$

By noting that $\mathbf{\Omega}$, $\mathbf{\Psi}$ and $\mathbf{X}(n)$ are block diagonal matrices, we can rewrite (5.11) in a block-wise form as follows:

$$\mathbf{p}_i(n+1) = \Big(\mathbf{I} + (\mathbf{I} - \mathbf{\Psi}_{ii} \otimes \mathbf{H}_{ii})^{-1}\mathbf{\Omega}_{ii}(\mathbf{X}_{ii}(n) - \mathbf{I})\Big)\mathbf{p}_i(n) \stackrel{\text{def}}{=} \boldsymbol{\mathcal{I}}_{BPC_i}(\mathbf{p}(n)) \tag{5.16}$$

where $\mathbf{p}_i(n)$ denotes the power levels of the transmitters of the block i at iteration n. Equations (5.11) and (5.16) are mathematically equivalent. The only difference between them is that the latter utilizes measurable information, $\mathbf{H}_{ii}$ and $\mathbf{X}_{ii}(n)$, within block i.

In UBPC given by the equation (5.16), the elements in $\mathbf{\Psi}_{ii}$ represent availability and reliability of the corresponding elements in the normalized link gain matrix, $\mathbf{H}_{ii}$. For example, if the users in block i have a full confidentiality on an element in $\mathbf{H}_{ii}$, then the corresponding element in $\mathbf{\Psi}_{ii}$ can be set to its maximum value given by the bound (5.10). However, the zero element in $\mathbf{\Psi}_{ii}$ corresponds to the opposite case, where the information is either not available or has poor reliability. When $\mathbf{\Psi}_{ii} = \mathbf{0}$, we can verify through (5.16) that the power update within block i becomes fully distributed, requiring only local CIR measurement. In fact, if we choose $\mathbf{\Psi} = \mathbf{0}$ or

if every block is composed of a single user, then UBPC becomes equivalent to FMA. As in FMA, the diagonal elements of $\mathbf{\Omega}_{ii}$ constitute a damping factor of the power control algorithm. The damping factor can be used to increase the robustness of the power control algorithm by adjusting the step size of power update. For example, in the case of power control errors, such as a CIR measurement error, smaller fault can be achieved decreasing the damping factor. The damping factor can also be used for taking into account the "sluggishness" of the transmitter, i.e., the power amount that can be varied in one update. Nevertheless, as will be stated in proposition 5.2, the largest $\mathbf{\Omega}_{ii}$ and $\mathbf{\Psi}_{ii}$ will generate the best convergence speed, provided that the link gains and the CIRs are measured accurately in block i.

Proposition 5.2. *Among those $\mathbf{\Omega}_{ii}$ and $\mathbf{\Psi}_{ii}$ that fulfill inequalities (5.8) and (5.10), the choice $\mathbf{\Omega}_{ii} = \mathbf{I}$ and $\mathbf{\Psi}_{ii} = \mathbf{1}$ is the best with respect to asymptotic average rate of convergence.*

Proof. For notational convenience, let us denote the iteration matrix $\mathbf{M}^{-1}\mathbf{N} = (\mathbf{I} - \mathbf{\Psi} \otimes \mathbf{H})^{-1}\mathbf{\Omega}(\mathbf{\Omega}^{-1} - \mathbf{I} + (\mathbf{1} - \mathbf{\Omega}^{-1}\mathbf{\Psi}) \otimes \mathbf{H})$ in (5.11) by $\mathbf{Z}_{BPC}(\mathbf{\Omega}, \mathbf{\Psi})$. As in the proof of proposition 3.8 let $\bar{\mathbf{\Omega}}_{ii} = \mathbf{I}$ and $\bar{\mathbf{\Psi}}_{ii} = \mathbf{1}$. Assume that $\mathbf{\Omega}_{ii} \neq \bar{\mathbf{\Omega}}_{ii}$ and $\mathbf{\Psi}_{ii} \neq \bar{\mathbf{\Psi}}_{ii}$. It follows that

$$\begin{aligned} \mathbf{Z}_{SOPC}(\mathbf{\Omega}, \mathbf{\Psi}) &= \mathbf{\Omega}^{-1} - \mathbf{I} + (\mathbf{1} - \mathbf{\Omega}^{-1}\mathbf{\Psi}) \otimes \mathbf{H} && (5.17) \\ &\geq \bar{\mathbf{\Omega}}^{-1} - \mathbf{I} + (\mathbf{1} - \mathbf{\Omega}^{-1}\mathbf{\Psi}) \otimes \mathbf{H} && (5.18) \\ &\geq \bar{\mathbf{\Omega}}^{-1} - \mathbf{I} + (\mathbf{1} - \bar{\mathbf{\Omega}}^{-1}\bar{\mathbf{\Psi}}) \otimes \mathbf{H} = \mathbf{Z}_{SOPC}(\bar{\mathbf{\Omega}}, \bar{\mathbf{\Psi}}) && (5.19) \end{aligned}$$

where in the inequalities (5.19) and (5.19) the equality is excluded. Thus, by proposition 3.6, we have $\rho(\mathbf{Z}_{BPC}(\mathbf{\Omega}, \mathbf{\Psi})) > \rho(\mathbf{Z}_{BPC}(\bar{\mathbf{\Omega}}, \bar{\mathbf{\Psi}}))$. □

Example 5.2. To illustrate how to choose $\mathbf{\Omega}_{ii}$ and $\mathbf{\Psi}_{ii}$, we consider an example in which three base stations, each communicating with exactly one mobile, form a block. Assume that for some reason we do not have information about the link gain $g_{12} = g_{21}$. Let us choose

$$\mathbf{\Omega}_{11} = \begin{bmatrix} \omega_1 & 0 & 0 \\ 0 & \omega_2 & 0 \\ 0 & 0 & \omega_3 \end{bmatrix} \tag{5.20}$$

then it must hold that

$$\mathbf{0} \geq \mathbf{\Psi}_{11} = \begin{bmatrix} \psi_{11} & \psi_{12} & \psi_{13} \\ \psi_{21} & \psi_{22} & \psi_{23} \\ \psi_{31} & \psi_{32} & \psi_{33} \end{bmatrix} \leq \begin{bmatrix} \omega_1 & 0 & \omega_1 \\ 0 & \omega_2 & \omega_2 \\ \omega_3 & \omega_3 & \omega_3 \end{bmatrix} \tag{5.21}$$

That is, we must choose $\psi_{12} = \psi_{21} = 0$. By choosing the strict upper bound for $\mathbf{\Psi}_{11}$, the convergence rate is maximized.

The sizes and structures of submatrices $\mathbf{\Psi}_{ii}$ (the size and structure of each block) define the computational complexity and distributiveness of UBPC. They also give a paramount effect on the convergence speed. If the block sizes are large and the elements in the corresponding $\mathbf{\Psi}_{ii}$-matrices are also large, then the convergence speed is going to be fast. Actually, the best possible performance with respect to the convergence speed, assuming that the link gains could be measured accurately, is achieved by including all the users into one block. In this special case, UBPC becomes fully centralized. One drawback of using large block sizes with dense $\mathbf{\Psi}_{ii}$ is that the computational complexity is high, since we need to invert large $(\mathbf{I} - \mathbf{\Psi}_{ii} \otimes \mathbf{H}_{ii})$ at each iteration. Another drawback is that the degree of signaling is high, since a large amount of measurement information must be collected. To reduce the complexity, we can use sparse $\mathbf{\Psi}_{ii}$ or reduce the block size. However, this is done at the cost of reducing the convergence speed. In practice, the sizes and structures of $\mathbf{\Psi}_{ii}$ are upper limited by the amount of signaling, the availability of the link gain estimates, and the computational complexity of the matrix inversion operation. However, it is generally difficult to compare between utilizing small blocks with reliable information and utilizing larger blocks with information of inferior quality. In example 5.3, we will illustrate a practical way of choosing blocks such that the computational complexity is kept low.

Example 5.3. Consider a DS-CDMA system, where all the mobiles assigned to a particular base station constitute one block. The link gains between mobiles and the base station within the same block are assumed to be known. Further, in the downlink case, we assume that the normalized cross-correlation between different channels in the block k is uniform, i.e., $\theta_{ij} = \theta$ if $i, j \in \mathcal{B}_k$. If we choose $\mathbf{\Omega}_{kk} = \mathbf{I}$ and $\mathbf{\Psi}_{kk} = \mathbf{1}$, $k = 1, \ldots, N$; then UBPC becomes, in up- and downlink cases,

$$p_i(n+1) = \frac{\gamma_i^t}{(1+\gamma_i^t)(1 - \sum_{j \in \mathcal{B}_k} \frac{\gamma_j^t}{1+\gamma_j^t})} \frac{I_i(n)}{g_{ii}}, \quad i \in \mathcal{B}_k \tag{5.22}$$

and

$$p_i(n+1) = \frac{\gamma_i^t}{1+\theta\gamma_i^t} \Big(\frac{\theta \sum_{j \in \mathcal{B}_k} \frac{\gamma_j^t}{1+\theta\gamma_j^t} \frac{I_j(n)}{g_{jj}}}{1 - \theta \sum_{j \in \mathcal{B}_k} \frac{\gamma_j^t}{1+\theta\gamma_j^t}} + \frac{I_i(n)}{g_{ii}} \Big), \quad i \in \mathcal{B}_k \tag{5.23}$$

respectively. For user i, the *external interference* from the outside of block k, is given by

$$I_i(n) = \frac{g_{ii} p_i(n)}{\gamma_i(n)} - \sum_{\substack{j \in \mathcal{B}_k \\ j \neq i}} g_{jj} p_j(n), \quad i \in \mathcal{B}_k \tag{5.24}$$

and

$$I_i(n) = \frac{g_{ii}p_i(n)}{\gamma_i(n)} - \theta g_{ii} \sum_{\substack{j \in \mathcal{B}_k \\ j \neq i}} p_j(n), \quad i \in \mathcal{B}_k \tag{5.25}$$

in up- and downlink cases, respectively. Note that, from our definition in section 3.1, the link gains g_{jj} in (5.24) and g_{ii} in (5.25) can be replaced by g_{ij} (see appendix A for the derivation of above results). Also, we can easily verify that if $\mathcal{B}_k = \{i\}$, then both (5.22) and (5.23) will be reduced to the fully distributive form, $p_i(n+1) = \frac{\gamma_i^t}{\gamma_i(n)} p_i(n)$.

5.2 Constrained case

Let us consider a more realistic case, where we have an upper limit for transmission powers as given in (3.3). The constrained block power control (CBPC) algorithm is given by

$$\mathbf{p}(n+1) = \min\{\bar{\mathbf{p}}, \boldsymbol{\mathcal{I}}_{BPC}(\mathbf{p}(n))\} \stackrel{\text{def}}{=} \boldsymbol{\mathcal{T}}_{BPC}(\mathbf{p}(n)) \tag{5.26}$$

For block i, the update rule can be expressed as

$$\mathbf{p}_i(n+1) = \min\{\bar{\mathbf{p}}, \boldsymbol{\mathcal{I}}_{BPC_i}(\mathbf{p}(n))\} \stackrel{\text{def}}{=} \boldsymbol{\mathcal{T}}_{BPC_i}(\mathbf{p}(n)) \tag{5.27}$$

To give a proof for the convergence of CBPC, we first note the following lemma.

Lemma 5.1. *If the system is feasible, there exists a positive definite diagonal matrix* $\mathbf{W}$ *such that* $||\mathbf{Z}_{BPC}(\boldsymbol{\Omega}, \boldsymbol{\Psi})||_\infty^{\mathbf{W}} < 1$ *for all* $\boldsymbol{\Omega}$ *and* $\boldsymbol{\Psi}$ *that fulfill inequalities (5.8) and (5.10).*

Proof. By definition, $\mathbf{H}$ is a positive matrix and by lemma 3.1 it is also an irreducible matrix. Therefore, the *Perron-Frobenius Theorem* (proposition 3.1) guarantees that there exits a positive vector $\mathbf{e} = (e_1 e_2 \cdots e_M)'$, called the *Perron eigenvector*, such that

$$\mathbf{He} = \rho(\mathbf{H})\mathbf{e} \tag{5.28}$$

It follows that

$$\mathbf{Z}_{BPC}(\boldsymbol{\Omega}, \boldsymbol{\Psi})\mathbf{e} = (\mathbf{I} - \boldsymbol{\Psi} \otimes \mathbf{H})^{-1}\boldsymbol{\Omega}(\boldsymbol{\Omega}^{-1} - \mathbf{I} + \mathbf{H} - \boldsymbol{\Omega}^{-1}\boldsymbol{\Psi} \otimes \mathbf{H})\mathbf{e} \tag{5.29}$$

$$= (\mathbf{I} - \boldsymbol{\Psi} \otimes \mathbf{H})^{-1}(\mathbf{I} + \boldsymbol{\Omega}(\rho(\mathbf{H}) - 1) - \boldsymbol{\Psi} \otimes \mathbf{H})\mathbf{e} \tag{5.30}$$

$$= (\mathbf{I} + (\mathbf{I} - \boldsymbol{\Psi} \otimes \mathbf{H})^{-1}\boldsymbol{\Omega}(\rho(\mathbf{H}) - 1))\mathbf{e} \tag{5.31}$$

Since the system is feasible, we have $\rho(\mathbf{H}) < 1$ and by Proposition 5.1, we have $\mathbf{Z}_{BPC}(\boldsymbol{\Omega}, \boldsymbol{\Psi}) \geq \mathbf{0}$, equality excluded. It is also clear that $\mathbf{Z}_{BPC}(\boldsymbol{\Omega}, \boldsymbol{\Psi})$ has a full rank. Therefore,

$$\mathbf{0} < \mathbf{Z}_{BPC}(\boldsymbol{\Omega}, \boldsymbol{\Psi})\mathbf{e} < \mathbf{e} \tag{5.32}$$

If we choose $\mathbf{W} = \text{diag}(\frac{1}{e_i})$, which is clearly a positive definite diagonal matrix, we have

$$||\mathbf{Z}_{BPC}(\mathbf{\Omega}, \mathbf{\Psi})||_{\infty}^{\mathbf{W}} < 1 \tag{5.33}$$

Thus by constructing a matrix $\mathbf{W}$, we have shown the existence of it. □

Proposition 5.3. *CBPC converges to* $\mathbf{p}^*$ *of a feasible system, starting from any power vector* $\mathbf{p}(0)$ *that is in the range of (3.3).*

Proof. The result follows directly from lemma 5.1 and proposition 3.9. □

Corollary 5.4. *Proposition 5.2 also holds for CBPC.*

Proof. By proposition 5.3, CBPC is a pseudo-contraction mapping. Thus, there exits $0 < n_0 < \infty$ such that $\boldsymbol{\mathcal{T}}_{BPC}(\mathbf{p}(\mathbf{n})) < \bar{\mathbf{p}}$, for all $n > n_0$ and for all $\mathbf{\Omega}$, $\mathbf{\Psi}$ fulfilling (5.8) and (5.10). So for $n > n_0$, the dynamics are described by UBPC and thus proposition 5.2 applies. See also remark 3.2. □

In the non-stationary case where $\mathbf{\Omega}_{ii}$ and $\mathbf{\Psi}_{ii}$ are allowed to vary from iteration to another, the CBPC can be written as

$$\begin{aligned} \mathbf{p}_i(n+1) &= \max\left\{\bar{\mathbf{p}}, \Big(\mathbf{I} + (\mathbf{I} - \mathbf{\Psi}_{ii}(n) \otimes \mathbf{H}_{ii})^{-1}\mathbf{\Omega}_{ii}(n)(\mathbf{X}_{ii}(n) - \mathbf{I})\Big)\mathbf{p}_i(n)\right\} \\ &\stackrel{\text{def}}{=} \boldsymbol{\mathcal{T}}_{BPC}(\mathbf{p}(n), n) \end{aligned} \tag{5.34}$$

Corollary 5.5. *If* $\mathbf{\Omega}_{ii}(n)$ *and* $\mathbf{\Psi}_{ii}(n)$ *fulfill (5.8) and (5.10) at every iteration, then the non-stationary CBPC converges to* $\mathbf{p}^*$ *of a feasible system, starting from any power vector* $\mathbf{p}(0)$ *that is in the range of (3.3).*

Proof. By Lemma 5.1, there exists a positive definite diagonal matrix $\mathbf{W}$ such that $||\mathbf{Z}_{BPC}(\mathbf{\Omega}, \mathbf{\Psi})||_{\infty}^{\mathbf{W}} < 1$ for all $\mathbf{\Omega}$ and $\mathbf{\Psi}$ that fulfill (5.8) and (5.10). Therefore $||\mathbf{Z}_{BPC}(\mathbf{\Omega}(n), \mathbf{\Psi}(n))||_{\infty}^{\mathbf{W}} < 1$ for all n and it follows, as in proof of proposition 4.4, that $\boldsymbol{\mathcal{T}}_{BPC}(\mathbf{p}, n)$ is a pseudo-contraction mapping. Hence, the non-stationary iteration converges. □

Corollary 5.5 states that the damping factor and the amount of link gain information utilized by the power control can vary from iteration to another without causing any problem to the convergence. In addition, we have the following property that the algorithm converges even if the power updates are done in asynchronous fashion:

Proposition 5.6. *The asynchronous CBPC converges to* $\mathbf{p}^*$ *of a feasible system, starting from any power vector* $\mathbf{p}(0)$ *that is in the range of (3.3).*

Proof. The result follows directly from lemma 5.1 and proposition 3.14. □

So far we have been focusing on the feasible system. However, it is noticeable that UBPC and CBPC may result in nonpositive power values when the system becomes infeasible; we cannot support every transmitter. In this case, the inequality (5.12) may no longer hold because $\rho(\mathbf{\Psi}_{ii}\mathbf{H}_{ii}) \geq 1$ (see also proposition 3.3). This means that the block i, and therefore the whole system, is overloaded and some of the users must be removed. Unfortunately, this condition alone is not enough to detect infeasibility since it may happen that the block i is feasible but the interference coming from other cells is too high ($\rho(\mathbf{H}_{ii}) \leq \rho(\mathbf{H}) < 1$ but $\mathbf{p}^*$ is not in the range of (3.3) or $\rho(\mathbf{H}_{ii}) < 1$ but $\rho(\mathbf{H}) \geq 1$) or it may even happen that $\mathbf{\Psi}_{ii}$ is chosen in such a way that the inverse matrix is positive although the block is overloaded ($\rho(\mathbf{H}_{ii}) \geq 1$ but $\rho(\mathbf{\Psi}_{ii}\mathbf{H}_{ii}) < 1$). In the case of negative powers, we could, if all the link gains in $\mathbf{H}_{ii}$ are known, utilize some advanced removal strategy like removing the worst interferer (the user that has the smallest link gain) first. Another approach that could be useful, especially if the link gain information has poor reliability, is to force the inverse of $\mathbf{I} - \mathbf{\Psi}_{ii} \otimes \mathbf{H}_{ii}$ matrix to become positive by decreasing some of the elements in $\mathbf{\Psi}_{ii}$. This effect can also be achieved by dividing the block into several smaller ones although this may require more signaling effort. After the inverse is made positive, the overall system can still be infeasible. If this is the case, the power vector will converge to a fixed point where some (or all) of the users are using the maximum power but are not supported. To cope with this situation, standard removal schemes like *gradual removal* [6] should be applied.

To relate the derivation in this chapter to our general framework described in chapter 3, we note that corollary 5.5 enables us to expand the "coverage" of our framework to some of the log-linear controllers like I-controller given by (3.29):

Proposition 5.7. *The power control algorithm (3.29) converges to* $\mathbf{p}^*$ *of a feasible system, starting from an arbitrary initial vector* $\mathbf{p}(0)$.

Proof. We start by noting that (3.29) can be interpreted as non-stationary Foschini and Miljanic algorithm with

$$\omega_i(n) = \frac{\left(\frac{\gamma_i^t}{\gamma_i(n)}\right)^{\frac{1}{T_{I_i}}} - 1}{\frac{\gamma_i^t}{\gamma_i(n)} - 1} \tag{5.35}$$

Since $T_{I_i} > 1$ and $\lim_{\gamma_i(n)\to\gamma_i^t} \omega_i(n) = \frac{1}{T_{I_i}} < 1$, we have $0 < \omega_i(n) < 1$. Hence, by corollary 5.5, the algorithm converges to $\mathbf{p}^*$. □

Remark 5.1. Similarly to proposition 5.7 we could prove the stability of B-BPC algorithm.

In that case B-BPC can be interpreted as non-stationary Foschini and Miljanic algorithm if $\left|\ln\gamma_i^t - \ln\gamma_i(n)\right| > \ln\Delta$. Hence, if the error increases FMA step is taken

to decrease it. However in the vicinity of γ_i^t the algorithm can not be described as non-stationary FMA and thus convergence is not guaranteed.

5.3 Computational results

We investigate how quickly CBPC converges to $\mathbf{p}^*$ of a feasible system. DCPC is used as a reference algorithm. The DS-CDMA system with 19 omni-bases located in the centers of 19 cells is used as a test system (figure 2.1). We consider both up- and downlink cases of an DS-CDMA example in which the *processing gain* is 128 (21 dB). For a given instance, a total of 190 mobiles are generated in the uplink case, whereas 380 mobiles are considered in the downlink case. The reason for the difference in the number of users is to keep the relative load approximately the same for both up- and downlinks.

The receiver noise at both mobiles and base stations is taken to be 10^{-12}. The relative maximum power of a mobile, and in the downlink case the relative maximum power of a traffic channel assigned to a mobile is set to one. The base that gives the lowest attenuation is assigned to each mobile. The target SIR is set to 8 dB for both up- and downlinks of each mobile.

When applying CBPC, we have used the same assumption as in example 5.3. That is, all the mobiles assigned to a particular base station constitute one block. The link gains between mobiles and the base station within the same block are assumed to be known. We choose $\mathbf{\Omega}_{ii} = \mathbf{I}$ and $\mathbf{\Psi}_{ii} = \mathbf{1}$ and apply (5.22) and (5.23), considering the maximum power constraint. In the downlink case, we use the normalized cross-correlation $\theta_{ij} = 0.4$ if mobiles i and j belong to the same base station.

The *outage probability* is used as a performance measure. To evaluate this, we have taken 1000 independent "feasible" instances of mobile locations and shadow fadings. In each instance, we have performed thirty power control steps. The initial power for each mobile is randomly chosen from the interval [0,1]. The outage probability at each iteration is computed over 1000 instances by counting the portion of the number of non-supported mobiles at the iteration. Figures 5.2 and 5.3 show the outage probabilities of CBPC and DCPC as a function of iteration in up- and downlink cases respectively. In the uplink case, CBPC takes about 7 iterations on average to reach the state with the outage probability of 10^{-4}. However, we can see that DCPC requires more than 30 iterations on average to reach that point. In the downlink, CBPC requires 8 iterations, whereas DCPC does 20 iterations. The reason for the performance difference in CBPC between up- and downlinks is that the uplink interference within a cell is much larger than that in the downlink and that main contribution of CBPC is to efficiently mitigate the interference within the cell (block).

Figures 5.4 and 5.5 show the Euclidean distance between the current power vector and $\mathbf{p}^*$. The distance is computed by averaging over 1000 instances. It is clear that CBPC also converges faster in terms of the Euclidean distance. The numerical results indicate that a significant improvement in the convergence speed has been obtained through utilizing link gain information. The speed difference becomes bigger as both algorithms approach $\mathbf{p}^*$. This coincides with the theoretical results of corollary 5.4 on

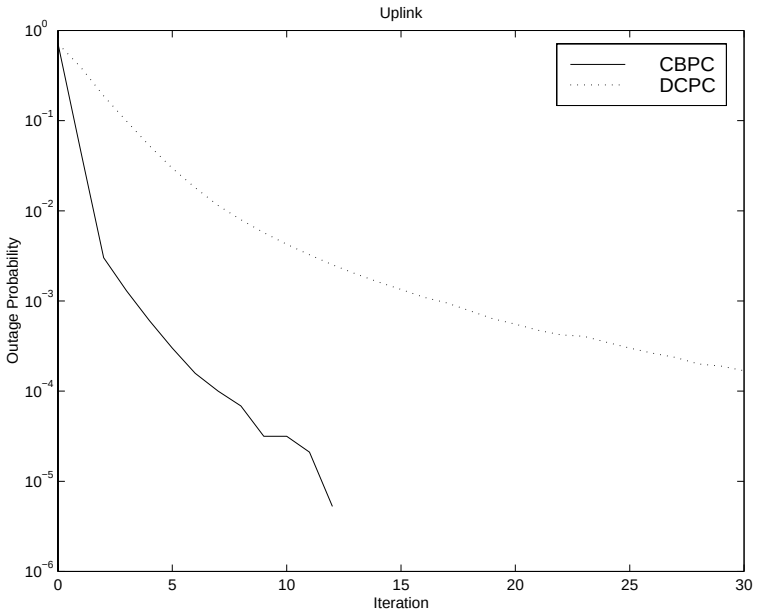

Figure 5.2: Uplink outage probability as a function of iteration.

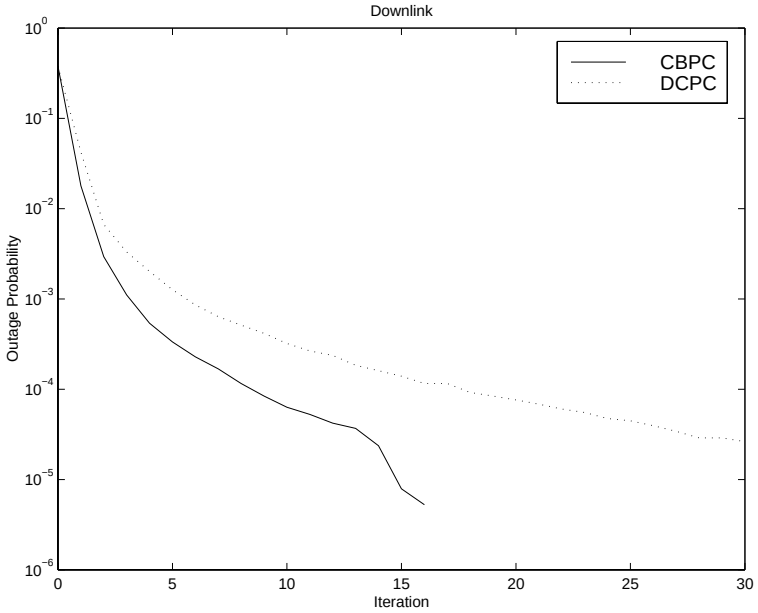

Figure 5.3: Downlink outage probability as a function of iteration.

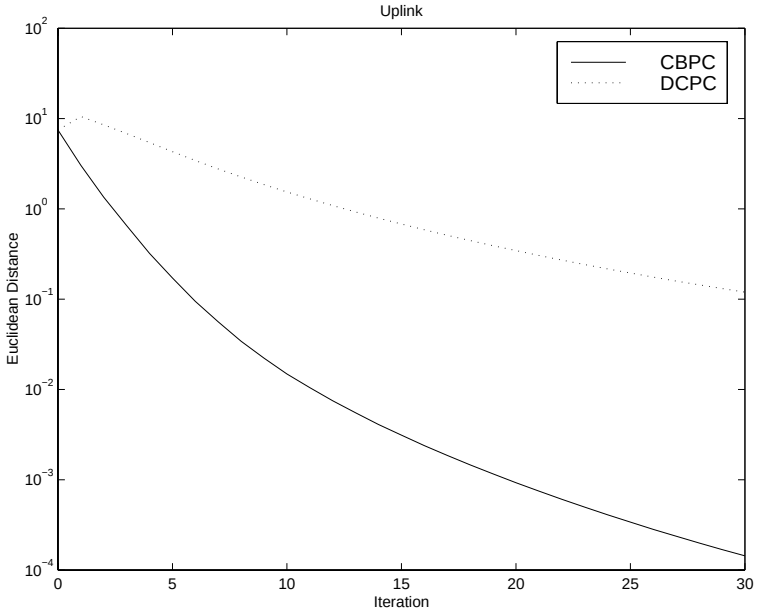

Figure 5.4: Uplink Euclidean distance between the current power vector and $\mathbf{p}^*$.

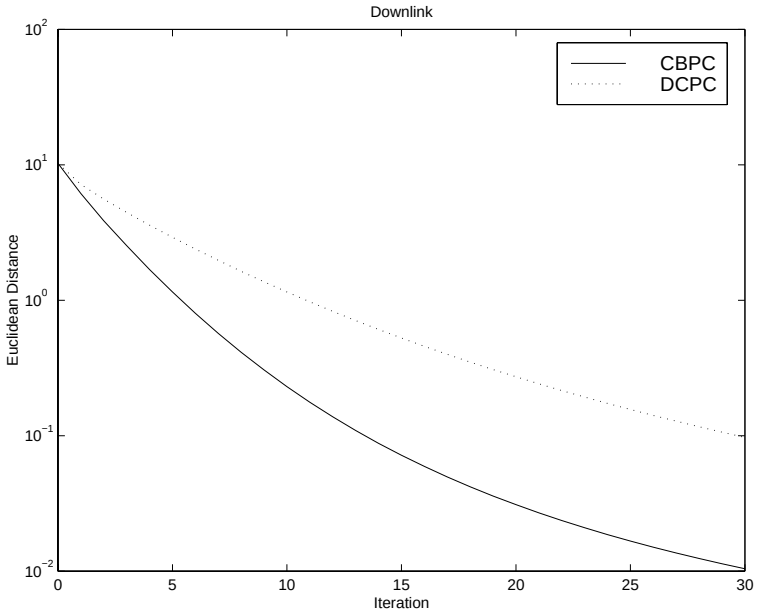

Figure 5.5: Downlink Euclidean distance between the current power vector and $\mathbf{p}^*$.

the asymptotic average rate of convergence.

5.4 Concluding remarks

In this chapter, we proposed a power control algorithm, which can incorporate available link gain information in a way that the convergence speed increases. Acceleration of convergence speed is based on the accurate measurement of link gains and received CIRs in each block. However, if those measurements were too erroneous, this would affect the power control negatively. To cope with the situation, we have introduced parameters $\mathbf{\Omega}$ and $\mathbf{\Psi}$ into our algorithm. Those parameters will determine the algorithm's key properties such as distributiveness, robustness and convergence speed.

The drawback of block power control algorithm is that it requires measured CIR values and large bandwidth for power control commands. However, the signaling burden can be decreased by only making CBPC steps if large changes in $\mathbf{H}$ are expected (e.g. a set of users have arrived/departed) and in the mean time bang-bang type of power control is used.

Finally, we note that our work opens possibility to have a power control algorithm that is between the fully distributed and the centralized ones.

Chapter 6

Generalized constrained power control

The *distributed constrained power control* (DCPC) is one of the most widely accepted algorithms by the academic community. It provides guidelines in designing power control algorithms for practical cellular systems and also constitutes a building block for other radio resource management algorithms.

With respect to *energy efficiency*, DCPC has a drawback that the power may reach the maximum level when a user is experiencing low channel quality. Unfortunately, even if the maximum power is used, this may not necessarily lead to sufficient improvement on channel quality. The impact will be high on power consumption and a severe interference, affecting other users. Therefore, in this chapter, we revisit and generalize DCPC in order not to necessarily use the maximum power when the channel quality is poor. Under poor conditions, the power may even be lowered to the minimum level, which we will call *temporary removal*. In that case, the user stays on the same channel and transmission will be resumed if the interference situation becomes favorable. In power control, if the power consumption level of a given algorithm were relatively low, it would be a great advantage, especially to the mobiles that could expect a prolonged operational time. In section 6.1, we explain how the generalized algorithm can improve the energy efficiency. In section 6.2, we show that, for the feasible system, the generalized algorithm converges to the fixed point that supports every active transmitter, as DCPC does. Based on the generalization, we suggest two power control algorithms and compare them with DCPC.

The dynamics of the two proposed algorithms in the infeasible case are discussed in section 6.3. When the system is infeasible so that all the active transmitters cannot be supported, some sort of *permanent* removal of users, e.g. handing over to another channel or dropping of users, is necessary to maximize the network capacity. For the infeasible system, we evaluate the suggested algorithms by combining them with the so called *gradual removal* [6] and compare the combined algorithms with GRR-DCPC [6].

Computational experiments on a DS-CDMA system, given in section 6.4, indicate that the suggested algorithms consume less energy while supporting more transmitters than DCPC.

6.1 Energy efficiency

The distributed constrained power control algorithm (DCPC), as explained in section 3.2.2, is given by

(**DCPC**)

$$\mathbf{p}(n+1) = \min\{\bar{\mathbf{p}}, \boldsymbol{\mathcal{I}}_{DCPC}(\mathbf{p}(n))\} \stackrel{\text{def}}{=} \boldsymbol{\mathcal{T}}(\mathbf{p}(n)) \tag{6.1}$$

where $\boldsymbol{\mathcal{I}}(\mathbf{p}(n)) = \mathbf{H}\mathbf{p}(n) + \boldsymbol{\eta}$.

Now consider the following generalized constrained power control algorithm:

(**GDCPC**)

$$p_i(n+1) = \begin{cases} \mathcal{I}_{DCPC_i}(\mathbf{p}(n)), & \mathcal{I}_{DCPC_i}(\mathbf{p}(n)) \leq \bar{p}_i \\ \tilde{p}_i(n), & \text{otherwise} \end{cases} \tag{6.2}$$

$$\stackrel{\text{def}}{=} \mathcal{G}_i(\mathbf{p}(n)) \tag{6.3}$$

where the power value $\tilde{p}_i(n)$ is taken within the range of (3.3). If we choose $\tilde{p}_i(n) = \bar{p}_i$, GDCPC is reduced to DCPC. When setting $\tilde{p}_i(n) = 0$, it can be interpreted as a temporary connection removal, allowing the removed user to stay on the channel and power up again if the interference has decreased. By setting the transmit power to zero, the user will not waste energy mitigating bad channel conditions and other users will benefit from lower interference. When $\tilde{p}_i(n) \neq \bar{p}_i$, GDCPC can not be described as general constrained iteration given by (3.24). Furthermore it violates the *monotonicity* property, and thus it is not a *standard interference function*. Thus neither of the two frameworks described in section 3.2.2 can be directly applied. However, we can prove the convergence of GDCPC to $\mathbf{p}^*$ in the feasible case, which will be given in the next section. To motivate the readers, we will first describe the energy saving property of GDCPC.

To simplify our notation in this chapter, let us redefine $\boldsymbol{\mathcal{T}}_{GDCPC} = \boldsymbol{\mathcal{G}}$, $\boldsymbol{\mathcal{T}}_{DCPC} = \boldsymbol{\mathcal{T}}$ and $\boldsymbol{\mathcal{I}}_{DPC} = \boldsymbol{\mathcal{I}}$.

Lemma 6.1. *$\boldsymbol{\mathcal{G}}^n(\mathbf{p}) \leq \boldsymbol{\mathcal{T}}^n(\mathbf{p}) \leq \boldsymbol{\mathcal{I}}^n(\mathbf{p})$ for all n and $\mathbf{p} \geq \mathbf{0}$.*

Proof. From definition of $\boldsymbol{\mathcal{I}}(\mathbf{p})$ and $\boldsymbol{\mathcal{T}}(\mathbf{p})$, we find that if $\mathbf{0} \leq \mathbf{q} \leq \mathbf{p}$, then $\boldsymbol{\mathcal{I}}(\mathbf{q}) \leq \boldsymbol{\mathcal{I}}(\mathbf{p})$ and $\boldsymbol{\mathcal{T}}(\mathbf{q}) \leq \boldsymbol{\mathcal{T}}(\mathbf{p})$. In addition $\boldsymbol{\mathcal{G}}(\mathbf{p}) \leq \boldsymbol{\mathcal{T}}(\mathbf{p}) \leq \boldsymbol{\mathcal{I}}(\mathbf{p})$. It follows that

$$\boldsymbol{\mathcal{I}}(\boldsymbol{\mathcal{G}}(\mathbf{p})) \leq \boldsymbol{\mathcal{I}}(\boldsymbol{\mathcal{T}}(\mathbf{p})) \leq \boldsymbol{\mathcal{I}}(\boldsymbol{\mathcal{I}}(\mathbf{p})) \tag{6.4}$$

Since

$$\boldsymbol{\mathcal{T}}(\boldsymbol{\mathcal{T}}(\mathbf{p})) \leq \boldsymbol{\mathcal{I}}(\boldsymbol{\mathcal{T}}(\mathbf{p})) \tag{6.5}$$

and

$$\boldsymbol{\mathcal{G}}(\boldsymbol{\mathcal{G}}(\mathbf{p})) \leq \boldsymbol{\mathcal{T}}(\boldsymbol{\mathcal{G}}(\mathbf{p})) \leq \boldsymbol{\mathcal{T}}(\boldsymbol{\mathcal{T}}(\mathbf{p})), \tag{6.6}$$

it follows that

$$\boldsymbol{\mathcal{G}}(\boldsymbol{\mathcal{G}}(\mathbf{p})) \leq \boldsymbol{\mathcal{T}}(\boldsymbol{\mathcal{T}}(\mathbf{p})) \leq \boldsymbol{\mathcal{I}}(\boldsymbol{\mathcal{I}}(\mathbf{p})). \tag{6.7}$$

By repeating the above reasoning n times, we get

$$\boldsymbol{\mathcal{G}}^n(\mathbf{p}) \leq \boldsymbol{\mathcal{T}}^n(\mathbf{p}) \leq \boldsymbol{\mathcal{I}}^n(\mathbf{p}) \tag{6.8}$$

□

Proposition 6.1. *If there exits n_0 and at least one i such that $\mathcal{I}_i^{n_0}(\mathbf{p}) > \bar{p}_i$, $\mathcal{I}_j^n(\mathbf{p}) \leq \bar{p}_j$, $n < n_0$ for all j and furthermore if $\tilde{p}_i(n) < \bar{p}_i$ for all n, then*

$$\sum_{i=1}^{M} \mathcal{G}_i^n(\mathbf{p}) < \sum_{i=1}^{M} \mathcal{T}_i^n(\mathbf{p}) \quad \forall n > n_0$$

Proof. By lemma 6.1, we have $\boldsymbol{\mathcal{G}}^n(\mathbf{p}) \leq \boldsymbol{\mathcal{T}}^n(\mathbf{p})$, thus it is sufficient to show that $\mathcal{J}(n) \neq \emptyset$ for all $n \geq n_0$ where $\mathcal{J}(n) = \{j : \mathcal{G}_i^n(\mathbf{p}) < \mathcal{T}_i^n(\mathbf{p})\}$. At iteration n_0, $i \in \mathcal{J}(n_0)$ because $\mathcal{G}_i^{n_0}(\mathbf{p}) = \tilde{p}(n_0) < \bar{p}_i = \mathcal{T}_i^{n_0}(\mathbf{p})$. At iteration $n_0 + 1$, from definition of $\mathcal{T}_i(\mathbf{p})$, we find that $\mathcal{G}_j^{n_0+1}(\mathbf{p}) < \mathcal{T}_j^{n_0+1}(\mathbf{p})$ for all $j \neq i$ thus $\mathcal{J}(n_0 + 1) \neq \emptyset$. In the same manner, we can see that $\mathcal{J}(n) \neq \emptyset$ hold for all $n > n_0$. □

Note that lemma 6.1 and proposition 6.1 are general and hold for both feasible and infeasible systems. Lemma 6.1 says that when starting from the same initial power vector, the power value from GDCPC is not greater than that of DCPC. Further, if there is an event that the required power is greater than the maximum allowed level, then from proposition 6.1, we can expect a certain amount of energy saving from GDCPC, compared with DCPC. For $\tilde{p}_i(n)$ of GDCPC, we can use any nonnegative value less than or equal to $\bar{p}_i$. However, from the proof of proposition 6.1, the setting $\tilde{p}_i(n) = 0$ will lead to the most energy-saving results. For simplicity, we will denote this version of GDCPC by GDCPC(I) throughout the chapter.

6.2 Convergence in feasible systems

As stated earlier, the convergence of GDCPC can be proven in the feasible case. Thus we have,

Proposition 6.2. *GDCPC converges to $\mathbf{p}^*$ of a feasible system, starting from any power vector $\mathbf{p}(0)$ that is in the range of (3.3).*

Proof. By lemma 6.1, we have

$$\boldsymbol{\mathcal{G}}^n(\mathbf{p}) \leq \boldsymbol{\mathcal{T}}^n(\mathbf{p}) \tag{6.9}$$

It was shown in section 3.2.2 that DCPC is a special case of general constrained iteration, so we know that in feasible case $\boldsymbol{\mathcal{T}}$ is a pseudo-contraction mapping. Therefore we can show, as in the proof of corollary 5.4, that there exits n_0 such that $\boldsymbol{\mathcal{T}}^n(\mathbf{p}) < \bar{\mathbf{p}}$ for all $n > n_0$. It follows that $\boldsymbol{\mathcal{G}}^n(\mathbf{p}) = \boldsymbol{\mathcal{I}}^{n-n_0}(\boldsymbol{\mathcal{G}}^n(\mathbf{p})) \leq \bar{\mathbf{p}}$ for all $n > n_0$ and the convergence of GDCPC follows from the convergence of DPC. □

Remark 6.1. So far we have focused on generalizing DCPC but similar results can be derived for other standard power control algorithms, like BPC and the general minimum power assignment algorithm [37], as well.

Besides the energy consumption, we are very interested in how fast the power value will converge. It has been reported that DCPC converges to $\mathbf{p}^*$ at a geometric rate [31, 37]. So far the convergence rate of GDCPC is an open issue. However, if we choose

$$\tilde{p}_i(n) = \max\{0, 2\bar{p}_i - \mathcal{I}_i(\mathbf{p}(n))\} \tag{6.10}$$

and denote this by GDCPC(II), then we have the following:

Proposition 6.3. *GDCPC(II) converges to* $\mathbf{p}^*$ *of a feasible system with the same geometric rate as DCPC starting from any power vector* $\mathbf{p}(0)$ *that is in the range of (3.3).*

Proof. Clearly $\max\{2\bar{p}_i - \mathcal{I}_i(\mathbf{p}(n))\} < \mathcal{I}_i(\mathbf{p})$ if $\mathcal{I}_i(\mathbf{p}) \geq \bar{p}_i$. Thus it follows that

$$\|\boldsymbol{\mathcal{G}}(\mathbf{p}(n)) - \mathbf{p}^*\|_\infty^{\mathbf{W}} \leq \|\boldsymbol{\mathcal{I}}(\mathbf{p}(n)) - \mathbf{p}^*\|_\infty^{\mathbf{W}} \leq \|\mathbf{H}\|_\infty^{\mathbf{W}} \|\mathbf{p}(n) - \mathbf{p}^*\|_\infty^{\mathbf{W}} \tag{6.11}$$

and we can conclude that $\boldsymbol{\mathcal{G}}$ is a pseudo-contraction mapping with rate $\|\mathbf{H}\|_\infty^{\mathbf{W}}$. □

With respect to proposition 6.3, we conclude that within the class of GDCPC, there exits at least one $\tilde{p}_i(n) \neq \bar{p}_i$ which gives the same convergence rate as DCPC and possibly increases the energy efficiency. In GDCPC(II), if the required power is larger than the maximum power $\bar{p}_i$, a power lower than $\bar{p}_i$ by the amount of the gap between the required power and $\bar{p}_i$ is used. If the required power is twice larger than the maximum power, the transmitter power is set to zero. Note that $\tilde{p}_i(n) < \bar{p}_i$ in GDCPC(II), and proposition 6.1 is applicable to GDCPC(II).

6.3 Convergence in infeasible systems

So far, in this chapter the emphasis has been on feasible systems. In the infeasible case, the DCPC is known to converge to a state where some (or all) of the powers reach the maximum value while the corresponding users are not supported. In GDCPC, however, convergence does not necessary occur if $\tilde{p}(n) < \bar{p}$.

In figure 6.1, a two-dimensional example of a noise-limited infeasible system in which $\rho(\mathbf{H}) > 1$ and maximum power of each mobile set to one, illustrates the possible fixed points. In addition one possible trajectory of DCPC, GDCPC(I) and GDCPC(II) is given. The dotted line represents the trajectory of DCPC starting from $\mathbf{p}(0)$ and the thin solid line is the trajectory of GDCPC(II) starting from the same point. In this special case the trajectory GDCPC(I) coincides with the trajectory of GDCPC(II) for

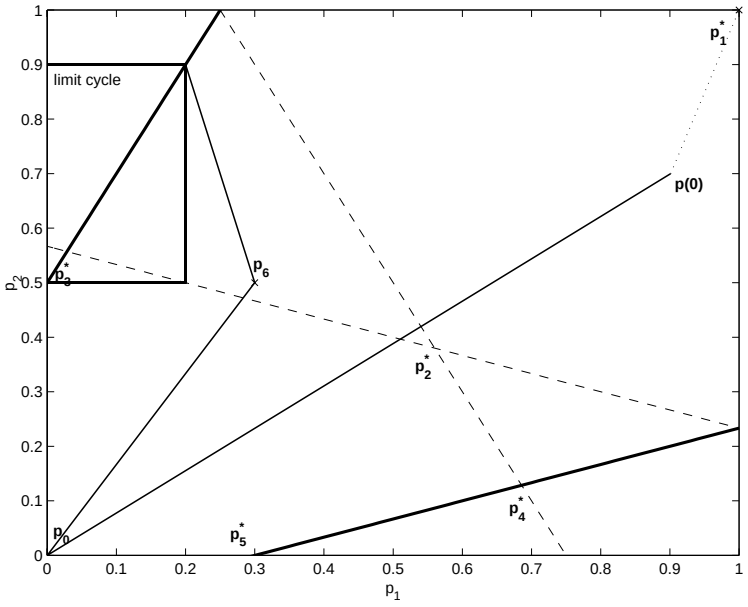

Figure 6.1: Trajectories and possible fixed points of DCPC, GDCPC(I) and GDCPC(II).

the three first points after which it oscillate between $\mathbf{p}_0$ and $\mathbf{p}_6$. The thick solid lines denote the CIR-targets (constrains) and the dashed lines represent equation (6.10) that could be interpreted as *virtual* targets.

In this example no more than one user can be supported. Hence the optimal fixed point would be $\mathbf{p}_5^*$ where user 1 is supported with the minimum power. The fixed point of DCPC will in this case be $\mathbf{p}_1^*$ due to the power constraints. Clearly this point is the worst, considering no user is supported while the power usage is maximized. GDCPC(I) will, depending on the starting point, oscillates between $\mathbf{p}_0$ and $\mathbf{p}_6$ or converge to $\mathbf{p}_5^*$. In GDCPC(II), the fixed point may be the intersection between the virtual targets, $\mathbf{p}_2^*$ or the intersection between virtual and real targets denoted by $\mathbf{p}_3^*$ and $\mathbf{p}_4^*$. However, GDCPC(II) unlike DCPC does not always converge to a fixed point. As illustrated in the figure 6.1, GDCPC may converge to a limit cycle.

As described above GDCPC(I) and GDCPC(II) may converge to a fixed point but the dynamics are more unpredictable. Due to the possibility of oscillating powers, each user may generally expect a more varying CIR and its impact on the bit error rate is not clear. Depending on power control interval, coding and interleaving strategies, the oscillation of CIR may or may not cause problems. For example if the data packet size is as short as the power control interval oscillating CIR (and thereby outage) could be interpreted as time sharing via power control. If on the other hand data packets are longer than one power control interval, then oscillating CIR causes additional symbol errors or erasures that the coding should correct. Thus stronger coding must be utilized

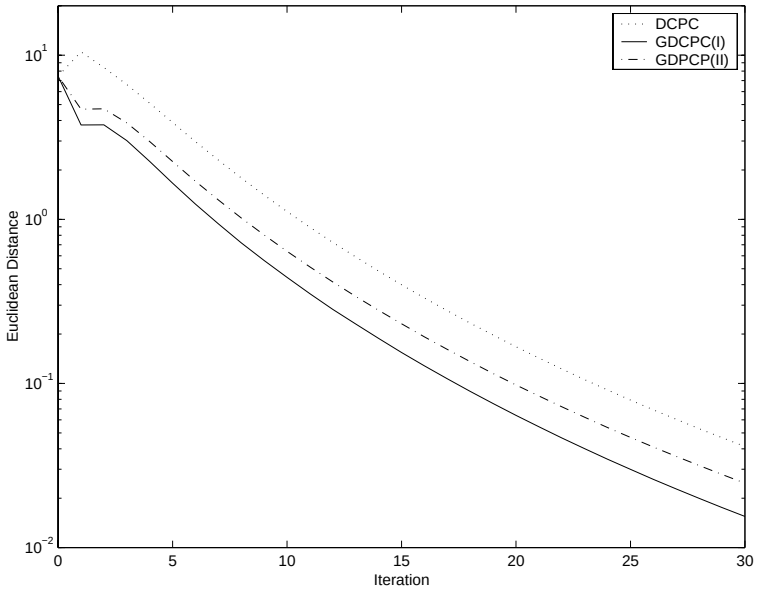

Figure 6.2: Euclidean distance between current power vector and $\mathbf{p}^*$.

to cope with oscillating CIR.

For an infeasible system, permanent connection removal could be utilized to increase system capacity. In GDCPC(I) and GDCPC(II), the powers may oscillate, and thus certain removal algorithms relying on convergence to some fixed points may not be utilized. For the purpose of permanent removal, we extend the previously suggested GRR-DCPC [6], which is an "on-the-fly" gradual removal combined with DCPC. Instead of DCPC, we combine the gradual removal with GDCPC(I) and GDCPC(II). That is, our modified gradual removal algorithm, which incorporates both temporary- and permanent removal GRR-GDCPC identifies user i as a candidate for permanent removal if $\mathcal{I}_i(\mathbf{p}(n_0)) > \bar{p}_i$ and sets $p_i(n) = 0$, with a given probability $\delta > 0$ for all $n > n_0$. Otherwise, $p_i(n_0 + 1) = \mathcal{G}_i(\mathbf{p}(n_0))$ and the power control proceeds with the next power iteration. In order to maximize system capacity, the removal probability δ, should be taken so that in each iteration, single removal is more probable than multiple removals. It has been shown that GRR-DCPC converges to a stationary power vector [6]. Since GRR-GDCPC uses the same decision procedure as GRR-DCPC, it is clear that also GRR-GDCPC converges.

6.4 Computational results

The main purpose of the experiments is to draw insight on how GDCPC(I) and GDCPC(II) perform in terms of energy saving, convergence and system capacity. To compare the performance of our proposed algorithms, we use DCPC as a reference

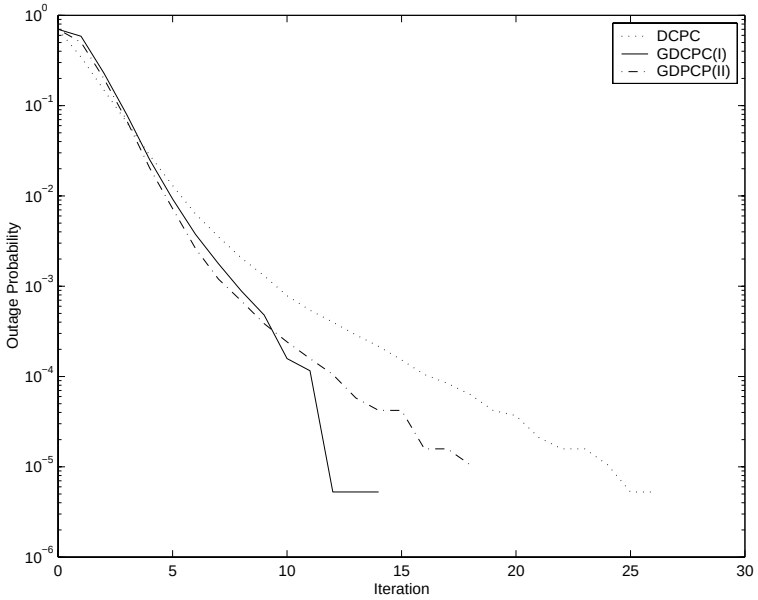

Figure 6.3: Outage probability in feasible case.

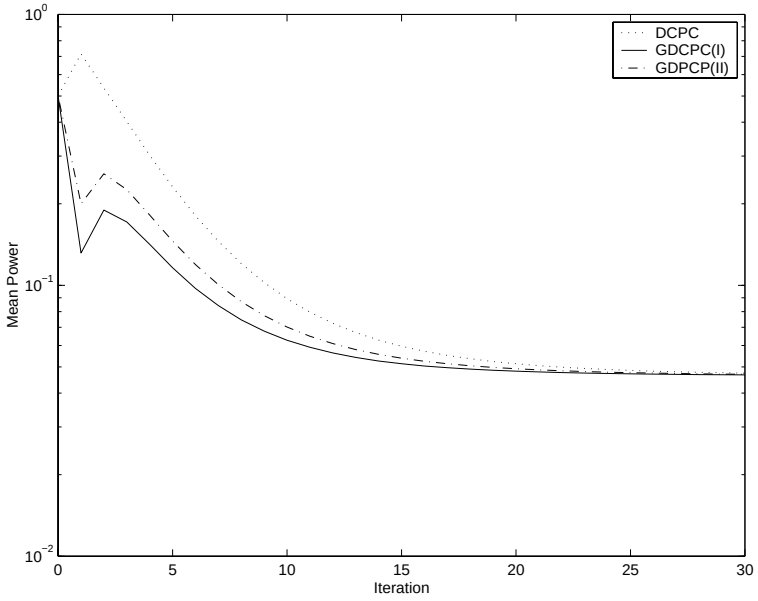

Figure 6.4: Mean transmission power in feasible case.

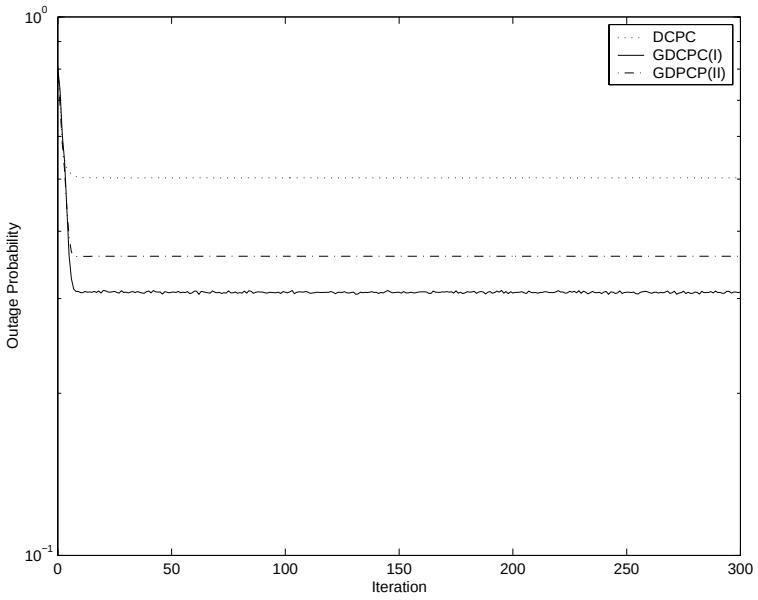

Figure 6.5: Outage probability in infeasible case.

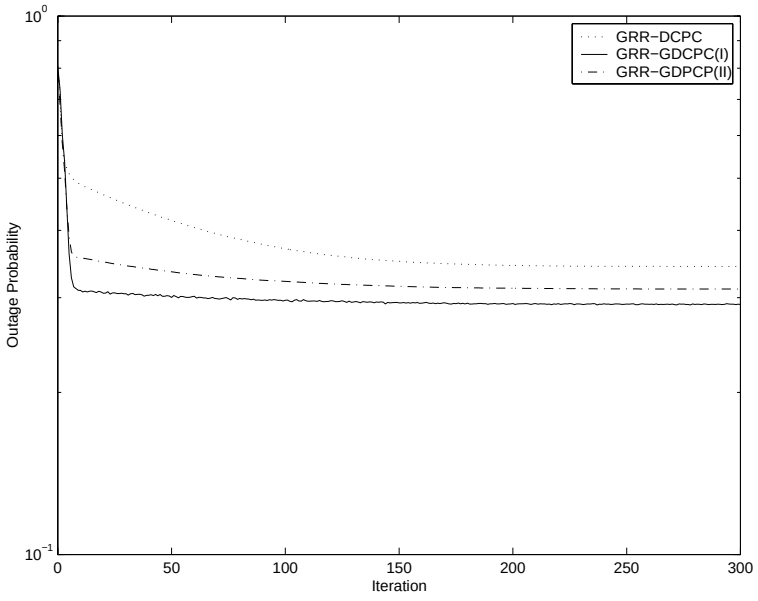

Figure 6.6: Outage probability in infeasible case with permanent removal.

algorithm. A DS-CDMA system with 19 omni-bases located in the centers of 19 hexagonal cells is used as a test system (figure 2.1). We consider an uplink example, in which the *processing gain* is 128 (21 dB). For a given instance, a total of 190 mobiles are generated, the locations of which are uniformly distributed over the 19 cells. The target SIR is set to 8 dB and 12 dB for each mobile when analyzing a feasible and an infeasible system, respectively.

As before the *outage probability* is used as a performance measure. The outage probability at each iteration is computed over the 1000 instances by counting the portion of the number of non-supported mobiles at the iteration. A connection is considered to be supported if SIR is above 7.5 dB in feasible case and above 11.5 dB in infeasible case. That is we have considered 0.5 dB SIR-margin.

In figure 6.2, the Euclidean distance between the current power vector and fixed point is shown. The figure indicates that GDCPC(I) is faster than GDCPC(II) and DCPC, both of which are proved to converge with a geometric rate. In figure 6.3, we see that the outage probability is lower over the whole range of iterations considered (except for the initial iterations) for both GDCPC(I) and GDCPC(II), compared to DCPC. It means that GDCPC(I) and GDCPC(II) support more users in average than DCPC during the iterations. Based on simulation results GDCPC(I) seems to outperform GDCPC(II) in terms of outage performance. The energy saving property is shown in figure 6.4, where obviously GDCPC(I) gives the best performance in both feasible and infeasible systems. The curves of GDCPC(I) and GDCPC(II) indicate that there are many mobiles in which the required power at iteration 1 is greater than the maximum and the rest of the iterations follow proposition 6.1. In conclusion, GDCPC(I) shows the best performance in terms of system capacity, energy saving and convergence speed, in the feasible systems.

Now let us consider the outage probability for infeasible systems. As can be seen in figure 6.5, where we compare GDCPC(I), GDCPC(II) and DCPC, both GDCPC(I) and GDCPC(II) support more mobiles in average than DCPC. However, the oscillating behavior is still seen, despite the use of 0.5 dB SIR-margin and averaging over 1000 snapshots, in GDCPC(I) while GDCPC(II) gives smoother outage. Compared with figure 6.5, the outage from DCPC and GDCPC(II) is decreasing when combined with gradual removal, while no significant difference is seen for GRR-GDCPC(I), according to figure 6.6. Thus GDCPC(I) alone seems to identify a proper number of mobiles for temporary removal at an early stage given that a proper SIR-margin is utilized. Although the outage was not improved, combining GDCPC(I) with gradual removal will guarantee convergence and therefore eliminate the oscillations in SIR. Also, note that both GRR-GDCPC(I) and GRR-GDCPC(II) are superior to GRR-DCPC that was known to be one of the best distributed removal algorithms [6].

6.5 Concluding remarks

In this chapter, we have proposed algorithms that are consuming less power and supporting more users than DCPC. The proposed algorithms are based on our general framework. The idea is that, when a user requires more power than is available, the

power will be decreased to benefit other users under favorable situations. It was shown that our algorithms converge to the fixed point of a feasible system, supporting every active user. For an infeasible system, convergence to a fixed point was exemplified not to necessarily occur. For that case, it was seen that power oscillations may cause a rapidly varying CIRs. However, this may not be a major obstacle, since the power control can be combined with a permanent removal algorithm. The difficulty with the proposed algorithms is that infeasibility may not be detected as for DCPC. This raises the question of how to combine a permanent removal algorithm with the proposed algorithms. We propose one possible approach by modifying a gradual removal algorithm that was originally designed for use with DCPC.

The practical applicability of the concept of temporary removals, which GDCPC(I) and GDCPC(II) benefit from, could for example be non-real time traffic where the flexibility of handling the transmission attempts is larger. Finding necessary and sufficient conditions for convergence for infeasible systems is still an open issue. Also, there is a possibility of designing more sophisticated removal algorithms suitable for our algorithms.

Finally, we would like to mention energy management, which was emphasized in [99]. It is expected that the need for low-power design principles will increase along with the more services available. Improving energy efficiency is of interest for both the operators (downlink) as well as for the customers (uplink). Therefore such design principles include all levels of the system, e.g., network architecture, circuit design, protocols and resource management algorithms. Our work can be considered as an effort to provide an energy efficient resource management.

Chapter 7

Radio resource knapsack packing

In this chapter, we consider data traffic in a bunched DS-CDMA system. Our assumption is that the incoming data bursts are converted into data packets that are one frame long (i.e. it takes one time period, called a frame, to send the whole packet with some fixed rate r_{2i}). The goal is to decide in the beginning of a frame which users are allowed to transmit (which packet are to be transmitted) so that the system is feasible during the frame. This problem is a special case of the combined power control and transmission rate selection problem, described in section 3.3, in which $K = 2$, $r_{i1} = 0$ and $r_{i2} \neq 0$. This problem has been considered in [47] where Lagrangian relaxation technique was used for deriving distributed removal algorithms by dualizing constraint (3.43). Based on the results in [22], it can be shown that dualizing constraint (3.42) leads to 0-1 knapsack problem. Instead of using the lagrangian relaxation technique, we first redefine the utility function (3.41) and then suggest a heuristic method similar to the knapsack packing method to maximize it.

The method considered here differs form the one suggested in [47] by the fact that our method tries to decide before transmission which users are allowed to transmit (which packets to send) during the next frame, while the the removal algorithm in [47] makes the decision after the transmission has begun. The other difference is that our method requires full knowledge about the link gain matrix within the bunch while the method in [47] is fully distributed and requires only knowledge about the received CIR. The radio resource knapsack packing method considered here is modification of the method suggested in [49] and it is similar to the bunched radio resource management algorithms suggested in [14, 13].

7.1 Problem formulation

The radio resource knapsack problem is based on the traditional knapsack problem: Maximize the sum of the values of the items included into knapsack within some known capacity limit. In our case the items (data packets to be transmitted) interfere with each other and thus the capacity limit in terms of number of users is not known.

We consider the following utility function

$$W = \sum_{i=1}^{M} W_i \stackrel{\text{def}}{=} \sum_{i=1}^{M} w_i f_i(\mathbf{p}) \tag{7.1}$$

in which the w_i corresponds to the value (reward that the operator gains by successfully transmitting the packet) of the packet. For example real time traffic should have higher value than non-real time traffic. The function $f_i(\mathbf{p})$ corresponds to the probability that the packet will be received correctly.

The packet transmission can further benefit from efficient ARQ-methods (Automatic Repeat reQuest), which gain energy also from the packets whose CIR-values are under the prefixed CIR-thresholds. The ARQ procedure will collect bit-energy of the packet by requesting the same packet to be transmitted again until the cumulative CIR sum yields a correctly received packet (see e.g. [58]). The ARQ-scheme, benefits also from those packets whose received CIR-values are below the set CIR-threshold and justifies giving value to partially received packets in (7.1).

7.2 Packing Algorithm

Because in the radio resource knapsack there is finite number of possible combinations, one method to find the optimal packing is to search all possible combinations and choose the best i.e. the one which gives the largest value of the utility function. This method is known to be NP-complete (non-polynomial) and is not efficient. To optimize the utility function there are much more efficient methods which do not perhaps give the global optima but very near to that in short search time. For example gradient-based methods can be used to find the optimal powers after allocation decisions. In here, the allocation by using dynamic programming based scheduling is considered. For each packet, which is at a time instant under consideration to be packed into the knapsack (called trial packet), the frame will be searched where the increase in the value of the total utility function of the knapsack is maximal if the new packet is allocated. If the value of the utility function does not improve in any frame, a frame is selected where the value decreases least. Allocation of the new packet follows the set of rules (see also B):

- **Rule 1:** It is required that the CIR-value of each packet is above some given threshold value (lower bound). This lower bound can be for example 3 dB for NRT-packets if the CIR-threshold for correctly received packet is 6 dB. Usually if some packet is not above the lower bound, it will remain in the transmission buffer of its base station. The lower bound of the RT-packets should be same as the CIR-threshold set for correctly received packets, since ARQ can not be applied.

- **Rule 2:** It is required that the contribution of each packet to the utility function W of the knapsack is above some given threshold. If it is not, the packet will remain in the base station buffer.

- **Rule 3:** If either rule 1 or rule 2 is not satisfied for some packets (called unfeasible packets), certain alternative choices are examined. Note that the trial packet can be an unfeasible packet as well. The alternatives are examined packet by packet for the unfeasible packets. This means that alternatives are checked first for the packet whose contribution to the total utility function of the knapsack has decreased most after the allocation of the new packet. If some changes are done to the already packed packets, the new CIR-value and new utility function value for each interfering packet are calculated again. If there are still some unfeasible packets, the alternatives will again be checked for those packets whose contribution to the utility function of the knapsack has decreased most after the allocation of the new packet.
- **Alternative 1** If some packet does not satisfy the rules above, this packet is tried to be changed with the most valuable feasible packet in the buffer.
- **Alternative 2** If the packet does not satisfy the rules above, it is left in the knapsack if the value of the utility function of the knapsack is more than it is when alternative 1 is selected.
- **Alternative 3** If a packet does not satisfy any of the rules above, the packet is removed from the knapsack, only if the value of the utility function of the knapsack is more than it is when alternative 1 or 2 is selected.

The frames of the first base station in the knapsack will be packed up to their capacity with the most valuable packets. This is done so that the most valuable packet at the moment is put to the most suitable frame in the knapsack. Then the secondmost valuable packet is considered and so on. For fairness reasons there should be a limit on how many packets one user is allowed to transmit in a frame. When the first base station's part of the knapsack is full, the packing continues in the next base station. Each base station is packed up to its capacity before the next base station is started to be packed. The packets are packed using the rules and in decreasing order of the value.

In addition, there is an option of the macro diversity. This means that the packet is transmitted from at least two different base stations or base station sectors. This is done by following the above rules. The CIR-value of that packet depends on how the packet combining is done at the receiver.

7.3 Power allocation

Independently of the method which is used to pack the packets into the frames of considered knapsack, the used powers can after packing be balanced so that they will maximize a given utility function, W. The optimal power allocation method is based on the maximization of the same (or same kind of a) utility function as in the knapsack packing. The optimization is done separately for each frame of the knapsack.

One iterative method to find the (sub)optimal initial transmission powers is as follows:

- For $i = 1 : M + 1$
  Step 1 Set counter, $c = 1$. Calculate the utility value of each interfering packet, W_i using the current transmission powers.
  Search for he packet whose utility value, W_i is the t^{th} lowest. Here $t = c$. Then calculate the utility values, W_i for each interfering packets after the transmission power of the considered packet is increased with some set fixed amount. The transmission power of the considered packet will be increased if the value of the utility function increases. If the value does not increase, the original transmission power of the considered packet remains valid. If the power is changed, then set $c = 1$ else set $c := c + 1$. The transmission powers p_i (i=1,2,...,M) are bounded between 0 or some other lower limit and $\bar{p}_i$. If the calculated powers are outside the bound, they are set to the closest limit.

  Step 2 If $c \leq M$, goto step 1. Else if $c = M + 1$, the power control procedure is stopped and (sub)optimal powers are found. This means that the total utility function does not increase any more. After that the algorithms will be used in the next frame of the knapsack.
  The trial packet will be discarded and put back to the buffer, if the CIR-value of a packet will decrease under the lower bound or the value of the utility function without this packet is higher than with this packet.

The knapsack packing and the optimal power control procedures should be applied together so that first the packets are packed using the scheduling method presented and then the powers are adjusted to maximize the utility function. Optimization of the powers can be done after every k^{th} ($k \geq 1$) packet is included in the knapsack.

Alternative method for finding the optimal initial power vector is to solve the power control problem (3.2) in the subspace of users (packets) included in the knapsack. If the dimension of the subspace is large, this will become computationally intensive. The need for reducing the amount of computations was the main motivation for introducing the above method.

In this power control scheme the fast closed-loop power control is not continuous and thus the knowledge about fast fading conditions are lost in the beginning of each frame. To reduce this error by open loop power control, closed-loop power control history can be used. One way of utilizing the power control history is to divide the link gain estimate between the mobiles and the serving base station by the product of past control actions, i.e. the link gain estimate g_{ii}, obtained by averaging over F_w frames, should be multiplied by factor, $\hat{c}_{ii}$:

$$\hat{c}_{ii}(F) = \frac{1}{\prod_{f=F-F_w}^{F-1} \prod_{c=1}^{C} u_i(f,c)} \tag{7.2}$$

where F is the number of current frame, F_w is the length of time window (in frames) and C is the number of power control steps in a frame. The variable $u_i(f,c)$ is the c^{th} control action taken ($\pm\Delta$ dB in the case of bang-bang control) in frame f by user i. If user i was not allowed to transmit a packet during a frame f then $u_i(f,c) = 1$ for all c. When the fading estimate is exploited, the open loop power control error

decreases provided that the probability of power control error is small. This implies that scheduling of packets is made more cautiously: the probability of a successful reception of the packets increases and the required transmission power decreases.

7.4 Computational results

We consider the downlink case of a DS-CDMA highway cellular system. Only non-real time traffic is considered, and all the incoming data burst are converted into equal sized packets. The processing gain is set to 64 (18 dB). One knapsack consist of five base stations and one frame. A frame is divided into 16 power control slots. The number of mobiles per cell is fixed and set to 50. The mobiles are assumed to be slowly moving at walking speed. The effect of shadow fading and the change in propagation parameter due to mobility are ignored. We consider both pseudorandom ($\theta_{ij} = 1$ for all i, j) and orthogonal codes within one cell ($\theta_{ij} = 0.4$ if users i and j are assigned to the same base station, otherwise $\theta_{ij} = 1$). In the first case, the interference power is high and thus it can be interpreted as being a heavy load case. Whereas, in the second case the interference power is smaller and thus we call it a medium load case.

As a closed loop power control method we apply the bang-bang controller. The SIR-target was set to 7 dB and 1 dB SIR-margin was used. The power control step size, Δ was set to 1 dB.

The utility function was chosen to be

$$W_i = w_1 x_i + w_2 \frac{g_i(\gamma_i)}{\gamma_i^t} \tag{7.3}$$

where x_i is set to one if current packet of user i is an ARQ packet (i.e. the last packet of that user was not received correctly) and zero otherwise. The weights are chosen to be $w_1 = 1$ and $w_2 = 0.1$. This is to force ARQ packets to get accepted into the knapsack. Similarly, we could increase the fairness of the system by giving more value to the packets of users that have not been allowed to transmit anything for a while. In our simulations, however, we are only interested in the overall throughput of the system. The function g_i limits the value of CIR to the range of CIR-target $\pm$ 3 dB for ARQ packets and CIR target + 3dB for others. For example if a user could achieve a CIR of 5 dB and it did receive a packet in the last frame, then $W_i = 0$ and it is not allowed to transmit in the next frame.

We compare our method with a method where each cell is packet with constant number of randomly chosen packets: 10 out of 50 packets in heavy load case and 40 out of 50 packets in medium load case. The number of packed packets is chosen to reflect to the overload case. We call this method as the over load method (OL) and our dynamic programming based method as the knapsack method (KS). The numerical results are obtained by averaging over 30 and 10 independent simulation runs of 10 frames in heavy and medium load cases respectively.

In table 7.1, and figures 7.1 and 7.2, the throughput statistics of both OL and KS methods are shown. The results in table 7.1 are normalized by setting the throughput

Table 7.1: Throughput statistics

algorithm	mean	std	min	max	mean $\frac{\text{kbit/s}}{\text{user}}$
Heavy load					
OL	1.00	0.032	1.93	1.06	1.64
KS	1.75	0.086	1.57	1.96	2.88
Medium load					
OL	1.00	0.032	0.95	1.05	3.54
KS	1.21	0.038	1.15	1.27	4.28

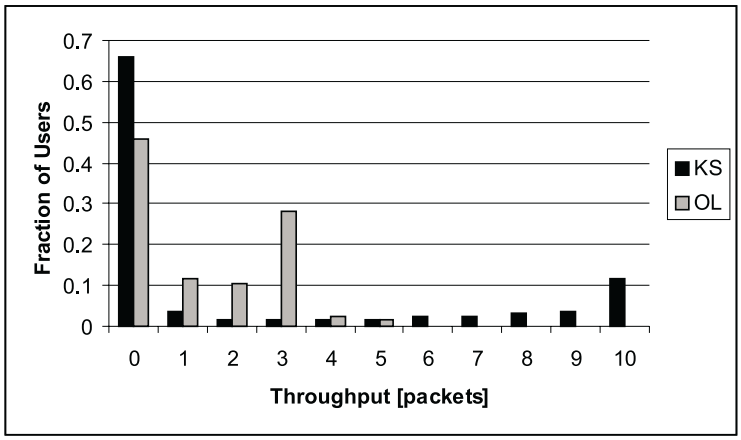

Figure 7.1: The histogram of throughput in heavy load case

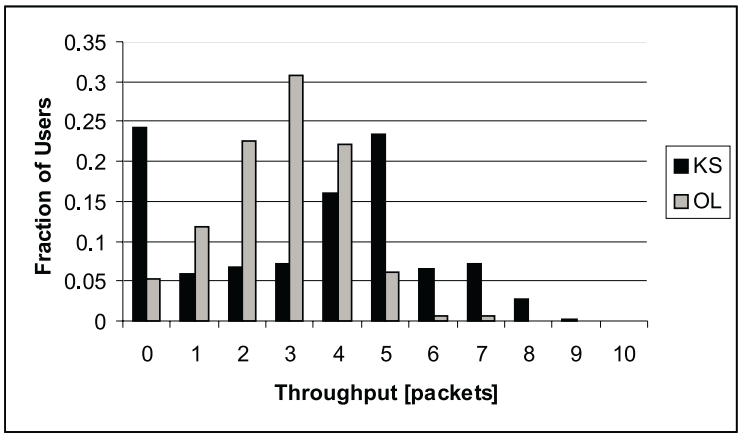

Figure 7.2: The histogram of throughput in medium load case

of the OL method to one. In the case of OL method, the power control problem is infeasible almost all the time, hence the throughput relies heavily on the performance of the utilized ARQ scheme. On the other hand the KS method is able to ensure feasibility and ARQ is only needed to repair the damage caused by the fast fading. As expected, the difference between OL and KS is large in the heavy load case in which the KS method achieves on the average 75% greater throughput. However, in the medium load case the gain of using KS method is on the average only 21%. From figure 7.1, we see that in heavy load case, the KS method favors some of the users (those who are close to the base station), while the others achieve only small or no throughput at all. In medium load case (figure 7.2) the KS method performs more fair. On the other hand, the OL method seems to be rather fair in both cases, but especially in the heavy load case, its performance is rather poor.

7.5 Concluding remarks

In this chapter, we proposed a centralized ("bunched") packet scheduling method that is able to ensure feasibility of the power control problem during the next frame. Gain compared to random packing was up to 75% depending on load.

Although, in this chapter, the radio resource knapsack method was considered in the case of single rate system, we claim that the method could be easily extended to case in which the transmission rates are selected from discrete set of possible rates by allowing each user to allocate several packets into one frame.

Unfortunately the proposed method is not well suited for distributed operation. Therefore, in the next chapter, we consider entirely different approach to the problem.

Chapter 8

Combined transmission rate selection and power control

In this chapter, we examine the combined rate selection and power control problem described in section 3.3. This problem was first addressed in [46] in which two distributed algorithms were suggested. The first one is based on *Lagrangian relaxation technique* and the second one, called *selective power control* (SPC), applies the *Generalized DCPC* and is therefore of special interest to us.

The major drawback of SPC is that it results in oscillatory CIRs and outage probability as a function of iterations. To remove this drawback, we revise SPC by combining it with the *active link protection* (ALP) [12], [10] and *gradual removal* (GRR) [6]. We denote the modified SPC by SPC-ALP. The idea behind SPC-ALP is as follows: ALP admission scheme is used in the admission of new users into the network and also for allowing old users to choose higher rates, SPC is then used to control the transmission rates of the supported users and GRR is to handle the congestion control. SPC-ALP has the same or slightly higher throughput than SPC. The advantage of SPC-ALP over SPC is in smoother CIRs and outage curve. This property is important, since the rapidly varying CIR, caused by the power control dynamics, could increase the number of erroneously received bits and thus require stronger coding. By decreasing the CIR oscillation, we can reduce the amount of the coding and thus increase throughput.

In the next section, we will examine SPC. Then in section 8.2, we will extend it by applying ALP and GRR. Section 8.3 briefly discusses the implementation aspects. Numerical results comparing SPC with SPC-ALP are provided in section 8.4 and finally section 8.5 gives concluding remarks.

8.1 SPC

SPC controls the transmission power as follows

$$p_i(n+1) = \max_j \left\{ \frac{\gamma_{ij}^t}{\gamma_i(n)} p_i(n) \chi \left(\frac{\gamma_{ij}^t}{\gamma_i(n)} p_i(n) \leq \bar{p}_i \right) \right\} \tag{8.1}$$

where $\chi(E)$ is the indicator function of event E ($\chi(E) = 1$ if event E occurs, otherwise $\chi(E) = 0$). SPC can be iterpreted as follows: It is a "recursive" GDCPC in which $\tilde{p}_i(n)$ of the first GDCPC using the maximum target is determined by another GDPC using smaller CIR target and so forth. Thus, it follows from proposition 6.2 that

Proposition 8.1 (Proposition 2 in [46]). *Starting with any power vector within the range of (3.3), SPC converges to a unique power vector* $\mathbf{p}^*$ *(*$\mathbf{0} \leq \mathbf{p}^* \leq \bar{\mathbf{p}}$*) that supports every active mobile with its maximum rate* r_{iK}*, using the minimal total transmission power, if such* $\mathbf{p}^*$ *exists.*

The structure of SPC has interesting similarity with the Combined Cell-Site Selection and Power Control [35], and the Integrated Power Control and Base Station Assignment [92] algorithms. The difference between these algorithms and SPC is that they seek the minimum interference assignment while SPC seeks the maximum. Unfortunately, when the problem is changed from minimization to maximization the convergence property can no longer be guaranteed in general case. This is because in general all the users can not be supported with maximum rate and thereby $\mathbf{p}^*$ does not exist. In section 6.3, it was noted that in infeasible case, GDCPC can result in oscillatory CIRs. Numerical results in [46] indicate that this is the case with SPC.

The actual rate selection function depends on the utilized coding and modulation techniques. In [46], it was assumed that infinitely fast adaptive modulation can be applied so that the transmission rate could be adapted to the received rate. That is, the transmission rate at time instant n depends on the received CIR at the same instant:

$$r_i(n) = \max_j \left\{ r_{ij} : \gamma_{ij}^t \geq \gamma_i(n) \right\} \tag{8.2}$$

In practice, the above can not be realized. Therefore, we suggest a more conservative method that is on the line with the power control part:

$$r_i(n+1) = \max_j \left\{ r_{ij} : \frac{\gamma_{ij}^t}{\gamma_i(n)} p_i(n) \leq \bar{p}_i \right\} \tag{8.3}$$

Depending on the used coding and modulation techniques the oscillatory behaviour of CIR and outage can be disadvantageous. For example, consider a system in which the length of data packet is several power control intervals long, power is controlled using (8.1) and the transmission rate is selected as in (8.3). Since the dynamics of SPC causes oscillating outage probability, some of the users utilizing nonzero rates are in outage at some iteration and supported at the next. When the user is in outage, some blocks of the data packet will be either received erroneously or entirely lost. To compensate for these errors and erasures, either error correction coding or ARQ has to be used. Both these methods decrease the maximum achievable data rate of the system. On the other hand, if the rate would be determined using (8.2) and the data packets would be only one power control interval long, the oscillating outage would not constitute any problem. In that case, the oscillating outage could be interpreted as time sharing of the channel.

8.2 SPC-ALP

In SPC-ALP, once the user is allowed to transmit, the power control tries to guarantee at least the minimum transmission rate to that user for the rest of the time. This means that the CIR of that user should be kept above the CIR target corresponding to the current rate. If there is any excess capacity, SPC-ALP tries to utilize it in the best way by dividing it between the active and the possible new users.

In SPC-ALP, each user has three different modes of operation: *standard*, *transition* and *passive* modes. At iteration n let us denote all the users in the standard mode by set $\mathcal{A}(n)$, all the users in the transition mode by set $\mathcal{B}(n)$ and all the users in the passive mode by set $\mathcal{C}(n)$. In what follows we describe each mode and the mode change conditions, and briefly discuss about the convergence of SPC-ALP.

8.2.1 Standard Mode

The system tries to support at least the minimum transmission rate at each iteration for all the users in the standard mode. In order to support the standard mode users the DPC-ALP power control scheme [12], [10] is utilized. DPC-ALP can be written as

$$p_i(n+1) = \begin{cases} \frac{\delta\gamma_i^t(n+1)}{\gamma_i(n)} p_i(n) & i \in \mathcal{A}(n) \\ \delta p_i(n) & i \in \mathcal{B}(n) \\ 0 & i \in \mathcal{C}(n) \end{cases} \tag{8.4}$$

where $\delta > 1$, $\gamma_i^t(n+1)$ denotes the target CIR of user i and $\gamma_i(n)$ denotes the received CIR value of user i based on the measurements done during the n^{th} iteration. DPC-ALP guarantees that if a user belongs to set $\mathcal{A}(n)$, it will be supported in the future given that the link gains are constant and there is no upper bound for transmission powers:

Proposition 8.2 (Proposition 1 in [12]). *For any fixed $\delta \in (1, \infty)$, we have that for every n and every $\mathcal{A}(n)$*

$$\gamma_i(n) \geq \gamma_i^t(n) \Rightarrow \gamma_i(n+1) \geq \gamma_i^t(n+1) \tag{8.5}$$

under the DPC-ALP updating algorithm. Therefore,

$$i \in \mathcal{A}(n) \Rightarrow i \in \mathcal{A}(n+1) \tag{8.6}$$

Remark 8.1. Note that in [12] it is assumed that $\gamma_i^t(n)$ is constant. However the above still holds if $\gamma_i^t(n+1) \leq \gamma_i^t(n)$.

In practice, we have an upper bound for the transmission power and therefore the above proposition does not necessarily hold. To remedy this problem, we will apply the concept of *distress signaling* [10]. The idea behind distress signaling is that if a supported user notes that utilizing its current transmission rate $r_i(n)$ would cause its power at the next iteration $p_i(n+1)$ to fulfill the inequality (8.7), then the network prohibits all the users in other sets to increase their powers. This procedure guarantees that the user broadcasting the distress signal will be supported in the future.

$$p_i(n+1) = \frac{\delta\gamma_i^t(n)}{\gamma(n)} p_i(n) > \frac{\bar{p}_i}{\delta^m} \tag{8.7}$$

In above, the parameter $m > 1$ is to consider the signaling delay of the distress signal. In practice, broadcasting of the distress signal must be limited to some subset of users (e.g., all the users assigned to one particular base station) and therefore the absolute warranty of support cannot be assured.

In order to stay supported in the case of high interference power, a user can decrease its transmission rate as long as the rate stays greater than the given minimum limit. This can be advantageous, since it may happen that the user i is using relatively high power to achieve moderate rates, but if it would decrease its rate then the other users could use higher rates and the overall throughput might increase. If rate decreasing is allowed, then the rate used at iteration $n+1$ by user i, $r_i(n+1)$, is chosen to be the best possible supportable rate $r_i^*(n+1)$ given by

$$r_i^*(n+1) = \max_j \left\{ r_{ij} : \frac{\delta\gamma_{ij}^t}{\gamma_i(n)} p_i(n) \leq \bar{p}_i \right\} \tag{8.8}$$

If the interference level is high enough, then $r_i^*(n+1)$ does not exist and therefore we cannot support the user i. If the unsupported user is still allowed to transmit, its power will saturate to the maximum value.

We suggest that the distress signal is sent only if it seems that the power of a user already using its minimum rate is drifting towards the maximum value. Under this strategy, the system divides excess resources fairly between all the users while guaranteeing the minimum transmission rate to the standard mode users.

It can be advantageous to remove some of the unsupported users, since this decreases the interference level in the system. This means that some of the unsupported users change their mode from standard to passive mode. Since it may happen that several users meet their maximum power limit simultaneously and if a subgroup of them became passive, then the rest could be supported. Therefore in order to decrease the dropping probability, we suggest a stochastic mode change strategy in which the user makes mode change with a certain probability $\pi_{A\to C}$. This strategy is similar to the *gradual removal* algorithm, GRR-DCPC, suggested in [6]. Of course, some other removal strategies than GRR-DCPC could be utilized in the mode change condition, but the gradual removal was chosen because it is simple and known to perform well.

Since we wanted to use the radio resources in the best way, there must exist a mechanism for increasing the rates of the standard mode users as well. To protect the other standard mode users, a user wishing to increase its rate is only allowed to do so if distress signal was not broadcast. If $r_i(n) < r_i^*(n+1)$, the user i expects that a better rate can be achieved and therefore changes its mode to transition mode.

8.2.2 Transition mode

Transition mode is used by users wishing to increase their transmission rates. They utilize the power control with limited power-up steps (see Equation (8.4)). This kind of power control guarantees that the CIR-values are increasing at each iteration and that the power increase does not harm users in the set $\mathcal{A}(n)$ (see also proposition 8.2).

Proposition 8.3 (Proposition 2 in [12]). *For any fixed $\delta \in (1, \infty)$, we have that for every n and every $\mathcal{B}(n)$*

$$\gamma_i(n) \leq \gamma_i(n+1) \tag{8.9}$$

In the transition mode the transmission rate to be used in the next iteration $r_i(n+1)$ is chosen to be the maximum rate that can be supported with the current power:

$$r_i(n+1) = \max_j \left\{ r_{ij} : \gamma_{ij}^t \leq \gamma_i(n) \right\} \tag{8.10}$$

In order to prohibit the transmission power of transition mode user from blowing up, we should have a mechanism to change mode from transition to either standard or passive mode. We use the following as a decision variable:

$$r_i^*(n+1) = \max_j \left\{ r_{ij} : \frac{\delta \gamma_{ij}^t}{\gamma_i(n)} p_i(n) \leq (1-d_i)\bar{p}_i + d_i p_i(n) \right\} \tag{8.11}$$

where $d_i = 1$ if the distress signal was sent, otherwise $d_i = 0$. If $d_i = 1$, $r_i^*(n+1)$ denotes the maximum rate that the user i can use in standard mode without increasing its power. Else if $d_i = 0$, $r_i^*(n+1)$ is the best possible rate that user i could achieve given that interference and link gain g_{ii} would be constant. If $r_i^*(n+1)$ does not exist, then the user expects not to be supported in the future and changes its mode to passive. If on the other hand the CIR-target corresponding to the rate $r_i^*(n+1)$ is less than or equal to the current CIR value $\gamma_i(n)$, then the user expects to be supported with its best possible rate in the future and thus have no need to further increase its power by δ. Therefore, the user chooses $r_i(n+1) = r_i^*(n+1)$ and changes its mode to standard mode. The CIR-target of that user is chosen to correspond to the rate $r_i^*(n+1)$.

8.2.3 Passive mode

A new user is initially in the passive mode. In addition, a user that cannot be further supported becomes a passive user. In the passive mode, users do not transmit, i.e., $p_i(n+1) = 0$ and $r_i(n+1) = 0$.

To become active a user must choose its initial rate and power, and change its mode to transition mode. The following conservative bound suggested by Bambos in [10] can be used to determine the initial power p_0 in such a way that the propositions 8.2 and 8.3 still hold.

$$p_0 < \frac{\delta - 1}{N_{max} g_{max}} \nu_{min} \tag{8.12}$$

where N_{max} is the maximum number of new users that are allowed to power-up simultaneously, g_{max} is the upper bound of the link gain that a user can have, and ν_{min} is the lower bound for the noise power. In practice, however, the initial power should be chosen to be larger, because using such a small initial power implies that the number of iterations required to increase the CIR value over even the smallest of targets is going to be extremely large. The drawback of larger initial values is, of course, that it can cause some standard mode users to become unsupported. To decrease this probability new transmissions should only be allowed when the distress signal is not broadcast and the number of new users should be limited. We suggest that a passive user changes its mode to the transition mode with certain probability $\pi_{C\to B}$ given that no distress signal is broadcast.

Clearly, equation (8.11) can not be directly applied for choosing the initial rate. But, if the link gain of the new user g_{ii} and the interference power at the receiver i would be known, then $\frac{p_i(n)}{\gamma_i(n)}$ could be replaced by $\sum_{\substack{j=1\\ j\neq i}}^{M} \frac{g_{ij}\theta_{ij}}{g_{ii}} p_j(n) + \frac{\nu_i}{g_{ii}}$ in equation (8.11) and it could be used for determining the initial rate. However, the initial power is expected to be small and thus the user is initially expected to be unsupported. Therefore, for the first iteration of the new user, it is enough to utilize the minimum rate.

8.2.4 Convergence

It follows from the above mentioned mode change criterion that the power vector of SPC-ALP does not generally converge to any fixed point solution. However, the convergence is guaranteed at least in the special case where all the users can be supported with the maximum rate and CIR margin δ.

Proposition 8.4. *If all the users can be supported with maximum rate and CIR-margin $\delta > 0$ simultaneously, SPC-ALP converges to that fixed point solution with probability 1 starting from any power vector within the range of (3.3).*

Proof. Let $\tilde{\gamma}_i^t(n)$ denote the the CIR target utilized by the nonstationary DCPC at iteration n. Then if we choose

$$\tilde{\gamma}_i^t(n+1) = \begin{cases} \delta\gamma_i^t(n+1), & i \in \mathcal{A}(n+1) \\ \delta\gamma_i(n), & i \in \mathcal{B}(n+1) \text{ and } i \notin \mathcal{C}(n) \\ \frac{p_0}{\sum_{\substack{j=1\\ j\neq i}}^{M} f_{ij}p_j(n)+u_i}, & i \in \mathcal{B}(n+1) \text{ and } i \in \mathcal{C}(n) \\ 0, & i \in \mathcal{C}(n+1) \end{cases} \tag{8.13}$$

then the nonstationary DCPC is equivalent to SPC-ALP. Furthermore with sufficiently small p_0, we have $\tilde{\gamma}_i^t(n) \leq \delta\gamma_{iK}^t$ for all n. Let $\boldsymbol{\mathcal{T}}_{DCPC}(\mathbf{p}(n))$ denote DCPC algorithm with $\delta\gamma_{iK}^t$ as CIR-targets, and let $\boldsymbol{\mathcal{T}}_{SPC-ALP}(\mathbf{p}(n), n)$ denote the SPC-ALP algorithm. Clearly

$$\boldsymbol{\mathcal{T}}_{SPC-ALP}(\mathbf{p}(0), 0) \leq \boldsymbol{\mathcal{T}}_{DCPC}(\mathbf{p}(0)) \tag{8.14}$$

It follows that,

$$\begin{aligned} \boldsymbol{\mathcal{T}}_{SPC-ALP}(\boldsymbol{\mathcal{T}}_{SPC-ALP}(\mathbf{p}(0),0),1) &\leq \boldsymbol{\mathcal{T}}_{DCPC}(\boldsymbol{\mathcal{T}}_{SPC-ALP}(\mathbf{p}(0),0)) \quad (8.15) \\ &\leq \boldsymbol{\mathcal{T}}_{DCPC}(\boldsymbol{\mathcal{T}}_{DCPC}(\mathbf{p}(0))) \quad (8.16) \end{aligned}$$

and thus

$$\boldsymbol{\mathcal{T}}^n_{SPC-ALP}(\mathbf{p}(0),n) \leq \boldsymbol{\mathcal{T}}^n_{DCPC}(\mathbf{p}(0)) \quad (8.17)$$

Since it was assumed that all the users could be supported with the maximum rate and CIR-margin δ, it follows that $\boldsymbol{\mathcal{T}}_{DCPC}$ is a pseudo-contraction mapping and thus convergent (proposition 3.10). Therefore, there exits n_0 such that for all $n > n_0$ there does not exist any user that would require more power than $\bar{p}_i$. That is, for $n > n_0$ the propositions 8.2 and 8.2 hold.

As n increases, the right hand side of (8.17) decreases and thus the interference level seen by the users in the transition mode also decreases. Therefore, the target rate of the users not yet utilizing the maximum rate, given by (8.11), increases. By proposition 2, those users have increasing CIRs and thus they will eventually achieve their CIR-targets corresponding to the maximum rate. As $n \to \infty$, all the passive users will change their mode to the transition mode with probability 1. Eventually all the users are in standard mode in which their dynamics are described by the fixed-rate DCPC dynamics. So we can conclude that the SPC-ALP converge to the same fixed point as the fixed-rate DCPC with probability 1. □

8.3 Implementation issues

The combined rate selection and power control algorithm described in the previous section is not directly suitable for practical implementation, because DPC-ALP would require a large bandwidth for the power control commands. Fortunately, the active link protection property can be achieved also by utilizing the bang-bang controller:

Proposition 8.5. *Propositions 8.2 and 8.3 hold for bang-bang controller with a CIR-margin of* δ^2.

Proof. Let $\mathcal{D}(n+1) = \left\{i : \gamma_i(n) \geq \delta^2 \gamma_i^t(n+1)\right\}$ and let $\mathcal{E}(n+1) = \{i : \gamma_i(n) < \delta^2\gamma_i^t(n+1)\}$. The bang-bang control algorithm with the CIR-margin is given by

$$p_i(n+1) = \begin{cases} \frac{1}{\delta} p_i(n) & i \in \mathcal{D}(n+1) \\ \delta p_i(n) & i \in \mathcal{E}(n+1) \end{cases} \quad (8.18)$$

First consider a case where $i \in \mathcal{D}(n+1)$

$$\gamma_i(n) = \frac{g_{ii}p_i(n)}{\sum_{\substack{j=1 \\ j\neq i}}^{M} g_{ij}\theta_{ij}p_j(n) + \nu_i} \geq \gamma_i^t(n) \quad (8.19)$$

Using the bang-bang control algorithm we get

$$\gamma_i(n+1) = \frac{g_{ii}\frac{1}{\delta}p_i(n)}{\sum_{\substack{j\in\mathcal{D}(n+1)\\ j\neq i}} g_{ij}\theta_{ij}\frac{1}{\delta}p_j(n) + \sum_{j\in\mathcal{E}(n+1)} g_{ij}\theta_{ij}\delta p_j(n) + \nu_i} \tag{8.20}$$

$$\gamma_i(n+1) = \frac{g_{ii}\frac{1}{\delta^2}p_i(n)}{\sum_{\substack{j\in\mathcal{D}(n+1)\\ j\neq i}} g_{ij}\theta_{ij}\frac{1}{\delta^2}p_j(n) + \sum_{j\in\mathcal{E}(n+1)} g_{ij}\theta_{ij}p_j(n) + \frac{1}{\delta}\nu_i} \tag{8.21}$$

$$\gamma_i(n+1) \geq \frac{1}{\delta^2}\frac{g_{ii}p_i(n)}{\sum_{\substack{j=1\\ j\neq i}}^{M} g_{ij}\theta_{ij}p_j(n) + \nu_i} \tag{8.22}$$

$$\gamma_i(n+1) \geq \frac{1}{\delta^2}\gamma_i(n) \tag{8.23}$$

$$\gamma_i(n+1) \geq \gamma_i^t(n) \geq \gamma_i^t(n+1) \tag{8.24}$$

For $i \in \mathcal{E}(n+1)$ we have

$$\gamma_i(n+1) = \frac{g_{ii}\delta p_i(n)}{\sum_{\substack{j\in\mathcal{D}(n+1)\\ j\neq i}}^{M} g_{ij}\theta_{ij}\frac{1}{\delta}p_j(n) + \sum_{j\in\mathcal{E}(n+1)}^{M} g_{ij}\theta_{ij}\delta p_j(n)\nu_i} \tag{8.25}$$

$$\gamma_i(n+1) = \frac{g_{ii}p_i(n)}{\sum_{\substack{j\in\mathcal{D}(n+1)\\ j\neq i}}^{M} g_{ij}\theta_{ij}\frac{1}{\delta^2}p_j(n) + \sum_{j\in\mathcal{E}(n+1)}^{M} g_{ij}\theta_{ij}p_j(n) + \frac{1}{\delta}\nu_i} \tag{8.26}$$

$$\gamma_i(n+1) > \frac{g_{ii}p_i(n)}{\sum_{\substack{j=1\\ j\neq i}}^{M} g_{ij}\theta_{ij}p_j(n) + \nu_i} = \gamma_i(n) \tag{8.27}$$

Thus we can conclude that Propositions 8.2 and 8.3 hold. □

The only modifications required in order to use the rate selection procedure described in section 8.2 with B-BPC is that the distress signaling should be decided based on the B-BPC step instead of DPC step (inequality 8.7). We denote this modified version of SPC-ALP by M-SPC-ALP.

The amount of signaling overhead depends on the number of possible rates. For example, if there are K possible rates, it takes $\lceil \log_2(K) \rceil$ ($\lceil \cdot \rceil$ denotes the the ceiling operator) bits to transmit the rate change command. In addition to the rate selection information, the distress signaling requires one to two bits. In downlink case, the distress signal (bit) can be determined by the base station controller and directly be broadcast to the whole cell. In the uplink case, each mobile has to send its distress signal individually to the base station which then broadcasts it to the whole cell. If the transmission rates are small, then relatively large bandwidth is wasted carrying only control information, but if the rates are high then the fraction of control information becomes negligible.

8.4 Computational results

The testbed is a CDMA system with 19 omni-bases located in the centers of 19 hexagonal cells (figure 2.1). We consider the uplink of the system in which $\theta_{ij} = 1$. Chip

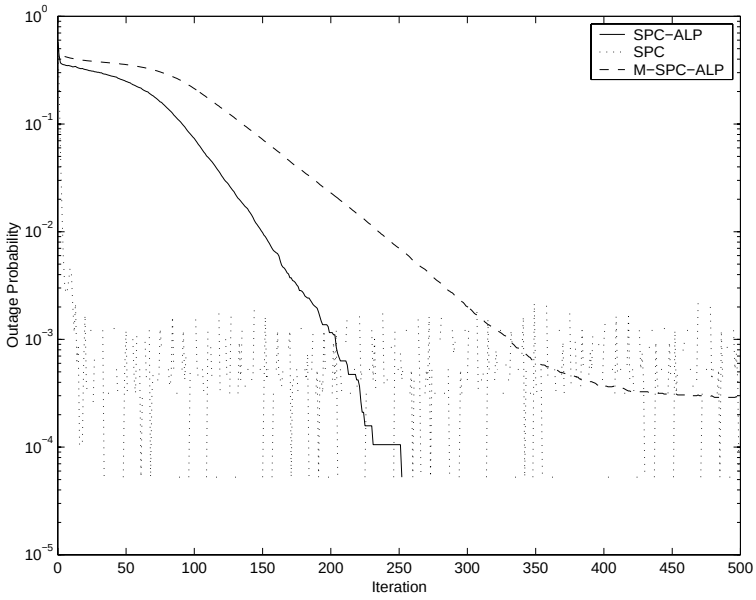

Figure 8.1: Outage probability under light load ($\gamma = -14$ dB).

rate is taken to be 1.2288 Mcps and it is assumed that the radio link can support four data rates, $r_i j = 9.6 \cdot \frac{1}{2^{j-1}}$ kbps ($j = 1,\ 2,\ 3,\ 4$). At any given instance, a total of 190 mobiles are generated and uniformly distributed over the 19 cells. The base receiver noise is taken to be 10^{-12}, and the maximum mobile power is set to 1. At each instance, the initial transmission rate and power of each mobile is randomly chosen and each mobile is connected to the base station that provides the lowest attenuation. The tuning parameters are taken to be $p_0 = 10^{-4}$, $\pi_{A\to C} = \pi_{C\to B} = 0.05$ and $\delta = 1.05$. The CIR-margin is also utilized in the case of SPC.

We consider the single-code system in which multiple rates are realized by the variable processing gain that is defined as the ratio of chip rate to the user information bit rate. The required minimum CIR before *despreading* is assumed to be $\gamma_i^k = \gamma \cdot \frac{1}{2^{k-1}}$ for each $9.6 \cdot \frac{1}{2^{k-1}}$ kbps. Three values, -14 dB, -10 dB and -6 dB are considered for γ, representing light, medium and heavy loads, respectively. The required E_b/I_o, *bit energy-to-interference power spectral density*, is calculated by adding the processing gain to the corresponding CIR value (in dB), which is constant, regardless of target data rates. For example, when $\gamma = -14$ dB, the required E_b/I_o is about 7 dB, which is actually the uplink target for a 9.6 kbps voice call with BER 10^{-3} in the IS-95 system [80]. The model used here is adopted from the *variable rate voice calls* in the IS-95 system and is the same as used in [46].

The *average throughput per mobile*, the *outage probability* and the *average transmission power per mobile* are used as performance measures. The averages are computed over 190 users in 100 instances. The number of instances is chosen to be small in order to elaborate the oscillatory behavior of SPC.

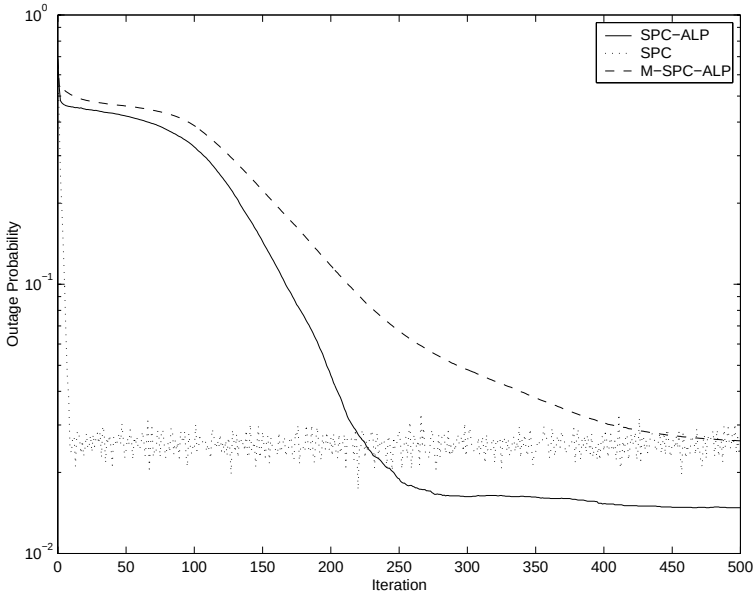

Figure 8.2: Outage probability under medium load ($\gamma = -10$ dB).

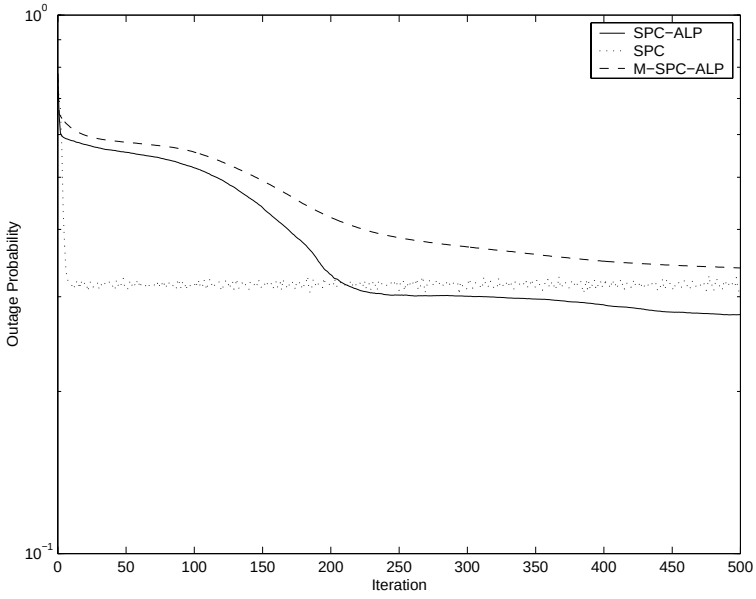

Figure 8.3: Outage probability under heavy load ($\gamma = -6$ dB).

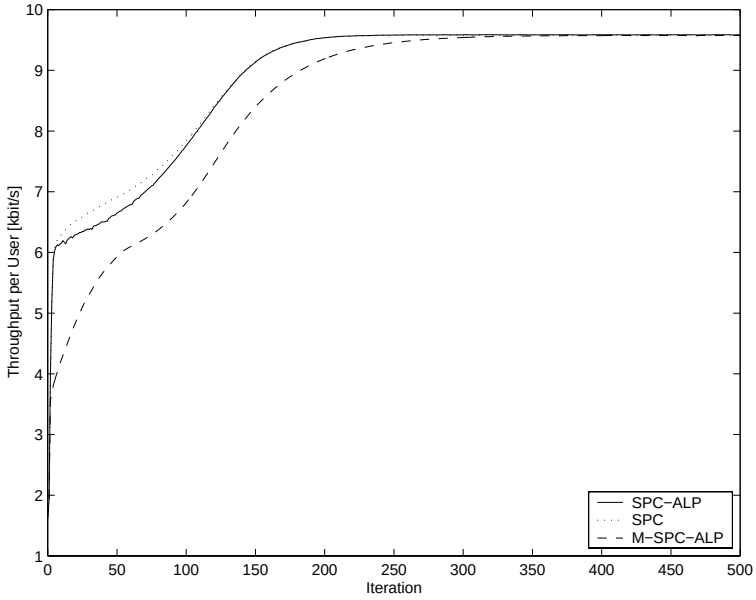

Figure 8.4: Average throughput per mobile under light load ($\gamma = -14$ dB).

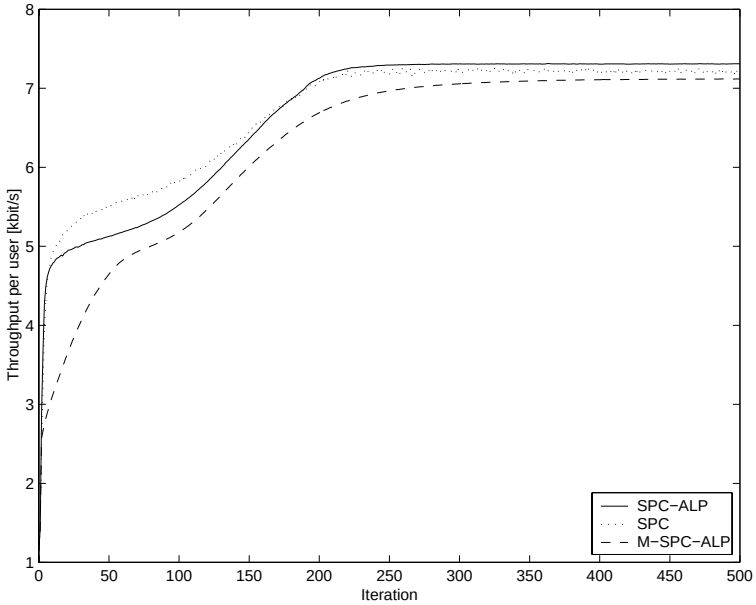

Figure 8.5: Average throughput per mobile under medium load ($\gamma = -10$ dB).

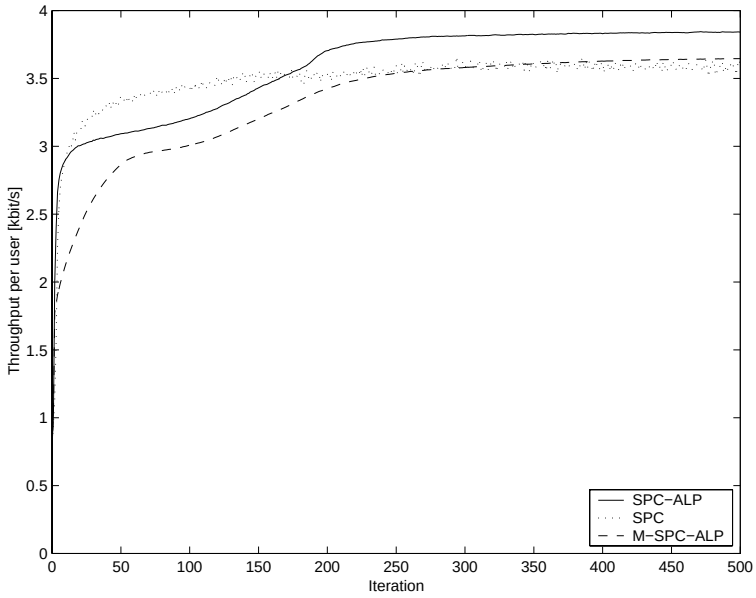

Figure 8.6: Average throughput per mobile under heavy load ($\gamma = -6$ dB).

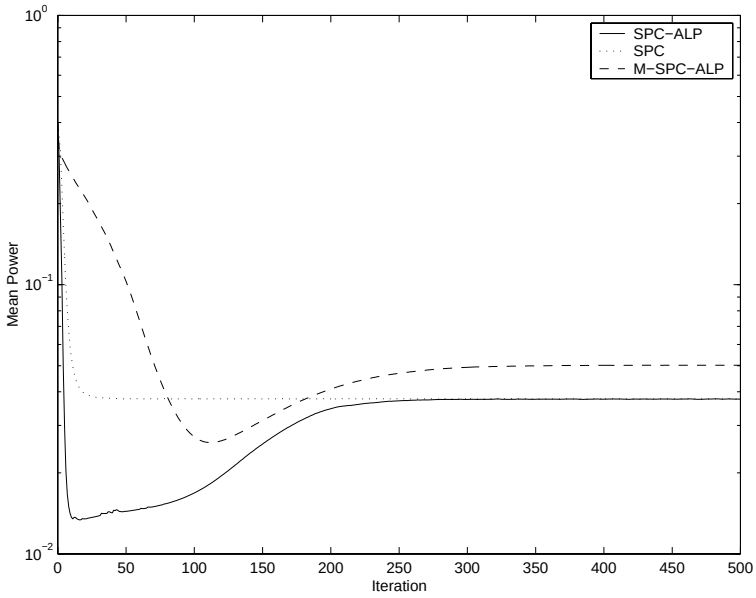

Figure 8.7: Average transmission power per mobile under light load ($\gamma = -14$ dB).

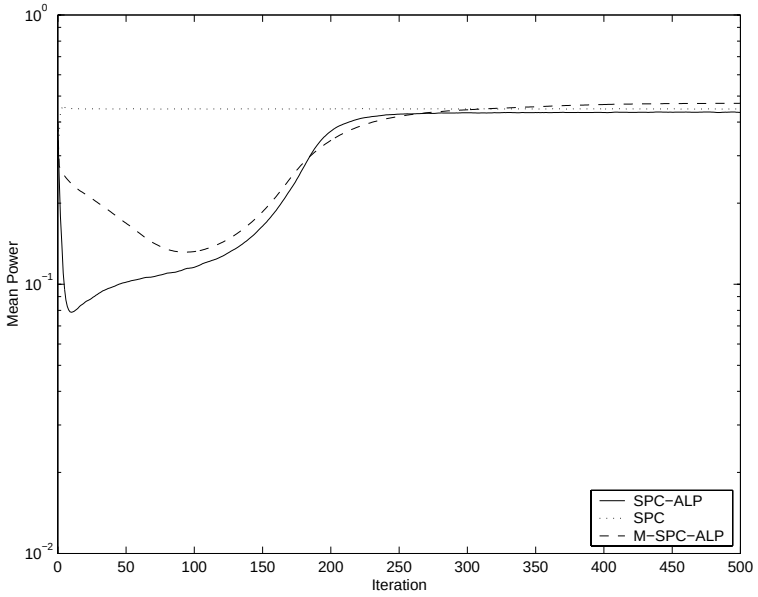

Figure 8.8: Average transmission power per mobile under medium load ($\gamma = -10$ dB).

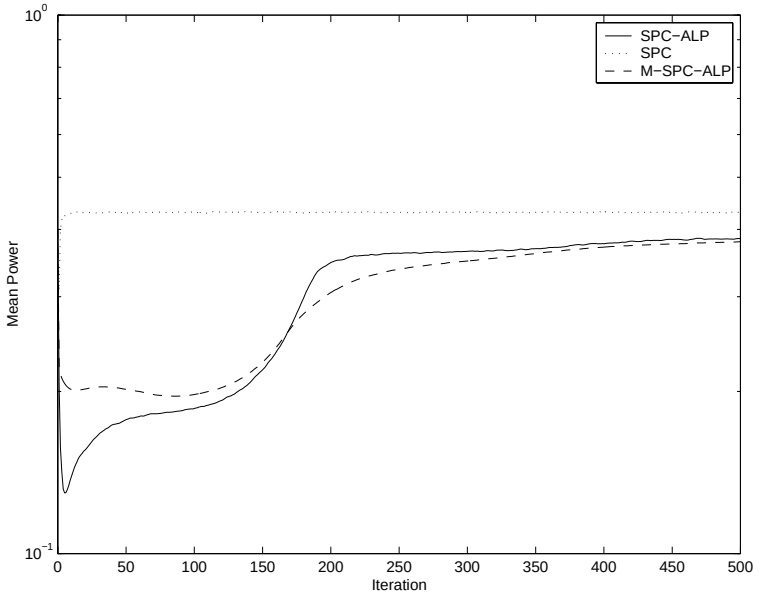

Figure 8.9: Average transmission power per mobile under heavy load ($\gamma = -6$ dB).

If the CIR value $\gamma_i(n)$ is greater than or equal to the CIR target $\gamma_i^t(n)$ corresponding to the chosen transmission rate $r_i(n)$ then it is assumed that mobile i successfully transmitted $r_i(n)$ bits at iteration n. Otherwise it is assumed that all the data transmitted by user i at that iteration is lost. Outage at iteration n is defined as fraction of users that did not get any throughput during the iteration. No CIR-margin is used in the outage computation, but instead CIR-margins are used in all the algorithms.

The outage probability is shown in figures 8.1, 8.2 and 8.3. The results indicate that SPC-ALP outperforms SPC in terms of outage probability. SPC has highly oscillating CIR and thus it alternates the set of users that are supported from iteration to another resulting in oscillating outage curve while the SPC-ALP gives much smoother outage as can be seen from the figures. It is noticeable that in the low load case, SPC-ALP converges to a fixed point solution while SPC does not necessarily do so. However, according to proposition 8.1 SPC converges to the fixed point solution if all the users can be supported with the maximum rate. The reason why SPC does not always converge in the low load case is that even in the low load case there exists some combination of user positions in which all the users can not be supported with the maximum rate. If these cases would be removed from the results, the outage of SPC would go to zero as the proposition states.

The average throughput per mobile is shown in figures 8.4, 8.5 and 8.6. In the medium and maximum load cases, the SPC-ALP gave about 1% and 7% better throughput than SPC respectively. In the low load case the difference is negligible.

The energy consumption in terms of average transmission power of the two algorithms is shown in figures 8.7, 8.8 and 8.9. SPC utilizes more power than SPC-ALP, since it assigns CIR target for individual users so that if all the other users would keep their powers constant, the best possible rate would be achieved for that particular user. Since all the users utilize the same strategy, CIR targets seem to be much higher than the targets corresponding to actual transmission rates.

As can be seen from the figures 8.1, 8.2 and 8.3; compared to SPC-ALP, M-SPC-ALP has as a smooth outage curve, but the outage probability is higher. This is because M-SPC-ALP utilizes much higher CIR-margin than SPC and therefore requires more power as can be seen form figures 8.7, 8.8 and 8.9. Figures 8.4, 8.5 and 8.6 indicate that M-SPC-ALP achieves almost the same throughput as SPC.

8.5 Concluding remarks

In this chapter, we studied the combined rate and power control for a cellular radio system that can support different transmission rates in a single connection. A new SPC-ALP algorithm based on ALP, SPC and GRR was suggested. Computational experiments carried on a CDMA system indicate that SPC-ALP achieves the same or slightly higher throughput than the SPC algorithm . Another property that can be seen from the numerical results is that SPC alternates the set of users that are supported from iteration to another resulting in oscillating outage curve while the SPC-ALP seems to give much smoother outage. The major drawback of SPC-ALP is that the number of tuning parameters that the network operator has to set in the

commission phase of the system is rather high.

It seems that the SPC-ALP could be realized by utilizing bang-bang controller instead of the DPC-ALP. This modified SPC-ALP has approximately the same throughput performance as SPC with smoother CIRs and outage. The drawback of M-SPC-ALP is its high energy consumption.

Chapter 9

Discussion

9.1 Conclusions

In this thesis, two problems are considered. The first one is the fixed-rate CIR based power control problem and the second one is the combined transmission rate selection and power control problem.

Our work on power control is parallel to the work of Yates [90], i.e., we suggest a framework for analyzing and developing power control algorithms. Our framework, unlike the Yates', establishes analytical means for comparing the convergence speeds of different algorithms. As a convergence speed measure, we suggest the asymptotic average rate of convergence that is commonly used in the field of numerical linear algebra [84, 89]. Unfortunately, this measure is not very well suited for nonstationary algorithms.

In convergence speed analysis, we assume that the system is feasible. That is, we assume that there exits some admission control scheme that can prevent the system to become overloaded. Of cause, this assumption is idealistic and does not hold for practical systems. However, it is needed in order to evaluate the power controller performance without the effects of other radio resource management functions.

Utilizing our framework we develop three new power control algorithms and compare them with DCPC. To justify our choice of reference algorithm, we note that DCPC has become one of the most widely accepted algorithms by the academic community. It provides guidelines in designing power control algorithms for practical cellular systems. DCPC is also used as a building block for connection removal [6, 47], admission control [7], combined power control and base station assignment [90] and radio network simulators. We consider two aspects of power control: The effect of available information on convergence speed and the energy efficiency. The convergence rate of power control is especially important when propagation and traffic conditions are changing rapidly. It is expected that future wireless traffic will become much more bursty than today's voice dominated traffic. With bursty traffic, slow algorithms will perhaps not even be able to converge before the data burst ends. To track these changes, the power control algorithm must converge quickly. It is also expected that the need for low-power de-

sign principles will increase along with the more services available. Improving energy efficiency is of interest for both the operators (downlink) as well as for the customers (uplink). Therefore such design principles include all levels of the system, e.g., network architecture, circuit design, protocols and resource management algorithms.

The weak point of our framework is that it is only applicable to time independent (snapshot) analysis. Thus, the resulting algorithms are deterministic in nature. However, we assume that the deterministic power control algorithms can be adapted to the statistics of the random radio channel by changing the CIR-targets. This kind of strategy is considered, e.g., in [5, 17, 69].

It is shown in chapter 4 that the convergence speed can be improved considerably by utilizing both current and previous power values in the computation of power update command. Computational results indicate that practical version of the algorithm, M-CSOPC, performs considerably better in terms of outage than the bang-bang controller. The drawback of the algorithm is that the performance of it depends on one free parameter ω. The optimal value of ω depends on the spectral radius of the $\mathbf{H}$-matrix and is thus generally unknown. To overcome this problem, tuning of ω based on distribution of $\rho(\mathbf{H})$ is suggested. In practice, obtaining this distribution can be difficult and some on-line optimization procedure may be needed.

In chapter 5, the problem of how to incorporate known link gain information into the power control algorithm in order to increase the convergence speed is investigated and a block power control is suggested. Acceleration of convergence speed is based on the accurate measurement of link gains and received CIRs in each block. However, if those measurements were too erroneous, this would affect the power control negatively. To cope with the situation, we have introduced parameters $\mathbf{\Omega}$ and $\mathbf{\Psi}$ into our algorithm. Those parameters will determine the algorithm's key properties such as distributiveness, robustness and convergence speed. The convergence is shown to occur even if $\mathbf{\Omega}$ and $\mathbf{\Psi}$ are allowed to vary from iteration to another. In addition, we note that our work opens possibility to have a power control algorithm that is between the fully distributed and the centralized ones. Therefore, it is especially suited for "bunched" systems. The major drawback of the block power control algorithm is that it is not expected to work with one bit quantization and thus relatively large signaling overhead may be required.

In chapter 6, a generalized DCPC algorithm that consumes less power and supports more users than DCPC is proposed. The idea is that, when a user requires more power than is available, the power will be decreased to benefit other users under favorable situations. It is shown that our algorithm converges to the fixed point of a feasible system, supporting every active user. For an infeasible system, convergence to a fixed point is exemplified not to necessarily occur. Finding necessary and sufficient conditions for convergence for infeasible systems is still an open issue. In infeasible case, it can be seen that oscillating powers may cause a rapidly varying CIRs as well. However, this may not be a major obstacle, since the power control can be combined with a permanent removal algorithm. The difficulty with the proposed algorithms is that infeasibility may not be detected as in DCPC. This raises the question of how to combine a permanent removal algorithm with the proposed algorithms. We propose one possible approach by modifying a gradual removal algorithm that was originally

designed for use with DCPC. We note that, there is a possibility of designing more sophisticated removal algorithms suitable for our algorithm. The practical applicability of the concept of temporary removals, which GDCPC can benefit from, could for example be non-real time traffic where the flexibility of handling the transmission attempts is larger.

It is common assumption that transmission rates may take any nonegative real values. That is, the throughput of a radio channel is a continuous function of the channel's SIR. However, in practice, the feasible transmission rates are limited to a small number of discrete values. In the discrete case the problem can be shown to be NP-complete [46]. Therefore, it is justified to consider heuristic algorithms that do not perhaps find the exact optimal solution, but instead find a "good" feasible one.

We start our multirate study by considering the rate management and power control problems separately. Here, the function of the rate management is beforehand to decide which users are allowed to transmit in the next frame so that the feasibility is guaranteed. For this purpose we suggest an algorithm based on the knapsack packing dynamic programming method. Unfortunately, the suggested knapsack method is not suited for distributed operation because it requires full knowledge about the link gain matrix. Thus, it can only be used for "bunched" systems.

Since the the dynamics of the system is dominated by the dynamics of the power control loop, it is natural to consider other radio resource management functions in combination with the power control. One such combination is the selective power control algorithm suggested by Kim, Rosberg and Zander [46]. SPC is based on the GDCPC and suffers from the same drawback, namely rapidly varying CIRs. Depending on the used coding and modulation techniques this oscillating CIR may cause additional errors to the receiver. To remove this drawback, we combine SPC with with the active link protection scheme. Computational experiments indicate that the proposed algorithm achieves the same or slightly higher throughput as the SPC algorithm with smoother CIRs and outage. In addition, SPC-ALP algorithm seems to be more energy efficient than SPC. Practical version of the algorithm utilizing only 1 bit power up/down commands, called M-SPC-ALP, seems to achieve approximately the same throughput as SPC. The drawback of M-SPC-ALP compared to SPC-ALP is in higher power consumption. The major drawback of SPC-ALP and M-SPC-ALP algorithms is the number of tuning parameters that the network operator has to set in the commission phase of the system. It is rather high and therefore can be difficult.

To conclude this thesis: We have considered both fixed-rate and multirate systems and suggested new algorithms that outperform the existing ones either in convergence speed, energy efficiency or in capacity.

9.2 Further studies

In the study of power control algorithm, it was assumed that the link gain matrix was constant and that the CIR could be measured accurately. The robustness analysis of the power control algorithms in the case of measurement errors and stochastic link gains constitute an interesting and challenging research topic.

The results concerning combined transmission rate selection and power control problem presented in this thesis were preliminary in nature. More sophisticated analysis of the problem is needed in order to suggest practical solutions. Here, as well as in the case fixed-rate power control problem, the estimation errors and stochastic nature of link gains should be taken into account. Open issues are: What are the general conditions for the algorithms to converge to a stable state? And, what are the factors that will affect the convergence speed of the algorithms. Most importantly, how much QoS can be enhanced through combined power control and rate selection?

Appendix A

Derivation of example 5.3

Since $\mathbf{A} = \mathbf{M} - \mathbf{N}$, from (2.8) and the definition of $\mathbf{M}$ and $\mathbf{N}$ in UBPC, we get

$$\mathbf{p} = (\mathbf{\Psi} \otimes \mathbf{H} + \mathbf{I} + \mathbf{\Omega}(\mathbf{1} - \mathbf{\Omega}^{-1}\mathbf{\Psi}) \otimes \mathbf{H})\mathbf{p} + \mathbf{\Omega}\boldsymbol{\eta} \tag{A.1}$$

Substituting $\mathbf{\Omega}_{kk} = \mathbf{I}$ and $\mathbf{\Psi}_{kk} = \mathbf{1}$ into the above and writing the equation system row by row, we get

$$p_i = \gamma_i^t\Big(\sum_{\substack{j \in \mathcal{B}_k \\ j \neq i}} \frac{g_{ij}}{g_{ii}}\theta_{ij}p_j + \frac{I_i}{g_{ii}}\Big), \quad i \in \mathcal{B}_k, \tag{A.2}$$

where

$$I_i = \sum_{j \notin \mathcal{B}_k} g_{ij}p_j + \nu_i \quad i \in \mathcal{B}_k \tag{A.3}$$

is the total noise plus external interference experienced by user i.

Consider first the uplink case. Since in our example a block is equal to a cell, all the receivers are co-located and thus $g_{ij} = g_{jj}$ and $I_i = I_j$ for all $i, j \in \mathcal{B}_k$. Therefore, by noting that $\theta_{ij} = 1$ for all $i, j \in \mathcal{B}_k$, we can rewrite (A.2) as follows:

$$g_{ii}p_i = \frac{\gamma_i^t}{1+\gamma_i^t}\Big(\sum_{j \in \mathcal{B}_k} g_{jj}p_j + I_i\Big), \quad i \in \mathcal{B}_k \tag{A.4}$$

Summing (A.4) over $i \in \mathcal{B}_k$ yields

$$\sum_{i \in \mathcal{B}_k} g_{ii}p_i = \sum_{i \in \mathcal{B}_k}\Big(\frac{\gamma_i^t}{1+\gamma_i^t}\Big(\sum_{j \in \mathcal{B}_k} g_{jj}p_j + I_i\Big)\Big) \tag{A.5}$$

From the above, we get

$$\sum_{i \in \mathcal{B}_k} g_{ii}p_i = \frac{\sum_{i \in \mathcal{B}_k} \frac{\gamma_i^t}{1+\gamma_i^t} I_i}{1 - \sum_{i \in \mathcal{B}_k} \frac{\gamma_i^t}{1+\gamma_i^t}} \tag{A.6}$$

Substituting (A.6) into (A.4) and dividing the result by g_{ii} yields

$$p_i = \frac{\gamma_i^t}{(1+\gamma_i^t)(1 - \sum_{j \in \mathcal{B}_k} \frac{\gamma_j^t}{1+\gamma_j^t})} \frac{I_i}{g_{ii}} \tag{A.7}$$

In the downlink case, all the intra-block interference is coming from the same source and therefore we have $g_{ij} = g_{ii}$ for all $i, j \in \mathcal{B}_k$. It was assumed that $\theta_{ij} = \theta$ for all $i, j \in \mathcal{B}_k$. So, the equation (A.2) becomes

$$p_i = \gamma_i^t(\theta \sum_{\substack{j \in \mathcal{B}_k \\ j \neq i}} p_j + \frac{I_i}{g_{ii}}), \quad i \in \mathcal{B}_k \tag{A.8}$$

By following the same steps as in (35)-(37) but keeping in mind that $I_i \neq I_j$, we get

$$p_i = \frac{\gamma_i^t}{1 + \theta\gamma_i^t}\Big(\frac{\theta \sum_{j \in \mathcal{B}_k} \frac{\gamma_j^t}{1+\theta\gamma_j^t} \frac{I_j}{g_{jj}}}{1 - \theta \sum_{j \in \mathcal{B}_k} \frac{\gamma_j^t}{1+\theta\gamma_j^t}} + \frac{I_i}{g_{ii}}\Big), \quad i \in \mathcal{B}_k \tag{A.9}$$

Appendix B

Radio resource knapsack packing algorithm

Pseudo-code of the packing algorithm

set $\mathcal{K}_c = \emptyset$
for i=1 to N
  set $\mathcal{P}_{t,j} = \mathcal{P}_{c,j} \forall j = 1, \cdots, N$
  while $\mathcal{P}_{t,i} \neq \emptyset$
    set $\mathcal{K}_t = \mathcal{K}_c \cup v\left(\mathcal{P}_{t,i}\right)$
    set $\mathcal{P}_{t,i} = \mathcal{P}_{t,i} \backslash v\left(\mathcal{P}_{t,i}\right)$
    set $\mathcal{P}_{s,j} = \mathcal{P}_{t,j} \forall j = 1, \cdots, N$
    while $\mathcal{I}\left(\mathcal{K}_t\right) \neq \emptyset$
      set $\mathcal{K}_s = \left(\mathcal{K}_t \backslash u\left(\mathcal{K}_t\right)\right) \cup v\left(\mathcal{P}_{s,I(u(\mathcal{K}_t))}\right)$
      set $\mathcal{P}_{s,I(u(\mathcal{K}_t))} = \mathcal{P}_{s,I(u(\mathcal{K}_t))} \backslash v\left(\mathcal{P}_{s,I(u(\mathcal{K}_t))}\right)$
      if $W\left(\mathcal{K}_s\right) < W\left(\mathcal{K}_t\right)$
        set $\mathcal{K}_r = \mathcal{K}_t \backslash u\left(\mathcal{K}_t\right)$
        if $W\left(\mathcal{K}_r\right) < W\left(\mathcal{K}_t\right)$
          set $\mathcal{I}\left(\mathcal{K}_t\right) = \mathcal{I}\left(\mathcal{K}_t\right) \backslash u\left(\mathcal{K}_t\right)$
        else
          set $\mathcal{K}_t = \mathcal{K}_r$
          if $I\left(u\left(\mathcal{K}_t\right)\right) \neq i$
            $\mathcal{P}_{t,I(u(\mathcal{K}_t))} = \mathcal{P}_{t,I(u(\mathcal{K}_t))} \cup u\left(\mathcal{K}_t\right)$
          end if
      else
        set $\mathcal{P}_{t,j} = \mathcal{P}_{s,j} \forall j = 1, \cdots, N$
        set $\mathcal{K}_t = \mathcal{K}_s$
      end if
    end while
    if $W\left(\mathcal{K}_t\right) > W\left(\mathcal{K}_c\right)$
      set $\mathcal{P}_{c,j} = \mathcal{P}_{t,j} \forall j = 1, \cdots, N$
      set $\mathcal{K}_c = \mathcal{K}_t$
    end if
  end while
end for
return $\mathcal{K}_c$

The above routine is executed in every frame after the buffers have been updated (i.e. all retransmission packets have been moved into the original buffers, all non-allocated packets have been put into the buffer of the closest base station and all new packets have been put into the buffer of the closest base station).

In the above algorithm N denotes the total number of base stations. The set $\mathcal{K}_c$ corresponds to current knapsack, $\mathcal{K}_t$, $\mathcal{K}_s$ and $\mathcal{K}_r$ are the sets of packets corresponding to trial, swapped and reduced knapsacks respectively (i.e. auxiliary variables). The sets $\mathcal{P}_{c,i}$, $\mathcal{P}_{t,i}$ and $\mathcal{P}_{s,i}$ are current, trial and swapped packet buffers of the i^{th} base station respectively. The index $I(u(\mathcal{K}_t))$ denotes the pointer to the base station from which the packet $u(\mathcal{K}_t)$ was originally allocated. Function $W(\mathcal{X})$ is the utility function corresponding to the set of packets $\mathcal{X}$. $\mathcal{I}(\mathcal{X})$ denotes the set of infeasible packets included in the set $\mathcal{X}$. Infeasible packet is a packet whose CIR-value γ_i is below some CIR-threshold γ_i^t or its contribution W_i to the total utility function is below some threshold W_i^t. The values of the thresholds can be different for real time and non-real time packets. The operator $v(\mathcal{X})$ takes the most valuable packet from the set $\mathcal{X}$ and the operator $u(\mathcal{X})$ takes the most infeasible packet from the set $\mathcal{X}$. The most infeasible packet is that packet whose γ_i or contribution to W has decreased most after the last allocation of packet into the trial knapsack $\mathcal{K}_t$.

Bibliography

[1] F. Adachi, M. Sawahashi, and H. Suda. Wideband DS-CDMA for next-generation mobile communication systems. *IEEE Communications Magazine*, 36(9):56–69, 1998.

[2] J. M. Aein. Power balancing in system employing frequency reuse. *COMSAT Technical Review*, 3(2):277–300, 1973.

[3] M. Almgren, H. Andersson, and K. Wallstedt. Power control in a cellular system. In *Proc. IEEE VTC '94*, pages 833–837, 1994.

[4] E. Anderlind. *Resource Allocation in Multi-Service Wireless Access Networks*. PhD thesis, Royal Institute of Technology, Sweden, 1997.

[5] M. Andersin and Z. Rosberg. Time variant power control in cellular networks. In *Proc. IEEE PIMRC '96*, pages 193–197, 1996.

[6] M. Andersin, Z. Rosberg, and J. Zander. Gradual removal in cellular PCS with constrained power control and noise. *IEEE/ACM Wireless Networks*, 2(1):27–43, 1996.

[7] M. Andersin, Z. Rosberg, and J. Zander. Soft and safe admission control in cellular networks. *IEEE/ACM Transactions on Networking*, 5(2):255–265, 1997.

[8] M. Andersin, Z. Rosberg, and J. Zander. Distributed discrete power control in cellular PCS. *Wireless Personal Communications*, 6(3):211–231, 1998.

[9] S. Ariyavisitakul and L. C. Chang. Signal and interference statistics of a CDMA system with feedback power control. *IEEE Transactions on Communications*, 41(11):1626–1634, 1993.

[10] N. Bambos. Toward power-sensitive network architectures in wireless communications: Concepts, issues, and design aspects. *IEEE Personal Communications*, 5(3):50–59, 1998.

[11] N. D. Bambos, S. C. Chen, and D. Mitra. Channel probing for distributed access control in wireless communication networks. In *Proc. IEEE GLOBECOM '95*, pages 322–326, 1995.

[12] N. D. Bambos, S. C. Chen, and G. J. Pottie. Radio link admission algorithms for wireless networks with power control and active link quality protection. In *Proc. IEEE INFOCOM '95*, pages 97–104, 1995.

[13] M. Berg. *Capacity, robustness, and complexity of radio resource management in bunched personal communication systems.* Licentiate thesis, Royal Institute of Technology, Sweden, 1999.

[14] M. Berg, S. Pettersson, and J. Zander. A radio resource management concept for "bunched" personal communication systems. In *Proc. Multiaccess, Mobility and Teletraffic for Personal Communications Workshop MMT '97*, pages 259–271, 1997.

[15] F. Berggren, R. Jäntti, and S.-L. Kim. A generalized algorithm for constrained power control with capability of temporal removal. Submitted to *IEEE Transactions on Vehicular Technology*, 1999.

[16] D. P. Bertsekas and J. N. Tsitsiklis. *Paraller and distributed computation numerical methods.* Prentice-Hall, Englewood Cliffs, 1989.

[17] J. Blom and F. Gunnarsson. *Power Control in Cellular Radio Systems.* Licenciate thesis, Division of Automatic Control, Linkpings Universitet, 1998.

[18] F. Bock and B. Ebstein. Assignment of transmitter power by linear programming. *IEEE Transaction on Electromagnetic Compatibility*, 6:36–44, July 1964.

[19] P.-R. Chang and B.-C. Wang. Adaptive fuzzy power control for CDMA mobile radio systems. *IEEE Transactions on Vehicular Technology*, 42(2):225–239, 1996.

[20] P.-R. Chang and B.-C. Wang. Adaptive fuzzy proportional integral power control for a cellular CDMA system with time delay. *IEEE Journal on Selected Areas in Communications*, 14(9):1818–1829, 1996.

[21] E. Dahlman, B. Gudmundson, M. Nilsson, and J. Sköld. UMTS/IMT-2000 based on wideband CDMA. *IEEE Communications Magazine*, 36(9):70–80, 1998.

[22] M. L. Fisher. The lagrangian relaxation method for solving integer programming problem. *Management Science*, 27(1):1–18, 1981.

[23] G. J. Foschini and Z. Miljanic. A simple distributed autonomous power control algorithm and its convergence. *IEEE Transactions on vehicular technology*, 42(4):641–646, 1993.

[24] M. Frodigh and J. Zander. Joint power control in cellular radio systems. In *Proc. IEEE PIMRC '95*, pages 41–45, 1995.

[25] T. Fujii and M. Sakamoto. Reduction of cochannel interference in cellular systems by intra-zone channel reassignment and adaptive power control. In *Proc. IEEE VTC '88*, pages 668–672, 1988.

[26] A. Furuskär, S. Mazur, F. Müller, and H. Olofsson. EDGE - Enhanced data rates for GSM and TDMA/136 evolution. *IEEE Personal Communications*, 6(3):56–66, 1999.

[27] X. M. Gao, X. Z. Gao, J. M. A. Tanskanen, and S. J. Ovaska. Power control for mobile DS-CDMA systems using a modified Elman neural network controller. In *Proc. IEEE VTC '97*, pages 750–754, 1997.

[28] A. Goldsmith and P. Varaiya. Capacity of fading channel with channel side information. *IEEE Transactions on Information Theory*, 43(6):1986–1992, 1997.

[29] S. A. Grandhi. *Power Control in Mobile Radio Systems*. PhD thesis, Rutgers,The State University of New Jersey, USA, 1994.

[30] S. A. Grandhi, R. Viljayan, and D. J. Goodman. Distributed power control in cellular radio systems. *IEEE Transactions on Communications*, 42(2-4):226–228, 1994.

[31] S. A. Grandhi, J. Zander, and R. Yates. Constrained power control. *Wireless Personal Communications*, 1:257–270, 1995.

[32] S. Gupta, R. D. Yates, and C. Rose. Soft dropping power control-a power control backoff strategy. In *Proc. IEEE International conference on Personal Wireless Communications*, pages 210–214, 1997.

[33] Y. Han, H. G. Bahk, and S. Yang. CDMA mobile system overview: Introduction, background, and system concepts. *ETRI Journal*, 19(3):83–97, 1997.

[34] S. V. Hanly. *Information Capacity of Radio Networks*. PhD thesis, University of Cambridge, England, 1993.

[35] S. V. Hanly. An algorithm for combined cell-site selection and power control to maximize cellular spread spectrum capacity. *IEEE Journal on Selected Areas in Communication*, 13(7):1332–1340, 1995.

[36] S. V. Hanly and D. N. Tse. Multi-access fading channels: Part II: Delay limited capacities. *IEEE Transactions on Information Theory*, 44(7):2816–2831, 1998.

[37] C-.Y. Huang and R. D. Yates. Rate of convergence for minimum power assignment algorithms in cellular radio systems. *Wireless networks*, 4:223–231, 1998.

[38] W. C. Jakes. *Microwave Mobile Communication*. John Wiley & Sons, New York, 1973.

[39] H. Ji and C.-Y. Huang. Non-cooperative uplink power control in cellular radio systems. *Wireless Networks*, 4:233–240, 1998.

[40] R. Jäntti and S.-L. Kim. Power control based on partial knowledge about the link gain matrix. Submitted to *ACM/Balzer Wireless Networks Journal*, 1999.

[41] R. Jäntti and S.-L. Kim. Second-order power control with asymptotically fast convergence. To appear in *IEEE Journal on Selected Areas in Communications*, March 2000.

[42] R. Jäntti and S.-L. Kim. Selective power control with active link protection for combined rate and power control. To appear in *IEEE VTC2000-Spring*, May 2000.

[43] W. Kahan. *Gauss-Seidel methods for solving large systems of linear equations.* PhD thesis, University of Toronto, Canada, 1958.

[44] J. H. Kim, S. J. Lee, Y. W. Kim, M. Y. Chung, and D. K. Sung. Performance of single-bit adaptive step-size closed-loop power control scheme in DS-CDMA systems. *IEICE Transactions on Communications*, E81-B(7):1548–1552, 1998.

[45] S.-L. Kim. A two-mode algorithm for combined power control and base station assignment. In *Proc. PIMRC '99*, 1999.

[46] S.-L. Kim, Z. Rosberg, and J. Zander. Combined power control and transmission rate selection in cellular networks. In *Proc. IEEE VTC 1999 - Fall*, pages 1653–1657, 1999.

[47] S.-L. Kim and J. Zander. Optimization approach to gradual removal in a cellular PCS with distributed power control. To appear in *IEEE Transactions on Vehicular Technology*, 1999.

[48] J. Laakso, R. Jäntti, M. Rinne, and O. Salonaho. Radio resource knapsack packing for wcdma air interface. In *Proc. IEEE PIMRC '98*, pages 183 –187, 1998.

[49] J. Laakso, T. Koljonen, and M. Rinne. The radio resource knapsack packing for WTDMA air interface. In *Proc. IEEE ICUPC'98*, pages 255–260, 1998.

[50] C.-C. Lee and R. Steele. Closed-loop power control in CDMA systems. *IEE Proceedings-Communications*, 143(4):231–239, 1996.

[51] L. C. Y. Lee. *Mobile Communications Engineering.* McGraw-Hill, New York, 1982.

[52] T.-H. Lee and J.-C. Lin. A study on the distributed power control for cellular mobile systems. In *Proc. IEEE VTC '96*, pages 1130–1134, 1996.

[53] T.-H. Lee, J.-C. Lin, and Y. T. Su. Downlink power control algorithm for cellular radio systems. *IEEE Transactions on Vehicular Technology*, 44(1):89–94, 1995.

[54] K. K. Leung. Integrated power control and link adaptation for QoS in broadband wireless networks. In *Proc. IEEE PIMRC*, 1999.

[55] K. K. Leung. A Kalman-filter method for power control in broadband wireless networks. In *Proc. IEEE INFOCOM*, pages 948–956, 1999.

[56] Y.-W. Leung. Simplified power control method for cellular mobile communication. *Electronics letters*, 30(8):626–627, 1994.

[57] Y.-W. Leung. Power control in cellular networks subject to measurement error. *IEEE Transactions on Communications*, 44(7):772–775, 1996.

[58] S. J. Lin, D. J. Costello, and M. J. Miller. Automatic-repeat-request error-control schemes. *IEEE Communications Magazine*, 22(12):5–17, 1984.

[59] N. Mandayam, P.-C. Chen, and J. Holtzman. Minimum duration outage for CDMA cellular systems: A level crossing analysis. *Wireless Personal Communications*, 7(2-3):135–146, 1998.

[60] H. J. Meyerhoff. Method for computing the optimal power balance in multibeam satellite. *Comsat Technical Review*, 3(2), 1974.

[61] D. Mitra. An asynchronous distributed algorithm for power control in cellular radio systems. In *Proc. Fifth WINLAB Workshop on Third Generation Wireless Information Networks*, pages 249–259, 1993.

[62] R. W. Nettleton and H. Alavi. Downstream power control for spread spectrum cellular radio systems. In *Proc. IEEE GLOBECOM '82*, pages 84–88, 1982.

[63] R. W. Nettleton and H. Alavi. Downstream power control for spread spectrum cellular radio systems. In *Proc. IEEE VTC '83*, pages 242–246, 1983.

[64] S.-J. Oh and K. M. Wasserman. Dynamic spreading gain control in multiservice CDMA networks. *IEEE Journal on Selected Areas in Communications*, 17(5):918–927, 1999.

[65] J. G. Proakis. *Digital Communications*. McGraw-Hill, Singapore, third edition, 1995.

[66] X. Qiu and K. Chawla. Throughput performance of adaptive modulation in cellular systems. In *Proc. ICUPC '98*, pages 945–950, 1998.

[67] X. Qiu and K. Chawla. On the performance of adaptive modulation in cellular systems. *IEEE Transactions on Communications*, 47(6):884–895, 1999.

[68] F. Rashid-Farrokhi, L. Tassiulas, and K. J. Ray Liu. Joint optimal power control and beamforming in wireless networks using antenna arrays. *IEEE Transactions on Communications*, 46(10):1313–1324, 1998.

[69] Z. Rosberg. Transmitter power control with adaptive safety margins based on duration outage. *IBM Haifa Research Lab.*, 1999.

[70] Z. Rosberg and J. Zander. Towards a framework for power control in cellular systems. *Wireless Networks*, 4:215–222, 1998.

[71] J. M. Rulnick and N. Bambos. Mobile power management for maximum battery life in wireless communication networks. In *Proc. IEEE INFOCOM '96*, pages 443–450, 1996.

[72] J. M. Rulnick and N. Bambos. Performance evaluation of power-managed mobile communication devices. In *Proc. IEEE ICC '96*, pages 1477–1481, 1996.

[73] J. M. Rulnick and N. Bambos. Mobile power management for wireless communication networks. *Wireless networks*, 2:3–14, 1997.

[74] A. Sampath, P. S. Kumar, and J. Holtzman. On setting reverse link target SIR in a CDMA system. *Proc. VTC '97*, 2:929–933, 1997.

[75] A. Sampath, P.S. Kumar, and J. Holtzman. Power control resource management for a multimedia CDMA wireless system. In *Proc. IEEE PIMRC '95*, pages 21–25, 1995.

[76] M. L. Sim, E. Gunawan, B.-H. Soong, and C.-B. Soh. Performance study of closed-loop power control algorithms for a cellular CDMA system. *IEICE Transactions on Vehicular Technology*, 48(3):911–921, 1999.

[77] M. Soleimanipour, W. Zhuang, and G. H. Freeman. Modelling and resource allocation in wireless multimedia CDMA systems. In *Proc. VTC '98*, pages 1279–1283, 1998.

[78] C. W. Sung and W. S. Wong. The convergence of an asynchronous cooperative algorithm for distributed power control in cellular systems. *IEEE Transactions on Vehicular Technology*, 48(2):563–570, 1999.

[79] C. W. Sung and W. S. Wong. A distributed fixed-step power control algorithm with quantization and active link protection. *IEEE Transactions on Vehicular Technology*, 48(2):553–562, 1999.

[80] *TIA/EIA Interim Standard-95: Mobile station - base station compatibility standard for dual-mode wideband spread spectrum cellular system.* Telecommunications Industry Association, Englewood Cliffs, 1993.

[81] W. Tschirk. Effect of transmission power control on the cochannel interference in cellular radio networks. *Elektrotechnik und Informationstechnik*, 106(5):194–199, 1989.

[82] D. N. Tse and S. V. Hanly. Multi-access fading channels: Part I: Polymatroid structure, optimal resource allocation and throughput capacities. *IEEE Transactions on Information Theory*, 44(7):2796–2815, 1998.

[83] S. Ulukus and R. D. Yates. Stochastic power control for cellular radio systems. *IEEE Transactions on Communication*, 46(6):784–798, 1998.

[84] R. S. Varga. *Matrix Iterative Analysis.* Prentice-Hall, Inc., Englewood Cliffs, New Jersey, 1962.

[85] A. J. Viterbi. *CDMA Principles of Spread Spectrum Communication.* Addison-Wesley, Reading, Massachusetts, 1995.

[86] A. J. Viterbi, A. M. Viterbi, A. M. Gilhousen, and E. Zehavi. Soft handoff extends CDMA cell coverage and increases reverse link capacity. *IEEE Journal on Selected Areas in Communication*, 12(8):1281–1288, 1994.

[87] A. J. Viterbi, A. M. Viterbi, and E. Zehavi. Performance of power-controlled wideband terrestial digital communications. *IEEE Transactions on Communications*, 41(4):559–569, 1993.

[88] J. F. Whitehead. Signal-level-based dynamic power control for cochannel interference management. In *Proc. VTC '93*, pages 499–502, 1993.

[89] D. M. Yang. *Iterative solution of large linear systems.* Academic Press, New York, 1971.

[90] R. D. Yates. A framework for uplink power control in cellular radio systems. *IEEE Journal on Selected Areas in Communications*, 13(7):1341–1347, 1995.

[91] R. D. Yates, S. Gupta, C. Rose, and S. Sohn. Soft dropping power control. In *Proc. IEEE VTC '97*, pages 1694–1698, 1997.

[92] R. D. Yates and C-.Y. Huang. Integrated power control and base station assignment. *IEEE Transactions on Vehicular Technology*, 44(3):638–644, 1995.

[93] J. Zander. Distributed cochannel interference control in cellular radio systems. *IEEE Transactions on Vehicular Technology*, 41(3):305–311, 1992.

[94] J. Zander. Performance of optimum transmitter power control in cellular radio systems. *IEEE Transactions on Vehicular Technology*, 41(1):57–62, 1992.

[95] J. Zander. Transmission power control for co-channel interference management in cellular radio systems. In *Proc. Fourth WINLAB Workshop on Third Generation Wireless Information Networks*, pages 241–247, 1993.

[96] J. Zander. Radio resource management in future wireless networks - requirements and limitations. *IEEE Communications Magazine*, 35(8):30–36, 1997.

[97] J. Zander. Best effort radio resource management for non-real-time multimedia traffic in wireless networks. *Royal Institute of Technology, Radio Communication Systems Group*, 1999.

[98] J. Zander and M. Frodigh. Comment on performance of optimum transmitter power control in cellular radio systems. *IEEE Transactions on Vehicular Technology*, 43(3):636, 1994.

[99] *IEEE Personal Communications*, 5(3), June 1998. Special issue on energy management in personal communications and mobile computing. Ed. M. Zorzi.